THE GEOLOGY AND GEOCHEMISTRY of the PILOT-SMUGGLER SHEAR ZONE, RICE LAKE AREA, MANITOBA.

(1)

by

Alan H. Bailes

May, 1969

A THESIS

Presented to

The Faculty of the Department of Geology

Graduate Studies and Research

The University of Manitoba

In Partial Fulfillment

of the Requirements for the Degree

Master of Science

ABSTRACT

The gold and quartz bearing vein deposits of the Rice Lake area occur within shear and fracture zones that are spatially associated with a large oval-shaped intrusion of quartz diorite. A typical gold-quartz vein bearing shear zone, the Pilot-Smuggler, has been described in detail. The study includes a description of the structure, the petrology and alteration of the host rocks, the mineralization and geochemistry of the shear zone and attendant gold and quartz bearing veins.

The gold-bearing quartz veins are small lenses that are fractured and disjointed and contain ankerite and sulphide minerals. Pyrite, the dominant sulphide mineral, occurs as brecciated stringers and patches within the veins. Sphalerite, pyrrhotite, chalcopyrite and a host of copper bearing sulphide minerals occur as tiny blebs and veinlets within the pyrite. The gold assays of the quartz veins are proportional to their sulphide content.

Minor structures within the Pilot-Smuggler shear zone suggest two stages of deformation have affected the break. During the initial stage the zone ruptured and stresses were released by planar glide, which was followed by compression subparallel to the shear zone foliation causing numerous kink, chevron, and conjugate folds.

The alteration processes, as determined by examination of thin section and chemical analyses of altered rocks of the shear zone, have involved an influx of the volatile elements, H_2O, CO_2

and S, that have caused the host dacitic volcanic rocks to alter to a sericite-chlorite-carbonate bearing schist. Silica not required for the formation of the new minerals, sericite and chlorite, has been depleted from the altered rocks and could have migrated into the quartz veins. The distribution of elements within the altered zones suggests that many of the constituents of the mineralized quartz veins could be derived from the adjacent altered rocks.

ACKNOWLEDGEMENTS

The author gratefully acknowledges the assistance and guidance of Professors D. Anderson and W. Brisbin and Dr. I. Haugh, and is also indebted to them for their critical reading of this manuscript.

The author was employed by the Manitoba Department of Mines and Natural Resources with Project Pioneer during the summer of 1966 while field information for this study was collected. The assistance of the other geologists employed with Project Pioneer and the permanent members of the staff of the Manitoba Mines Branch is gratefully acknowledged.

The rock analyses were generously contributed by K.Ramlal of the staff of the Geology Department of the University of Manitoba. The gold assays were supplied by A. MacKay, Chief Chemist, Department of Mines and Natural Resources, Manitoba.

FRONTISPIECE

Quartz Vein of Pilot-Smuggler
Shear Zone, Gold Lake Mines'
Company Ltd. Property

TABLE OF CONTENTS

ABSTRACT		i
ACKNOWLEDGEMENTS		iii
TABLE OF CONTENTS		v
LIST OF ILLUSTRATIONS		vii
LIST OF TABLES		xi
CHAPTER I		
INTRODUCTION		
1.	GENERAL	1
2.	STATEMENT OF THESIS PROBLEM	1
3.	LOCATION OF THESIS AREA	3
4.	METHOD OF STUDY	6
CHAPTER II		
RESULTS OF PREVIOUS STUDIES OF GOLD DEPOSITS		
1.	TYPICAL FEATURES OF GOLD DEPOSITS	8
2.	THEORIES OF GOLD DEPOSITION	10
A.	Magmatic Hydrothermal Theory	10
B.	Lateral Secretion Theory	11
3.	NEUTRON ACTIVATION ANALYSIS FOR TRACE AMOUNTS OF GOLD	12
CHAPTER III		
GENERAL GEOLOGY		
1.	GENERAL GEOLOGY OF THE RICE LAKE AREA	14
2.	GOLD DEPOSITS OF THE RICE LAKE AREA	16
3.	GENERAL DESCRIPTION OF THE PILOT-SMUGGLER SHEAR ZONE	17
4.	QUARTZ VEINS OF THE PILOT-SMUGGLER SHEAR ZONE	36
CHAPTER IV		
STRUCTURAL GEOLOGY		
1.	INTRODUCTION	49
2.	DESCRIPTION OF STRUCTURAL FEATURES OF THE PILOT-SMUGGLER SHEAR ZONE	50
A.	Penetrative Planar Structures	50
(1)	Varieties of Penetrative Planar Structures	51
(2)	Categories of Penetrative Planar Structures	54

CHAPTER IV (Cont'd)

2.	B.	Minor Folds and Linear Structures	60
		(1) Minor Folds	60
		(2) Linear Structures	65
	C.	Joints	70
3.		INTREPRETATION AND DISCUSSION OF STRUCTURAL FEATURES OF THE PILOT-SMUGGLER SHEAR ZONE	70
4.		GENERAL DISCUSSION OF STRUCTURAL AND AGE RELATIONSHIPS OF GEOLOGICAL FEATURES OF THE RICE LAKE AREA	80

CHAPTER V
GEOCHEMISTRY OF THE GOLD-BEARING QUARTZ VEINS

1.	INTRODUCTION	83
2.	DESCRIPTION OF WALL ROCK ALTERATION	83
3.	DISTRIBUTION OF ELEMENTS IN THE ALTERATION ZONES	89
4.	ORIGIN OF THE GOLD-BEARING QUARTZ VEINS OF THE PILOT-SMUGGLER SHEAR ZONE	95

CHAPTER VI
SUMMARY AND CONCLUSIONS

SUMMARY AND CONCLUSIONS	99
LIST OF REFERENCES	102
APPENDIX I - MERCURY VAPOR ANALYSIS	106
APPENDIX II - GAMMA RAY SPECTROMETER SURVEY	109
APPENDIX III - CHEMICAL ANALYSES	112

LIST OF ILLUSTRATIONS

LIST OF FIGURES

FIGURE 1	-	Location Map	2
FIGURE 2	-	Distribution of Quartz Veins Rice Lake-Beresford Lake Area	4
FIGURE 3	-	General Geology, Rice Lake Area	5
FIGURE 4	-	Textures of Sulphide Minerals	42 - 43
FIGURE 5	-	Poles to Schistosity Surfaces (S_1), a Stereographic Plot	55
FIGURE 6	-	Poles to Shear Zone Schistosity (S_2), a Stereographic Plot	55
FIGURE 7	-	Poles to Strain Slip Cleavage (S_3), a Stereographic Plot	55
FIGURE 8	-	Average Orientations of S-Surfaces (S_1, S_2, S_3), a Stereographic Plot	55
FIGURE 9	-	Sketch of Minor 'S' Kink Folds (F_2)	58
FIGURE 10	-	Diagramatic Plan View Showing Strike of Shear Zone Relative to Strike of S_2	59
FIGURE 11	-	A Stereographic Plot of Axes of Minor Folds	61
FIGURE 12	-	A Stereographic Plot of Linear Structures	61
FIGURE 13	-	Minor Folds, Pilot-Smuggler Shear Zone	62
FIGURE 14	-	Contoured Equal Area Plot of Poles to 132 Joint Surfaces	69
FIGURE 15	-	Idealized Evolution of Shear Zone Structures Shown in Plan Views and Synoptic Stereographic Plots	73 - 75
FIGURE 16	-	Kinks and Kink Folds Formed by Compression Subparallel to a Previous Foliation	78
FIGURE 17	-	Representation of Structure South of Rice Lake by Strain Ellipsoid	82
FIGURE 18	-	Distribution of the Volatile Elements (H_2O+CO_2+S) Compared with that of SiO_2, 3+50N Grid Line	92
FIGURE 19	-	Distribution of the Volatile Elements (H_2O+CO_2+S) compared with that of FeO, 3+50N Grid Line	93
FIGURE 20	-	Distribution of Cations in the Alteration Zones	94

LIST OF FIGURES (Cont'd)

FIGURE 1A	-	Mercury Content of Rock Specimens, 3+50N Grid Line	107
FIGURE 2A	-	K Gamma Values for Unsheared Volcanic Rocks	110
FIGURE 3A	-	Al_2O_3 Content of Rock Specimens, 3+50N Grid Line	114
FIGURE 4A	-	FeO, Fe_2O_3, MgO & TiO_2 Contents of Rock Specimens, 3+50N Grid Line	115
FIGURE 5A	-	CaO, Na_2O & K_2O Contents of Rock Specimens, 3+50N Grid Line	116
FIGURE 6A	-	H_2O, CO_2, S Contents of Rock Specimens, 3+50N Grid Line	117

LIST OF PLATES

FRONTISPIECE	-	Quartz Vein of Pilot-Smuggler Shear Zone, Gold Lake Mines Property	iv
PLATE 1	-	Aerial view of Pilot-Smuggler Shear Zone	18
PLATE 2	-	Chilled bleached contact between volcanic flows	18
PLATE 3	-	Thin section photomicrograph of chilled contact between volcanic flows	20
PLATE 4	-	Thin section photomicrograph of typical fragmental volcanic rock	20
PLATE 5	-	Pyroclastic dacite breccia that contains fragments of various composition and size	21
PLATE 6	-	Thin section photomicrograph of a welded tuff containing shards and crystal fragments	21
PLATE 7	-	Thin section photomicrograph of a chlorite-sericite-carbonate schist with folded disjointed quartz veinlets	25
PLATE 8	-	Quartz stringers emanating from quartz feldspar porphyry dike intrude diabase dike	25
PLATE 9	-	Dark dacitic inclusions in quartz feldspar porphyry dike	29
PLATE 10	-	Thin section photomicrograph of quartz feldspar porphyry dike	29
PLATE 11	-	Thin section photomicrograph of contact between a dacitic volcanic rock and a quartz feldspar porphyry dike	32

LIST OF PLATES (Cont'd)

PLATE 12	-	Fractured quartz vein	34
PLATE 13	-	Conjugately folded (F_2) quartz vein	34
PLATE 14	-	Thin section photomicrograph of vein quartz with a cataclastic foliation (S_2)	35
PLATE 15	-	Thin section photomicrograph of strained quartz showing cataclastic foliation (S_2) with recrystalization in shear and tension fractures	35
PLATE 16	-	Mineralized quartz vein	37
PLATE 17	-	Brecciated pyrite	37
PLATE 18	-	Polished section photomicrograph of pyrite brecciated and veined by quartz	41
PLATE 19	-	Polished section photomicrograph of pyrite impregnated by quartz veinlets	41
PLATE 20	-	Polished section photomicrograph of quartz veining brecciated pyrite	44
PLATE 21	-	Polished section photomicrograph of chalcopyrite as veins and blebs within pyrite	44
PLATE 22	-	Polished section photomicrograph of chalcopyrite as blebs and veinlets in pyrite	45
PLATE 23	-	Polished section photomicrograph of sphalerite veining pyrite	45
PLATE 24	-	Polished section photomicrograph of a bleb of chalcopyrite and pyrrhotite in pyrite	46
PLATE 25	-	Polished section photomicrograph of chalcocite in quartz	46
PLATE 26	-	Polished section photomicrograph of gold in pyrite	47
PLATE 27	-	Folded and disjointed competent sedimentary unit	52
PLATE 28	-	Characteristic minor 'S' kink folds (F_2)	52
PLATE 29	-	'Strain slip cleavage' (S_3) that intersects shear zone schistosity (S_2)	53
PLATE 30	-	Thin section photomicrograph of small chevron folds	53
PLATE 31	-	Shallow plunging 'Z' assymmetrical fold (F_1) in a layer of sedimentary rock	64

LIST OF PLATES (Cont'd)

PLATE 32	-	Thin section photomicrograph of 'S' (F_2) minor fold	66
PLATE 33	-	Thin section photomicrograph of a feldspar phenocryst dappled by epidote, calcite, sericite alteration	87
PLATE 34	-	Thin section photomicrograph of a veinlet of epidote and calcite	87
PLATE 35	-	Thin section photomicrograph of zoisite-calcite alteration	88
PLATE 36	-	Thin section photomicrograph of a carbonate, sericite, shlorite schist	88

LIST OF TABLES

TABLE I	-	Table of Formations - Rice Lake Area	15
TABLE 2	-	Chemical Analyses of Typical Rock Types	31
TABLE 3	-	Gold Assays	40
TABLE 4	-	Mineralogy of the Alteration Zones, 3+50N Grid Line	86
TABLE 5	-	Changes in Chemical Composition of Alteration Zones	90
TABLE 6	-	Gold in Minerals of the Skaergaard Differentiated Intrusion	95
TABLE IA	-	Chemical Analyses of Rock Specimens, 3+50N Grid Line	113

CHAPTER I

INTRODUCTION

1. 1. General

Gold is at present the only mineral of economic importance in the Rice Lake-Beresford Lake belt of Precambrian volcanic, sedimentary, and derived metamorphic rocks (Figure 1, page 2). Interest in the area was sparked by its discovery in 1911 on the Gabrielle claim on the north shore of Rice Lake. Many small deposits have been discovered since and numerous small-scale mining operations have been attempted; however, the meagerness of the deposits and the irregularity of the gold assays, have combined to discourage large financial investment in the properties. There are, at this time, no producing mines in the area. The San Antonio gold mine, which was in operation since the early 1930's, was closed down in the summer of 1968.

A detailed geological investigation, known as Project Pioneer, a joint endeavour of the Manitoba Mines Branch and the Geology Department of the University of Manitoba, is being carried out on the Rice Lake greenstone belt. Studies on the gold deposits in the area form an important phase of the project.

1. 2. Statement of Thesis Problem

The Rice Lake-Beresford Lake area contains numerous shear and fracture zones, many of which are occupied by gold-bearing quartz veins. The shear and fracture zones,

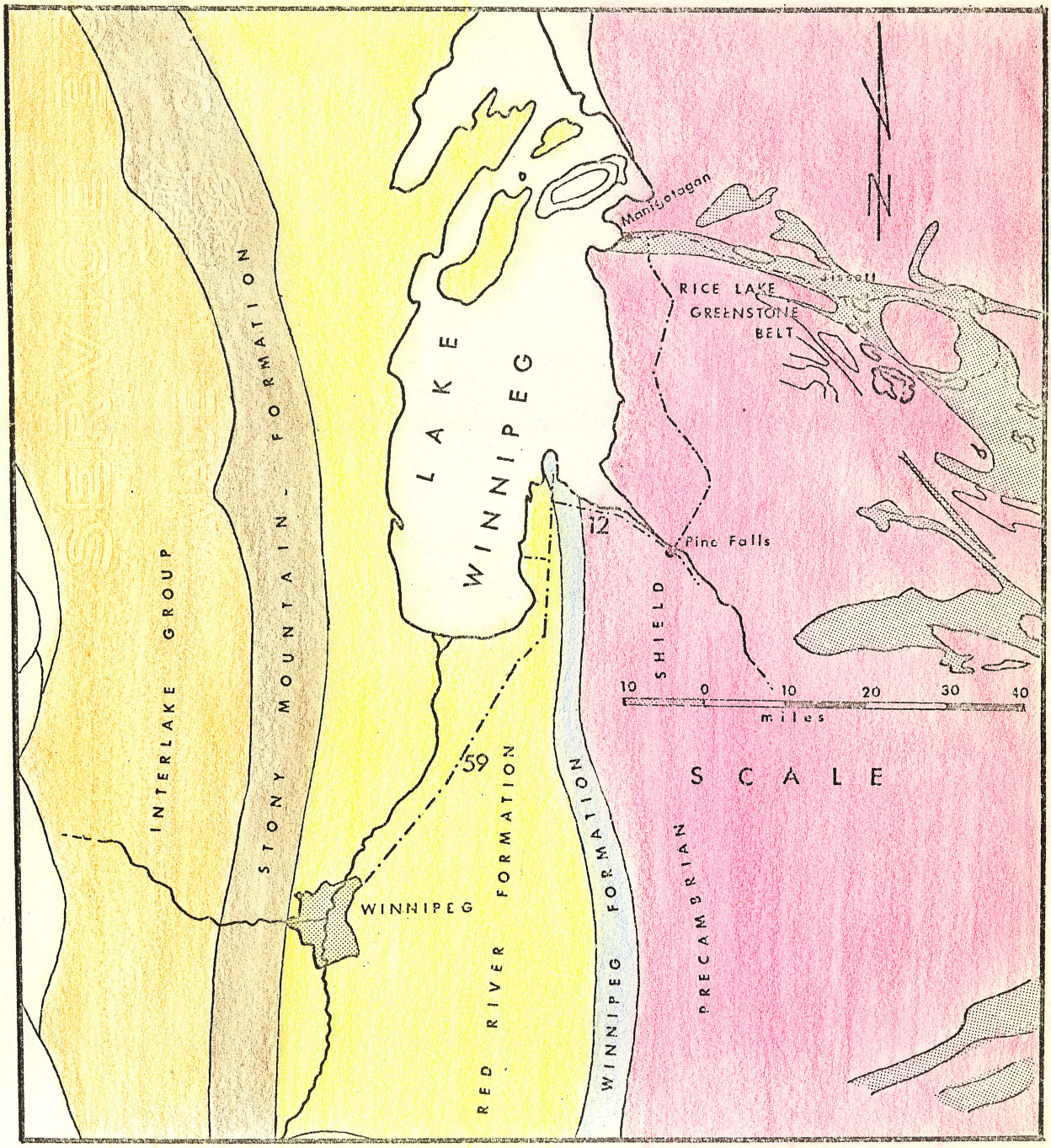

Location Map

FIGURE 1

and attendant gold-bearing quartz veins occur to the east and west of a large oval shaped intrusion of quartz-diorite.

This thesis presents the results of a detailed geological examination of a typical gold and quartz bearing shear zone, the Pilot-Smuggler shear zone, of the Rice Lake greenstone belt. This study includes a description of the structure, petrology, alteration of the host rock, and the mineralization and geochemistry of the shear zone and attendant gold-bearing quartz veins. Besides presenting a detailed description of the Pilot-Smuggler break, a further objective is to formulate a possible mechanism of emplacement of the gold-bearing quartz veins that occur within the shear zone.

The Pilot-Smuggler shear zone, and associated gold-bearing quartz veins, were chosen for study because they are prominent and easily accessible. (Figure 3, page 5).

1. 3. Location of Thesis Area

The Rice Lake greenstone belt trends east-southeast from Lake Winnipeg to the Manitoba-Ontario provincial boundary. The Town of Bissett is accessible by highway from Winnipeg via Pine Falls (Figure 1, page 2). The property of the Gold Lake Mines Company Ltd., situated on the Pilot-Smuggler break, is located approximately three miles south of the town. The Caribou Lake road, joining the main Pine Falls-Bissett road about three miles west of Bissett, crosses a section of the Pilot-Smuggler break about one mile north of Salveigh Lake (Figure 3, page 5). A small bush road nearby connects the Caribou Lake road with the abandoned Gold Lake Mine.

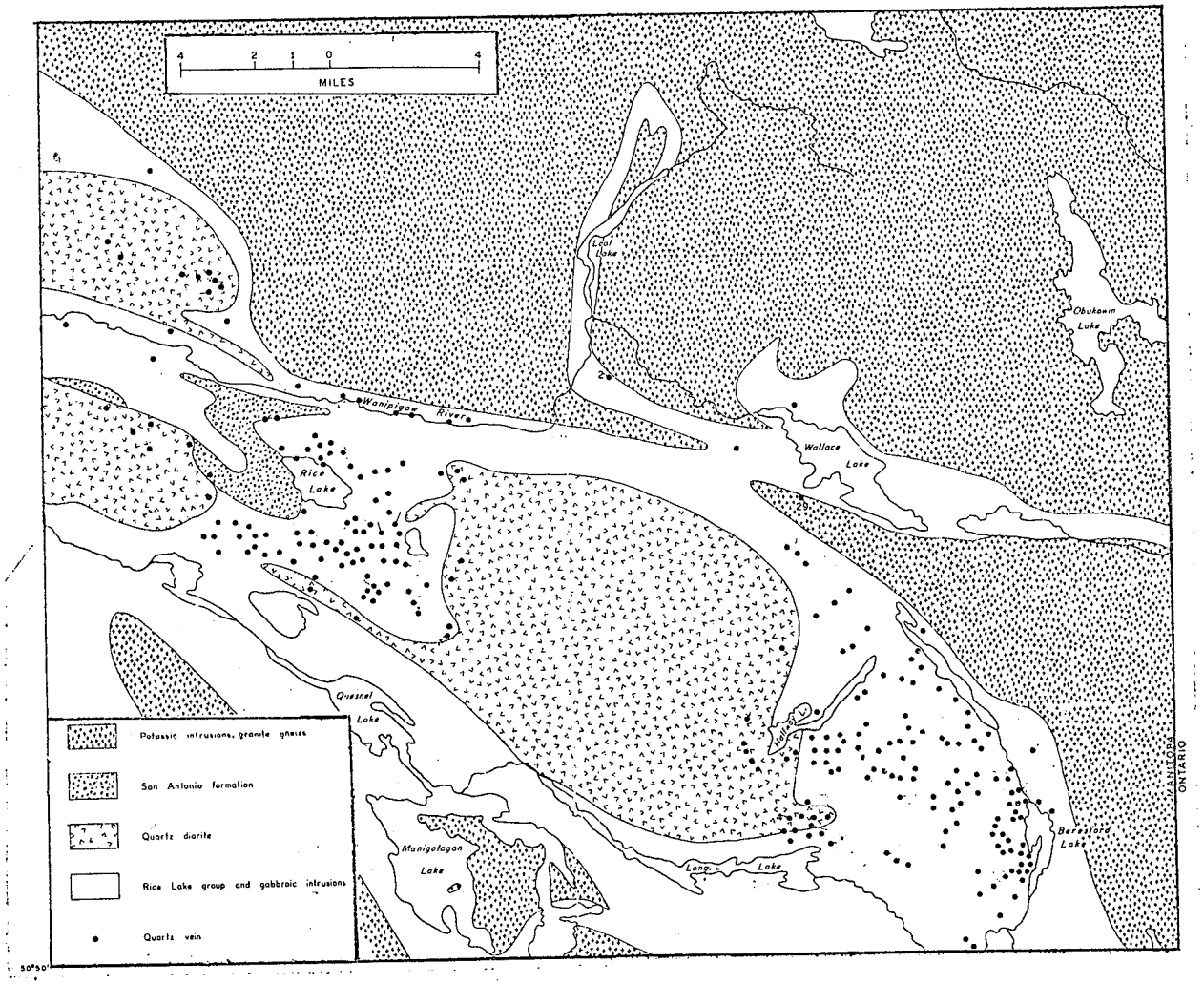

FIGURE 2

Distribution of Quartz Veins Rice Lake — Beresford Lake Area

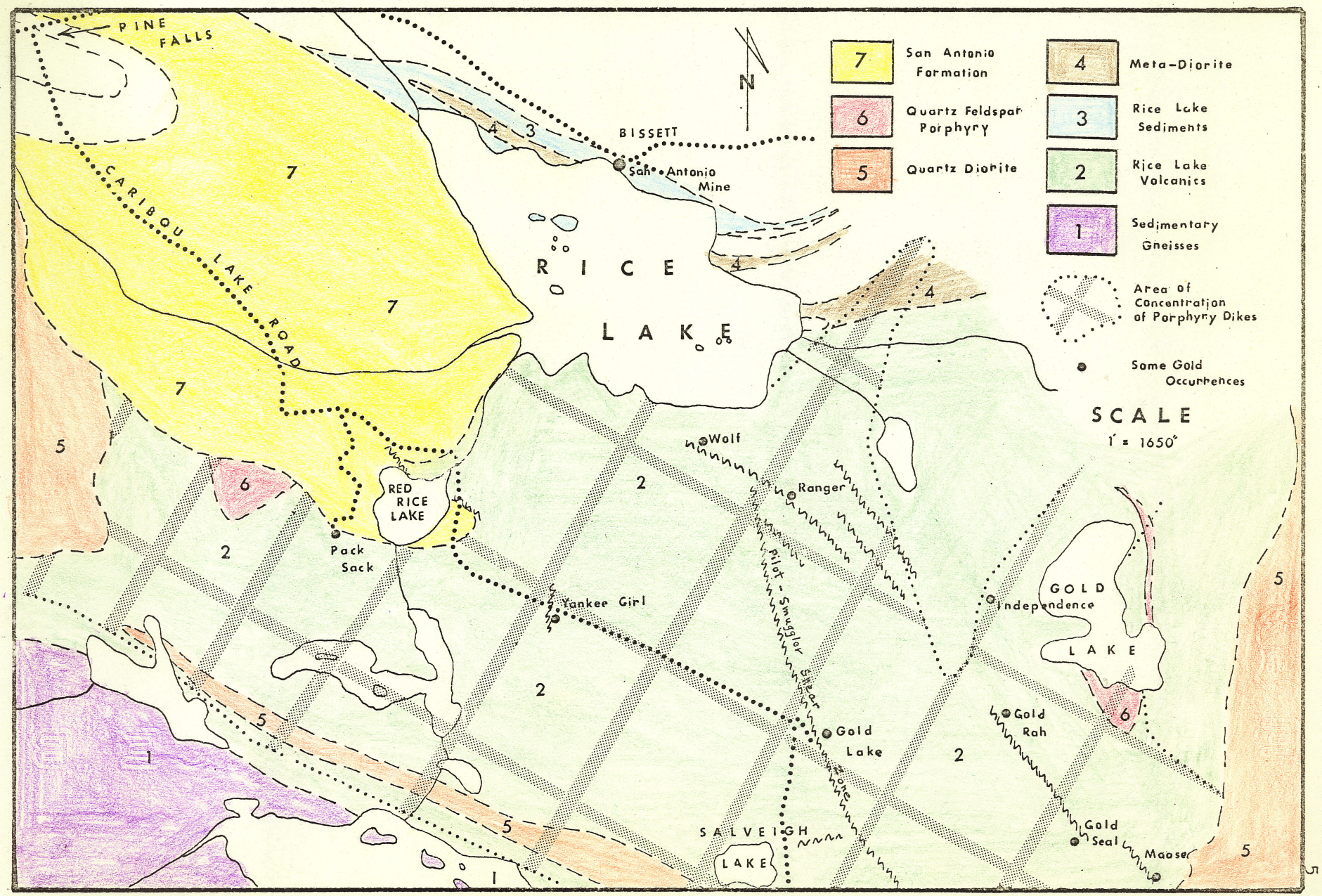

FIGURE 3

GENERAL GEOLOCY, RICE LAKE AREA
after Stockwell (1937)

I. 4. Method of Study

Field examination of the Pilot-Smuggler shear zone was made during the summer of 1966 while the writer was working for the Manitoba Mines Branch on Project Pioneer. Subsequently at the University of Manitoba, the field data were organized and laboratory studies carried out on specimens collected during the field season.

Projects carried out relating to this thesis problem are listed below:

(1) A general geological map, on a scale of 1 inch to 1/4 mile, of the Pilot-Smuggler shear zone was prepared. (Map 1).

(2) The orientations of minor structural features related to the Pilot-Smuggler break were measured and plotted on stereographic diagrams.

(3) A detailed geological map, on a scale of 1 inch to 25 feet, of a rectangular area, fourteen hundred feet by eight hundred feet, surrounding the two exploratory shafts on the property of the Gold Lake Mine Company Ltd. was prepared (Map 2). A grid was surveyed and cut for this area to ensure accuracy of mapping and for locating specimens for laboratory study.

(4) Ten polished sections of the quartz veins and associated sulphide minerals were prepared and studied.

(5) Approximately fifty thin sections were prepared and studied. The petrology of the individual rock units and the altered rocks of the shear zone, associated with gold-bearing quartz veins, was carefully examined.

(6) Chemical analyses of representative specimens of each rock unit were made. A suite of specimens collected across the quartz veins and into the country were analyzed chemically to determine the distribution of the major and minor elements.

CHAPTER II

RESULTS OF PREVIOUS STUDIES OF GOLD DEPOSITS

II. 1. Typical Features of Gold Deposits

The high price of gold and the low wages effective during the 1930's, made gold mining a profitable venture notwithstanding the general depression of the period. This is reflected in the geological literature of the era which contains many articles dealing with gold deposits. The work done by geologists during the 1930's on gold deposits was, generally, of high calibre and many of their observations are still pertinent; some of the more prevalent observations were:

(a) The association of gold deposits with large acid intrusives. (Bateman, 1940), (Gunning, 1937), (Pardie & Park, 1943), (Gallagher, 1940);

(b) The zonal arrangements of ore deposits around large acid batholithic intrusions. For example, a mineral study of the Province of British Columbia by H.C. Cooke (1946) suggested that gold deposits always occur near these igneous bodies; copper deposits further removed; and silver-lead-zinc deposits still more distant;

(c) The composition of associated granitic bodies is a factor in governing gold occurrences, viz., granitic bodies commonly grade into quartz feldspar porphyries where gold deposits are found. (Dougherty, 1935). The three important known gold-bearing localities in Manitoba, the Elbow-Morton, Herb Lake, and Rice Lake-Gold Lake areas, mapped by C.H.Stockwell (1935, 1937, 1938), were all found to be located near intrusions of "quartz eye" granite, a porphyritic granite with prominent blue quartz eyes. Gold deposits were also considered to be commonly associated with sodic granite bodies of intermediate composition. (Gallagher, 1940);

(d) The altered rocks surrounding gold-bearing quartz veins are typically rich in carbonates, sericite and chlorite. This has often been used to find and trace gold bearing veins. (Clarke et al, 1939), (Cooke, 1947), (Dougherty, 1935), (Lindgren, 1905-6), Pardie & Parke, 1943);

(e) The mineralogy of gold-bearing quartz vein deposits is simple and similar for all deposits. (White, 1943). Quartz is the dominant vein mineral accompanied by small proportions of tourmaline, beryl, albite, calcite, and sulphide minerals. (Cooke, 1946);

(f) The sulphide mineralization accompanying the gold-bearing quartz veins usually occurs as small brecciated patches and stringers. Pyrite is the dominant sulphide mineral with minor chalcopyrite, sphalerite, arsenopyrite, galena, pyrrhotite, tellurides, various copper sulphides and sulphosalts. The pyrite was often found to be veined by the other sulphides so that many geologists have postulated that more than one period of mineralization is involved in the formation of gold deposits (Byers, 1940);

(g) That many gold-bearing quartz veins have been brecciated (White, 1943). It is thought that this has facilitated the entry of successive periods of mineralizing fluids;

(h) The majority of paragenetic charts that have been prepared for gold deposits include several periods of fracturing and mineralization, and often numerous periods of deposition of gold. (Armstrong, 1943), (Byers, 1940), (Coleman, 1957). The interpretation of ore textures under the reflecting microscope is often difficult and it is likely that many of these paragenetic charts could be simplified. Most of the charts, however, do include the following two stages:

(1) quartz accompanied by pyrite (and sometimes arsenopyrite)

xxxx fracturing xxxx

(2) chalcopyrite, sulphosalts, sphalerite, galena gold;

(i) Gold values of the quartz veins increase with sulphide concentration, especially with the 'second' stage of sulphide minerals. Often chalcopyrite, galena and sphalerite in these veins are considered indicators of the presence of gold. (Gunning, 1937);

(j) Lode gold occurrences, almost without exception, are deposited in or near structural breaks such as shear or fracture zones. (Cooke, 1946).

The three major regions of gold occurrences in Canada are the Cordillera, the Canadian Shield, and the Nova Scotian

Appalachians. The Canadian Shield is the most important of these regions. The rocks in which gold deposits are found, on the Shield, consist mainly of ancient volcanic and sedimentary rocks. In a few instances, deposits have been found within small bodies of intrusive granite, syenite, or porphyry. Some instances are known of gold deposits in larger granitic masses but, in such cases, the gold-bearing quartz veins are confined to the edges of these bodies. (Cooke, 1946). Although the mineralogy of the gold deposits of the Canadian Shield is simpler than that of the British Columbian or Nova Scotian deposits, the descriptions in Cooke's article (1946) and those by other authors, indicate that all of the gold occurrences are similar. The similarity of lode gold deposits suggests that they may share a common mechanism of formation.

II. 2. Theories of Gold Deposition

There are two major theories that have been proposed to explain the mechanism of formation of lode gold deposits. One theory suggests that the gold-bearing veins have been precipitated from hydrothermal solutions that are genetically related to intrusive magmatic bodies. The theory that some, if not most, of the constituents of lode gold deposits, have been leached from the rocks hosting the veins, has also been considered a possible genesis for gold deposits.

II. 2A. Magmatic Hydrothermal Theory

According to the Glossary of Geology and Related Sciences, prepared by the American Geological Institute, 'hydrothermal' is a term "applied to heated or hot magmatic

emanations rich in water, to the processes in which they are concerned, and to the rocks, ore deposits, alteration products, and springs produced by them." The theory of hydrothermal genesis of ore deposits was originated by W. Lindgren and has proven useful in explaining many geological features. According to this theory, the gold is retained in the residual phase of the crystallizing magma and is carried by these fluids away from the solidifying magma to be deposited in structurally favorable localities. This theory explains the association of gold with granitic bodies, which have large associated vapour phases, and the deposition of gold in permeable shear and fracture zones.

II. 2B. Lateral Secretion Theory

The Glossary of Geology and Related Sciences, prepared by the American Geological Institute, defines 'lateral secretion' as "the theory that the contents of a vein or lode are derived from the adjacent wall rock." W.Lindgren (1905-6) was the first geologist to apply this theory to gold deposits, although he later changed his mind in favor of a magmatic hydrothermal origin.

Studies by many geologists have suggested that the silica of gold-bearing quartz veins has been leached from the vein wall rock. Chemical analyses of altered and unaltered wall rock by Byers (1940), Bateman (1940), Boyle, (1959), Clarke (1939), Cooke (1946), Hurst (1935), Lindgren(1905), Moore (1912), Knopf (1929) and Schmitt

(1954), and others, support this hypothesis.

Many of the proponents of the 'lateral secretion' theory are willing to attribute the quartz and some sulphide minerals of the gold-bearing veins, to having been leached from the altered host rocks. They believe, however, that the remaining vein material and the altering solutions (rich in CO_2, H_2O and S) are of magmatic hydrothermal origin. A recent study by R. W. Boyle (1961) on the Giant Yellowknife area in the Northwest Territories, suggested to him that most, if not all, vein materials could have been derived from a migration of elements under metamorphic gradients into or away from the vein sites.

II. 3. Neutron Activation Analysis for Trace Amounts of Gold

Until recently one of the major problems confronting geologists in their investigations of lode gold deposits has been the expense and difficulty of analyzing rock specimens for trace amounts of the metal. Gold is particularly well suited to analysis by neutron activation techniques because of its very high activation cross-section for thermal neutrons. With this method it is now possible to provide reliable data on the distribution of gold in common igneous rocks, silicate minerals, and also in the rocks hosting the gold deposits.

Studies by Vincent and Crocket (1960) and Shcherbakov and Perezhogin (1963), using the neutron activation technique have caused these authors to come to differing conclusions concerning the genesis of gold deposits, but further work on lode gold deposits using this analytical

tool should result in some valuable contributions to an understanding of their mechanism of formation.

CHAPTER III

GENERAL GEOLOGY

III. 1. General Geology of the Rice Lake Area

The Rice Lake and adjacent areas have previously been studied by Moore (1912), Delury (1921), Cooke (1921), Wright (1932), Stockwell (1938), and Davies (1953). These areas are now undergoing an intensive investigation by the Manitoba Mines Branch and the University of Manitoba.

The Rice Lake greenstone belt consisting of Archean volcanic and sedimentary rocks trends east-southeast from Lake Winnipeg towards the Manitoba-Ontario provincial boundary (Figure 1, page 2). C.H. Stockwell (1938) divides the rocks of the Rice Lake greenstone belt into the Rice Lake series, intrusive rocks, and the San Antonio formation (Table 1, page 15). The volcanic rocks comprise basalt, andesite, dacite, rhyolite and associated pyroclastic rocks, interbedded with sedimentary rocks which include impure quartzite, greywacke, slate, and conglomerate. The Rice Lake series of volcanic and sedimentary rocks has been intruded by a series of calcic intrusions, comprising diabase dikes and sills, irregular sill-like bodies of gabbro, batholithic bodies of quartz diorite, and sills, dikes and stocks of quartz feldspar porphyry (Figure 3, page 5). In the vicinity of Rice Lake, a sedimentary unit known as the San Antonio formation, unconformably overlies the Rice Lake series, one of the large quartz diorite bodies and other intrusive rocks

(Davies, 1953). There is no documented or observed occurrence where the San Antonio formation has been cut by dikes of igneous material, although it directly overlies the quartz diorite. J.F. Davies (1963) considers the volcanic rocks of the Rice Lake series, which are texturally, mineralogically, and compositionally similar to one another, to be the extrusive equivalents of the calcic intrusions. Gneissic and potassic granitic bodies occur to the north and south of the Rice Lake greenstone belt. (Figure 2, page 4).

TABLE I

Table of Formations - Rice Lake Area

San Antonio Formation
Feldspathic quartzite

Intrusive rocks
- Aplite and pegmatite dikes
- Porphyry, rhyolite, and andesite dikes
- Lamprophyre dikes
- Quartz diorite
- "Quartz-eye" granite
- Meta-diabase sills and dikes
- Meta-gabbro, meta-diorite, quartz diorite
- Porphyritic andesite sills and dikes

Rice Lake Series
- Trachyte breccia, porphyritic dacite breccia
- Porphyritic andesite
- Basalt
- Tuff, arkose, conglomerate
- Porphyritic basalt
- Rhyolite, trachyte, andesite, breccia
- Porphyritic andesite breccia

(After Stockwell - 1938)

Diabase and quartz feldspar porphyry dikes are numerous. They are common near the large quartz diorite intrusion and are often spatially related to many of the gold occurrences

(Figure 3, page 5). The diabase and porphyry dikes are thought by Stockwell (1938) and Davies (1953) to have been intruded contemporaneously. In some instances, the porphyry dikes cut the diabase dikes; in the others, the reverse relationship is true. Most of the cross-cutting relations, however, indicate the porphyry dikes to be slightly younger (Stockwell 1938). The quartz feldspar porphyry dikes emanate from the quartz diorite body; transitions from quartz diorite to quartz feldspar porphyry have been observed following these dikes from the quartz diorite source (Stockwell, 1938). It is possible that the source of the diabase dikes is basic material remobilized by the intrusion of the quartz diorite, or a basic differentiate of this intrusion.

III. 2. Gold Deposits of the Rice Lake Area

There are numerous gold occurrences in the Rice Lake area. Most of the gold deposits, however, are too small, and assays too irregular, for them to be of commercial importance. Many of the gold occurrences have been examined geologically with information on them available from the Manitoba Mines Branch's cancelled assessment files, from geological reports prepared by Stockwell (1938) and Davies (1953 & 1962), and in a thesis written by J. F. Davies (1963). Some of the typical features of the Rice Lake gold occurrences are listed below:

(1) The known gold occurrences are contained in shear zones or, in some cases, in fracture zones.

(2) The gold-bearing quartz veins have associated alteration zones rich in chlorite, sericite, ankerite and pyrite.

(3) The gold content of the quartz vein ore bodies is often proportional to the concentration of sulphide minerals in, or associated with, the quartz veins.

(4) Chalcopyrite has been considered by prospectors and geologists working in the Rice Lake area, to be an indication that quartz veins are gold-bearing.

(5) Although gold-bearing quartz veins occur in practically all rock types of the Rice Lake district, the majority of quartz veins with larger quantities of gold, occur in mafic intrusive or extrusive rocks.

The majority of shear zones and attendant gold-bearing quartz veins are spatially associated with the large oval-shaped body of quartz diorite that intrudes the Rice Lake series (Figure 2, page 4). The quartz veins are distributed to the east and west of this large body.

The shear zones of the Rice Lake area belong to two groups. (Stockwell, 1938). One group trends north-northwest and the other trends east-northeast; both groups dip steeply, often slightly to the north. The two groups appear to have developed contemporaneously, although over a considerable period of time. In some cases the group trending north-northwest cuts and displaces the other, or vice versa. The mode of formation of the shear zones is of particular interest because the gold deposits are contained within these structural breaks.

III. 3. General Description of the Pilot-Smuggler Shear Zone

The Pilot-Smuggler break is a prominent topographic feature that appears on aerial photographs as a strong linear system of almost continuous outcrop (Plate I, page 18). It is approximately three miles long and fifty to one

PLATE 1
Aerial view of Pilot-Smuggler shear zone. (1" = 1/4 mile)

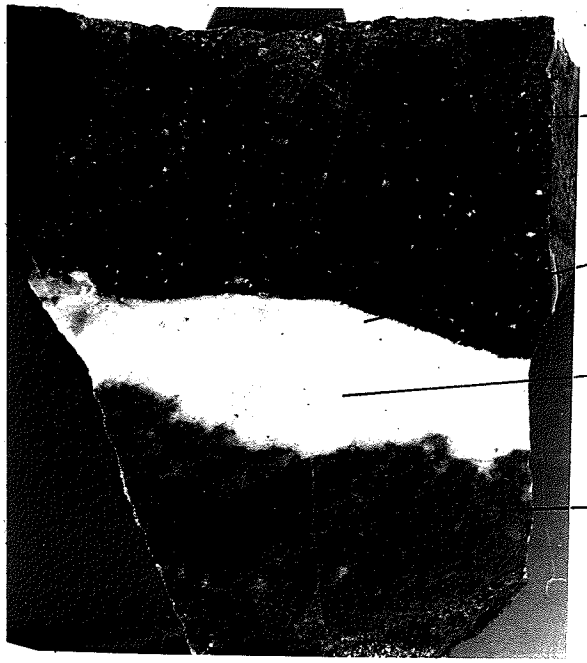

PLATE 2
Chilled bleached contact between volcanic flows (1X)

hundred feet wide. The zone is composed of schistose rock that dips steeply, usually northeast, and strikes between 335 and 350 degrees. The break curves slightly, with its northerly portion trending more to the north (Map 1). Most of the quartz veins, which occur as lenses and pods within the shear zone, are near the site of the abandoned Gold Lake Mine exploratory shafts where the break begins to veer north. It is possible that this change in direction plays a major part in localizing the quartz veins.

The Pilot-Smuggler shear zone transects dacitic and rhyolitic volcanic units of the Rice Lake series. Numerous quartz feldspar porphyry dikes trend perpendicular to the direction of the Pilot-Smuggler break and have been offset by it. A diabase dike trends parallel to the shear zone and portions of the dike have been incorporated into the shear zone. Well layered rocks, likely of sedimentary origin, are contained within the shear zone but are not found outside the boundaries of the break. A description of the rock types through which the shear zone cuts is given below:

Dacite & Rhyolite (1)*

The volcanic rocks that host the Pilot-Smuggler shear zone are comprised of many varieties. They may be volcanic flows (Plates 2 & 3, pages 18 & 20),

* Number of unit as given in legend of Map 2.

PLATE 3
Thin section photomicrograph of 'chilled' contact (same as shown in Plate 2) (10X, polarized light)

PLATE 4
Thin section photomicrograph of typical fragmental volcanic rock. (10X, non-polarized light)

PLATE 5
Pyroclastic dacite breccia that contains fragments of varying composition and size (IX)

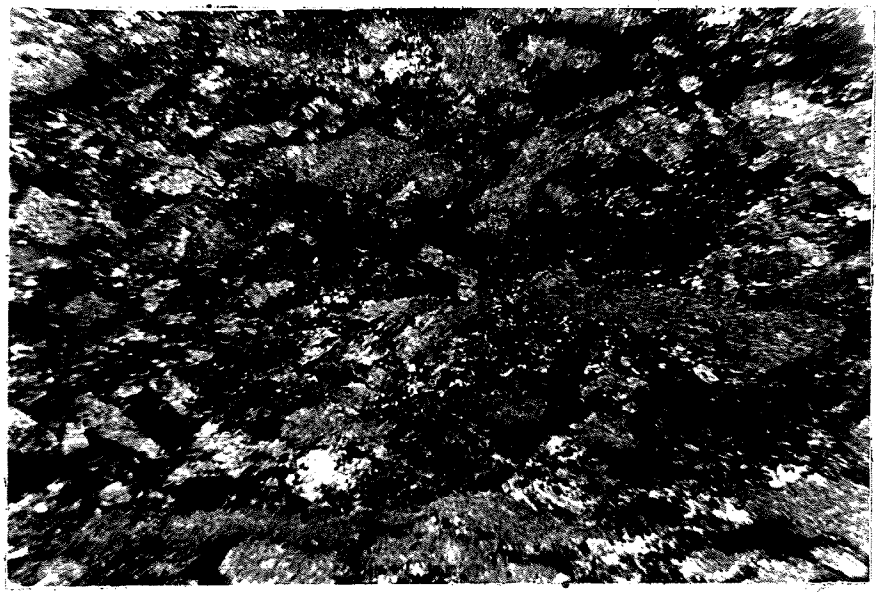

PLATE 6
A thin section photomicrograph of a welded tuff containing shards and crystal fragments. (10X, polarized light)

volcanic breccias (which include both flow and pyroclastic breccias) (Plates 4 & 5, pages 20 & 21), and lapilli and welded tuffs (Plate 6, page 21). Most of the volcanic rocks are porphyritic and contain well formed phenocrysts. In many cases the phenocrysts, generally andesine crystals two to three millimeters long, in these porphyritic volcanic rocks are so well formed that it is difficult to distinguish these rocks from the quartz-feldspar porphyry dikes. The volcanic rocks are typically fragmental (Plates 4 & 5, pages 20 & 21). The fragments vary considerably in size and shape; generally they range in size from 5 mm to 300 mm. It would appear that most of the volcanic rocks are pyroclastic breccias. The fragments may vary in composition (Plate 5, page 21) or may be of uniform composition (Plate 4, page 20).

The volcanic rocks are massive and unstratified and only two units could be mapped (Map 1). These two units consist of rocks of predominantly dacitic and rhyolitic composition respectively and the contacts between the units are gradational. Both the dacitic and rhyolitic volcanic units are porphyritic and fragmental. The rhyolitic rocks are variable in color and may be black, light grey, light

blue, a bluish grey, and in some cases have a greenish tint. The dacites vary less in color and are usually dark grey. Both the dacitic and rhyolitic rocks weather to a light grey color, often with a creamy tinge. The feldspar phenocrysts stand out in relief in the porphyritic varieties and give the rock a rough weathered surface.

Dacitic volcanic rocks host the shear zone near the exploratory shafts of the Gold Lake Mines Company Ltd. (Map 1). These dacitic rocks are composed essentially of plagioclase (An 30-40) and a fibrous green amphibole, likely actinolite. The plagioclase occurs both as large phenocrysts (1 - 3 mm) that are often twinned and zoned, and as smaller crystals (1/16 - 1/8 mm) within the fine grained matrix with the actinolite. The feldspar crystals are commonly dusted with sericite and calcite that have formed as alteration products. Epidote has formed as an alteration product of both plagioclase and actinolite. Chlorite, biotite, leuxocene, magnetite, apatite, and in some cases, quartz phenocrysts are also present in small quantities. The volcanic rocks hosting the Pilot-Smuggler shear zone belong to the epidote-amphibolite metamorphic facies.

The fragments within the volcanic rocks are commonly elongated in one direction when observed in thin section (Plate 4, page 20) or on a rock surface. A weak alignment of the platy minerals, such as sericite, chlorite, and the fibrous amphibole, parallel to the elongated fragments, forms a weak or incipient schistosity, referred to hereafter as S_1*. On the weathered surface this schistosity is evident as the alignment of the long directions of small siliceous fragments that weather in relief. This weak schistosity, which has a constant regional strike between 280 and 305 degrees and dips steeply, does not render the volcanic rocks fissile, except locally. As the shear zone is approached S_1 becomes more pronounced and better developed, and also veers in direction so that it becomes more parallel to the trend of the shear zone. (Figure 9a, page 58).

Chlorite-Sericite Schist (IS)

The volcanic rocks incorporated into the shear zone are altered to a chlorite-sericite schist composed of alternating layers of

* Both the planar and linear structural elements have been given symbols--see Chapter IV, page 54 for further information.

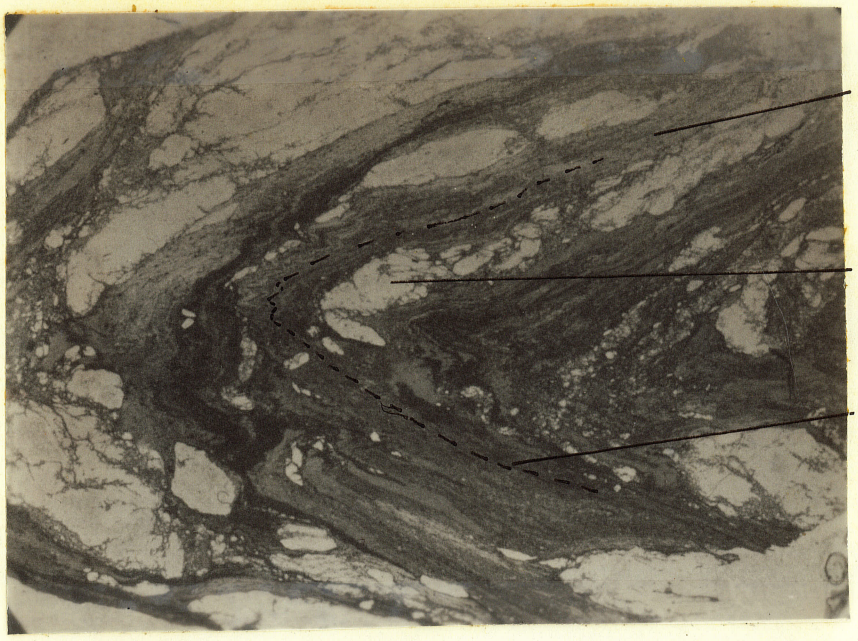

PLATE 7
Thin section photomicrograph of a chlorite-sericite-carbonate schist with folded disjointed quartz veinlets.

PLATE 8
Quartz stringers emanating from quartz feldspar porphyry dike intrude diabase dike.

Note: The compass points north in all pictures.

sericite, chlorite and albite, and albite and chlorite, impregnated by patches of ankerite and small lenses of quartz (Plate 7, page 25). The chlorite-sericite schist is generally crenulated and kinked. The volcanic rocks adjacent to the shear zone are altered to chlorite, sericite, and epidote or zoisite but have not developed a strong schistosity. These rocks have suffered a period of retrogressive metamorphism, associated with the formation of the shear zone and vein deposits, that has altered them to the greenschist metamorphic facies.

Diabase (2)

A diabase dike trending parallel to the shear zone is continuous along most of the length of the break. The diabase is a fine grained massive rock with a distinctive brown weathered surface. It is composed of a green fibrous amphibole, likely actinolite, with small proportions of plagioclase, chlorite, calcite, epidote, zoisite, leucocene, magnetite, ilmenite, pyrite, and chalcopyrite. The diabase is considerably altered to a mineral assemblage belonging to the epidote-amphibolite facies.

The intrusion of the dike preceded the conclusion of movements on the break and the dike has been rendered schistose for a large proportion of its length. The portions of the dike incorporated into the shear zone have been altered to a dark green chlorite schist (2S) having a rough weathered surface.

The diabase dike often has a sinuous contact with the volcanic rocks (Map 2) which could represent intrusion parallel to a contorted layering within the volcanic unit.

Quartz Feldspar Porphyry (3)

The porphyry dikes typically contain large zoned and twinned plagioclase phenocrysts (1 - 3 mm), quartz phenocrysts (1 - 2 mm), often hornblende and biotite phenocrysts, and a fine grained matrix composed of these minerals (Plate 10, page 29). Sericite, chlorite, calcite, and epidote are present as alteration products of these minerals.

The quartz feldspar porphyry dikes have a distinctive light cream colored weathered surface (Plates 8 & 9, pages 25 & 29). On fresh surfaces the porphyry dikes are dark or light grey in color depending on whether they have fine or coarse grained matrixes respectively.

Color, mineralogical and textural changes occur along or across the strike of individual dikes and are likely a result of variations in its cooling history.

The porphyry dikes may be altered to minerals of the epidote-amphibolite or also the greenschist facies (Plate 10, page 29). Often the margins of the porphyry dikes and adjacent host volcanic rocks are schistose over a width of a few feet (Map 2). The contacts of the dikes and the host volcanic rocks may also be sharp (Plate 11, page 32). In the schistose margins of the porphyry dikes the schistosity strikes parallel to the trend of the dikes and dips steeply. This relationship of the well developed schistosity to the contact suggests that the porphyry dikes also dip steeply.

The quartz feldspar porphyry dikes are offset by the shear zone. Portions of quartz feldspar porphyry dikes incorporated into the shear zone are highly altered to minerals of the greenschist facies and develop a strong schistosity. The quartz phenocrysts remain unaltered in the sheared quartz feldspar porphyry (3S) and protrude as small eyes that are a distinctive feature of the weathered

PLATE 9
Dark dacitic inclusions in quartz feldspar porphyry dike (note distinctive cream colored weathering surface of quartz feldspar porphyry dike).

PLATE 10
Thin section photomicrograph of quartz feldspar porphyry dike (10X, polarized light)

surface of this rock unit. Chemical analyses of the quartz feldspar porphyry and its sheared equivalent show that the altering processes accompanying the shearing have involved a decrease of SiO_2 accompanied by an increase of H_2O and CO_2 (Table 2, page 31).

Sedimentary Rocks

Zones of predominantly sedimentary material (Plates 27 & 28, page 52) have been recognized by N. Church (personal communication, 1968) within the Pilot-Smuggler shear zone. This material was previously considered by the author to be bands of mylonite and rocks with layering resulting from metamorphic segregation. Both metamorphic layering and cataclastic foliation do exist within the Pilot-Smuggler shear zone. However, the metamorphic layering is a discontinuous layering that consists of alternating layers of chlorite-albite, sericite, and sericite-chlorite a few millimeters in width; while the layering of the sedimentary rocks is continuous and often over a foot in width. In many instances metamorphic, cataclastic, and schistose foliations have developed parallel to the sedimentary layering. The sedimentary rocks have been contorted into many minor folds. Although the volcanic

TABLE 2

CHEMICAL ANALYSES OF TYPICAL ROCK TYPES

Rock Type:	SiO_2:	Al_2O_3:	Fe_2O_3:	FeO:	MgO:	CaO:	Na_2O:	K_2O:	H_2O:	CO_2:	TiO_2:	P_2O_5:	MnO:	Total:
Dacite (1)	59.10	19.24	0.91	4.08	2.72	7.14	2.70	0.83	1.69	0.16	0.75	0.32	0.09	99.73
Porphyritic Dacite (1)	64.05	15.62	1.88	2.84	2.81	4.16	5.14	1.44	0.89	0.18	0.60	0.23	0.06	99.90
Mildly Sheared Dacite(1S)	61.00	15.75	1.52	3.16	2.68	3.77	2.58	2.71	3.01	2.62	0.54	0.19	0.06	99.47
Diabase (2)	48.50	13.53	3.53	9.52	6.48	13.04	1.87	0.32	1.39	0.34	1.06	0.19	0.22	99.92
Mildly Sheared Diabase(2S)	49.05	14.62	6.25	6.88	6.25	10.33	1.15	0.08	2.96	0.37	1.19	0.18	0.21	99.52
Quartz Feldspar Porphyry(3)	67.85	15.36	2.13	0.96	2.02	3.62	4.75	1.49	0.85	0.35	0.30	0.21	0.04	99.93
Sheared Quartz Feldspar Porphyry (3S)	52.30	13.94	1.46	2.72	2.78	7.20	5.60	0.38	1.97	4.34	0.80	0.71	0.08	94.26

TABLE 2

CHEMICAL ANALYSES OF TYPICAL ROCK TYPES

PLATE II

Thin section photomicrograph of contact between a dacitic volcanic rock and a quartz feldspar porphyry dike. The plagioclase phenocrysts of the porphyry dike are zoned and twinned. The fine grained matrix is mildly altered to the epidote-amphibolite facies.

rocks also have been subjected to the same tectonic forces within the shear zone, folds and other minor structural features are not as obvious in the volcanic rocks as in the well layered sedimentary rocks.

The sedimentary rocks are not found outside the boundaries of the shear zone and are generally restricted to the northern portion of the Pilot-Smuggler break. The reason why the sedimentary rocks appear to be confined within the shear zone deserves further attention.

The geological units described above show an apparent horizontal offset that is right lateral. There are several geological features supporting a right lateral displacement on the shear zone, as follows:

(1) The fragmental rhyolite unit is displaced across the Pilot-Smuggler break and indicates a right lateral offset (Map 1).

(2) The regional schistosity, S_1, that has an average strike of 305 degrees and northeasterly dip of 78°, swings as it approaches the shear zone, in a manner that indicates a right lateral displacement (Figure 9a, page 58).

(3) The quartz feldspar porphyry dikes are drawn into the shear zone in a manner indicating a right lateral displacement (Map 2). An approximate tie-in of porphyry

PLATE 12
Fractured quartz vein: there are joints parallel to and perpendicular to the trend of the quartz vein, and a set of joints that cut diagonally across the quartz vein. The quartz vein parallels the shear zone.

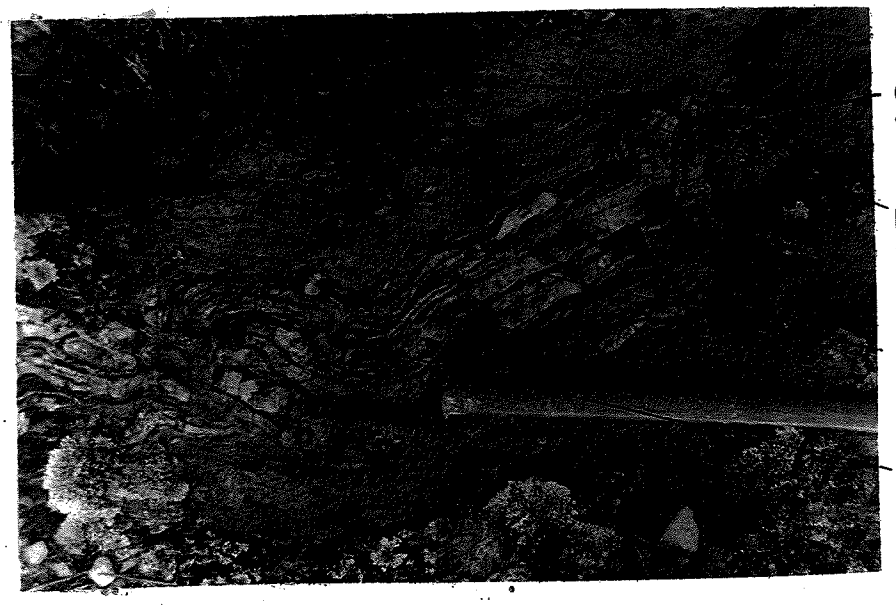

PLATE 13
Conjugately folded (F_2) quartz vein

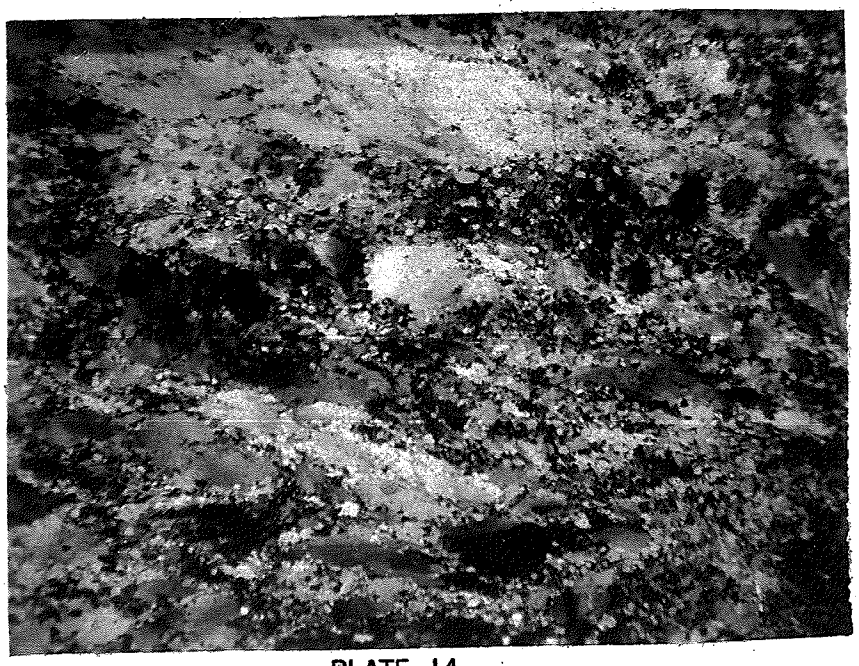

PLATE 14
Thin section photomicrograph of vein quartz showing a typical strongly developed cataclastic foliation (S_2) (10X, polarized light)

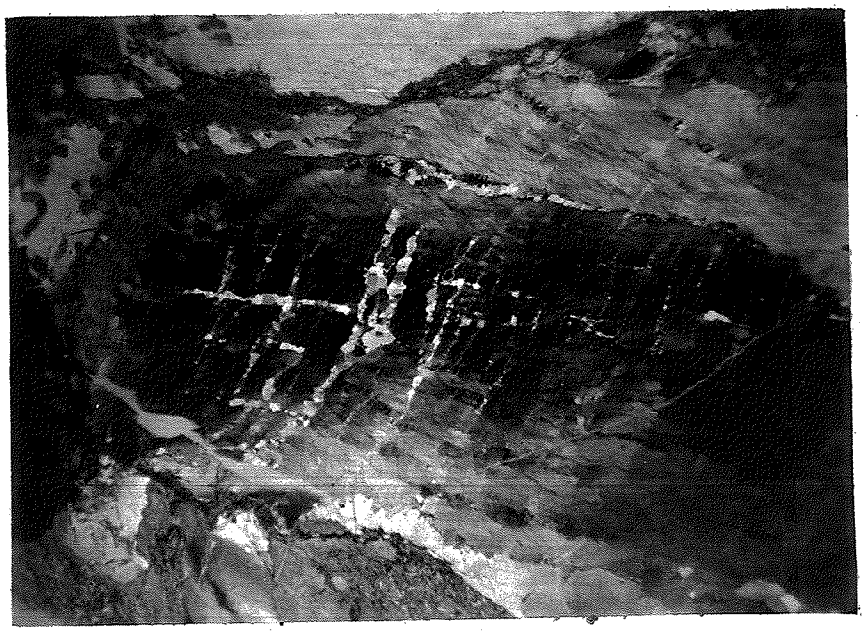

PLATE 15
Thin section photomicrograph of strained quartz showing cataclastic foliation (S_2) with recrystallization in shear and tension fractures. (100X, polarized light)

dikes across the shear zone is conceivable if a right lateral offset is assumed.

The mineralogy and general geological setting of the gold-bearing quartz veins is described in the following section. The minor structural features associated with the Pilot-Smuggler break are described in Chapter IV, page 50.

III. 4. Quartz Veins of the Pilot-Smuggler Shear Zone

The quartz veins are most numerous where the Pilot-Smuggler shear zone makes a slight swing in direction, near the site of the abandoned Gold Lake Mines Company Ltd. exploratory shafts. Surface trenching and test pitting on these quartz veins by the Gold Lake Mines Company indicated two ore zones. One was 315 feet long, averaging .424 ounces of gold per ton over a width of 5.4 feet, and the other 175 feet long, averaging .31 ounces per ton over a width of 3 feet (emens, 1936). A diamond drilling program in 1935 and underground development work in 1936, which included a 351 foot vertical shaft and 1,919 feet of lateral work on the 150 and 300 feet levels, indicated that the irregular and marginal ore shoots, indicated by surface work, did not continue at depth.

The gold-bearing quartz veins are irregular lenses, discontinuous veins, and pods that are strung out or aligned within, and parallel to the trend of, the shear zone. The largest vein traced was 75 feet in length with a maximum width of 5 feet (Map 2); most of the quartz veins are much smaller, usually only a few feet in length and one or two

PLATE 16

Mineralized quartz vein: Pyrite occurs as brecciated stringers, ankerite in patches, and quartz is ribboned by chlorite sericite schist. (IX)

PLATE 17

Brecciated pyrite: In polished sections these fractures are seen to be impregnated by quartz and other sulphide minerals. (IX)

feet in width. The quartz veins have been subjected to deformation since their emplacement. While the relatively incompetent volcanic rocks have developed a schistosity (S_2)* in response to shearing movements along the break, the competent quartz veins have developed a cataclastic foliation (Plates 13 & 14, pages 34 & 35). The veins are fractured (Plate 12, page 34) and are often interlaced with sheared enclosures of the host rock (see Frontispiece). Many of the lensoid quartz veins are sygmoidal in shape (Map 2, between 5+50N and 6+50N) and other veins have been contorted into conjugate folds (F_2) (Plate 13, page 34). Some of the quartz veins have developed boudinage structures whose long axes parallel the minor folds (F_2). The quartz veins may represent a single or two or more periods of emplacement, but the veins appear to have been emplaced prior to the conclusion of structural deformation which caused the development of the shear zone schistosity S_2.

The mineralogy of the quartz veins is simple; quartz, ferruginous carbonate (ankerite) and sulphide minerals (mainly pyrite) are present. The mineralogy of the quartz veins and associated sheared host rocks, has been examined in thin sections. The sulphide mineralogy and textures have been

* The symbols, representing structural features, are given here so information given in this chapter can be correlated to the discussion of the structural features in Chapter IV.

studied with a reflecting microscope. Ten polished sections were made for this latter study. Polished sections were difficult to prepare as the brecciated pyrite of the quart veins was often plucked from the polished surface during grinding.

The sheared volcanic rocks that host the quartz veins have been altered to a sericite-chlorite schist that is rich in ferruginous carbonate (Plate 7, page 25). A more detailed description of these rocks is given in Chapter V.

Small stringers of sulphides, dominantly pyrite, occur in fractures and as small pods within the quartz veins (Plates 16 & 17, page 37). The pyrite is brecciated (Figure 4a & Plates 18, 19 & 20, pages 42, 41 and 44), and quartz, in turn, impregnates the pyrite along fractures. It is possible this quartz, filling the fractures in the pyrite, was remobilized during the cataclasis of the quartz veins (Plate 14, page 35).

Samples were taken from the quartz veins near the Gold Lake Mines Company Ltd. shafts and assayed for gold (Table 3, page 40). The gold content of the quartz veins appears to be related directly to their sulphide content. A sample of quartz with no associated sulphides, assayed no gold, whereas a sample of almost pure sulphides assayed the highest gold content.

The sulphide samples collected for examination under the reflecting microscope were taken from the area near the exploratory shafts of the abandoned Gold Lake Mines Company

TABLE 3

GOLD ASSAYS

Location:	Sample Description:	Au (ounces/ton):	Au Value per ton @ $35/oz:
6+50N/0+76E	Highly fractured quartz vein - chalcopyrite is the dominant sulphide.	0.11	$ 3.85
3+40N/0+36E	Highly fractured quartz vein with stringers of brecciated pyrite (Plate 16, page)	0.31	10.85
'Mine' Tailings	Quartz vein with small brecciated stringers of pyrite.	0.17	5.95
3+25N/0+00E	Brecciated quartz and pyrite.	0.05	1.75
3+75N/0+10E	Brecciated pyrite	0.46	16.10
2+60N/0+10E	Cataclastic quartz vein (no associated sulphides).	Nil	Nil

Analysed by A. MacKay,
Chief Chemist, Mines
Branch Laboratory,
Province of Manitoba

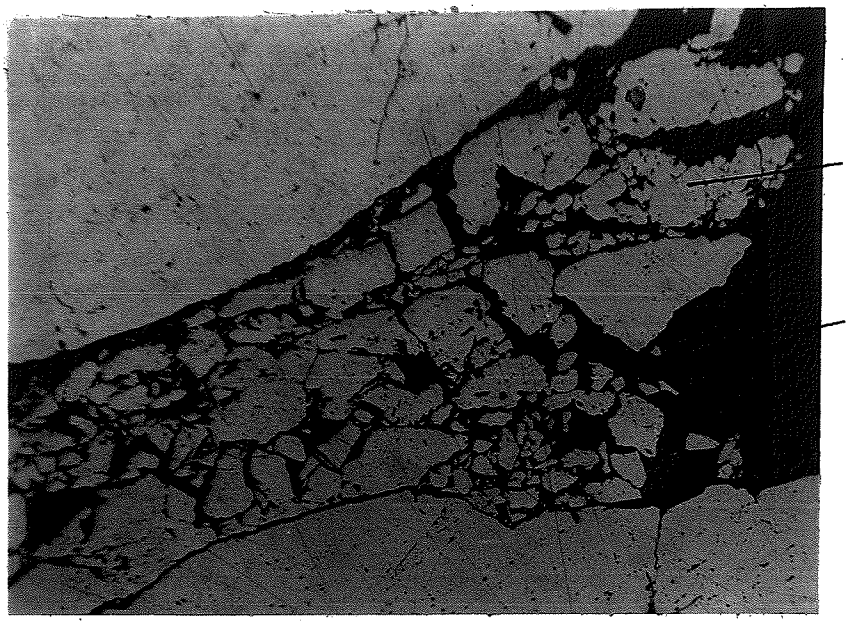

PLATE 18

Polished section photomicrograph of pyrite brecciated and veined by quartz. (50X)

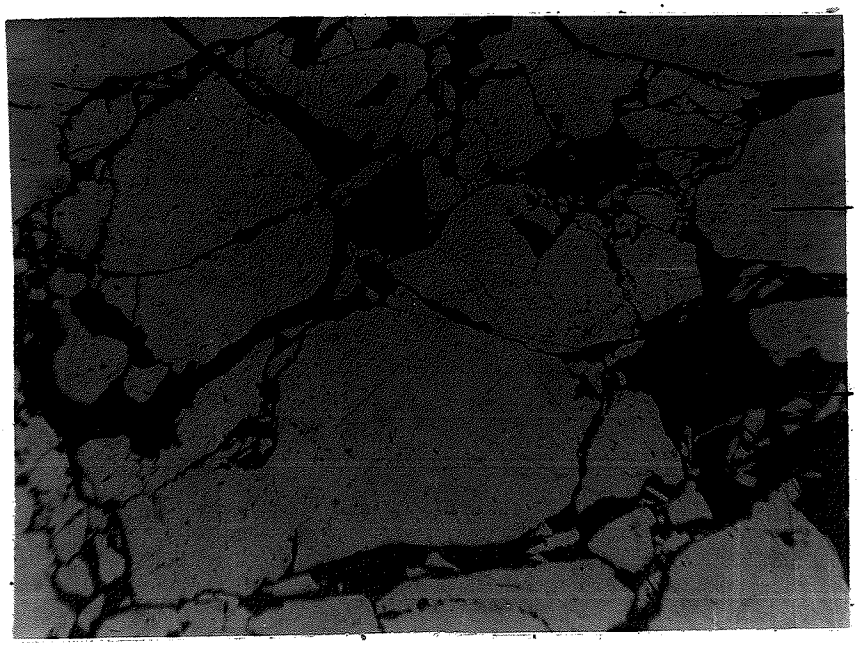

PLATE 19

Polished section photomicrograph of pyrite impregnated by quartz veinlets. (50X)

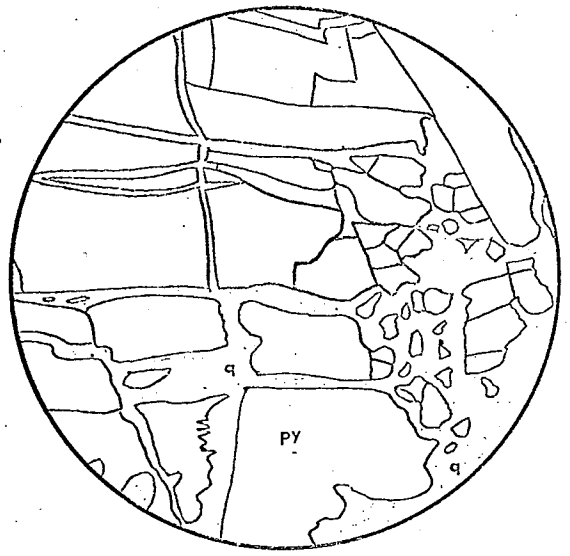

(a) Fractured pyrite cut by quartz stringers (32X).

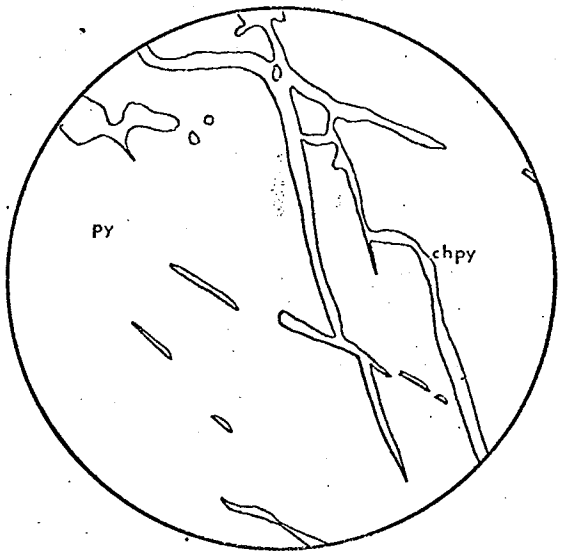

(b) Pyrite veined by chalcopyrite (1360X).

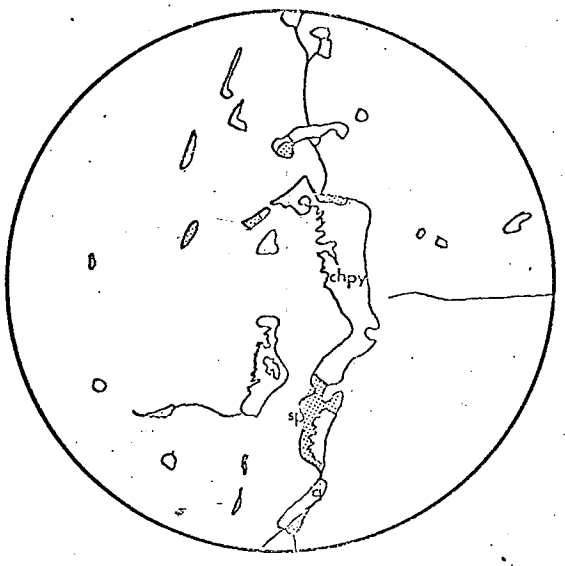

(c) Chalcopyrite and sphalerite as veinlets and 'blebs' in pyrite (225X).

(d) An exsolved 'bleb' in pyrite contains bornite, chalcocite, chalcopyrite and sphalerite (1360X).

FIGURE 4

Textures of sulphide minerals.

Figure 4 - continued:

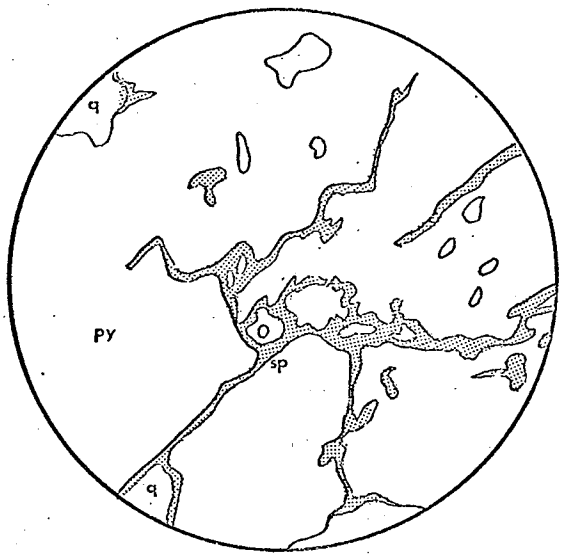

(e) Sphalerite veining pyrite (360X).

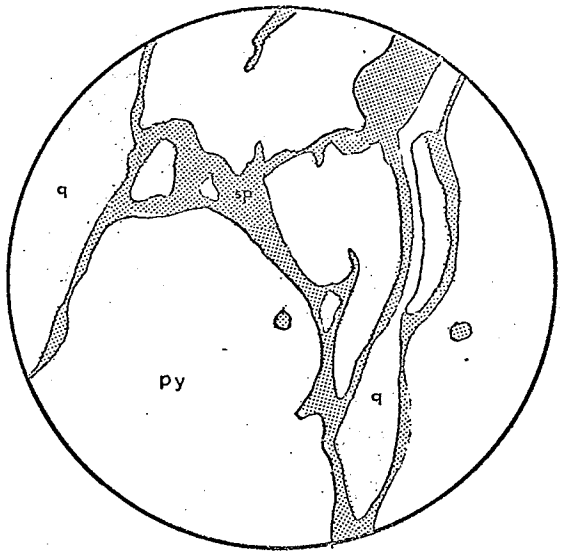

(f) Sphalerite veining pyrite - (Note - the sphalerite rims the quartz veinlets) (1360X).

Index to Symbols

- q - quartz
- py - pyrite
- chpy - chalcopyrite
- sp - sphalerite
- c - chalcocite
- po - pyrrhotite
- bo - bornite
- cov - covellite

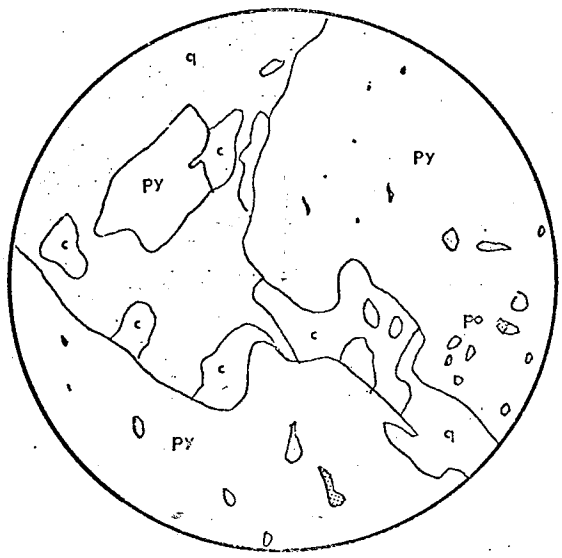

(g) Chalcocite within quartz impregnations in pyrite (270X).

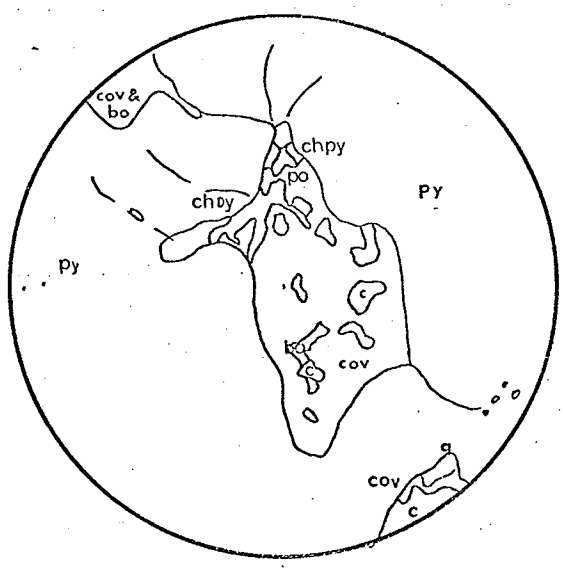

(h) An exsolution 'bleb' in pyrite contains an intimate mixture of covellite, bornite, chalcopyrite, pyrrhotite and chalcocite (680X).

FIGURE 4

Textures of sulphide minerals
(concluded)

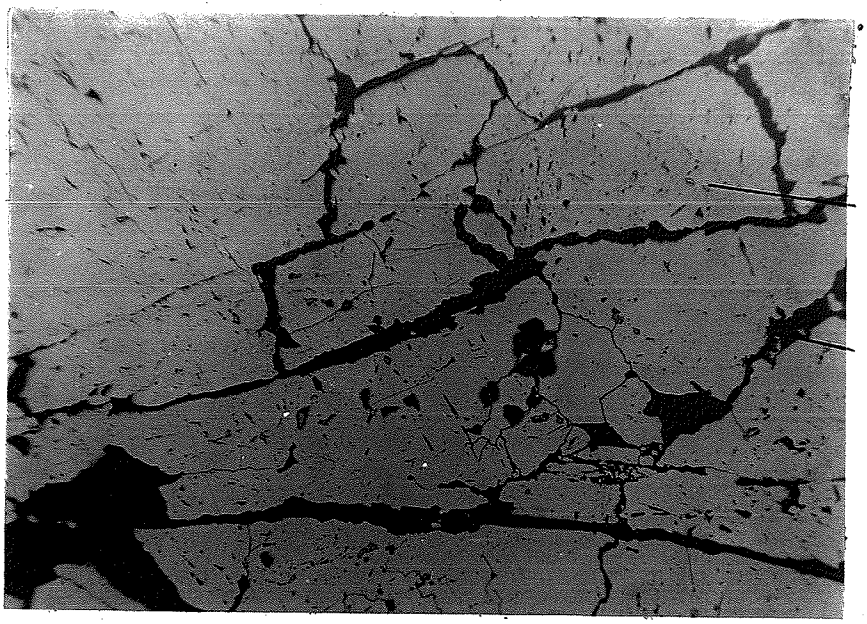

PLATE 20
Polished section photomicrograph of quartz veining brecciated pyrite. (50X)

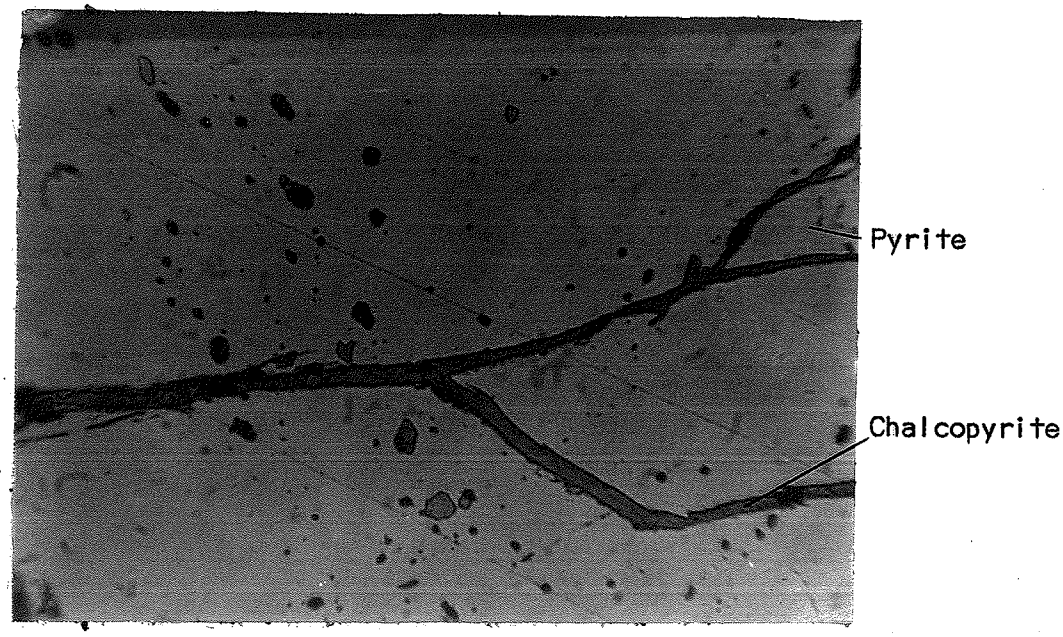

PLATE 21
Polished section photomicrograph of chalcopyrite as veins and small inclusions within the pyrite. (500X)

PLATE 22
Polished section photomicrograph of chalcopyrite that occurs as blebs and veinlets in pyrite (700X)

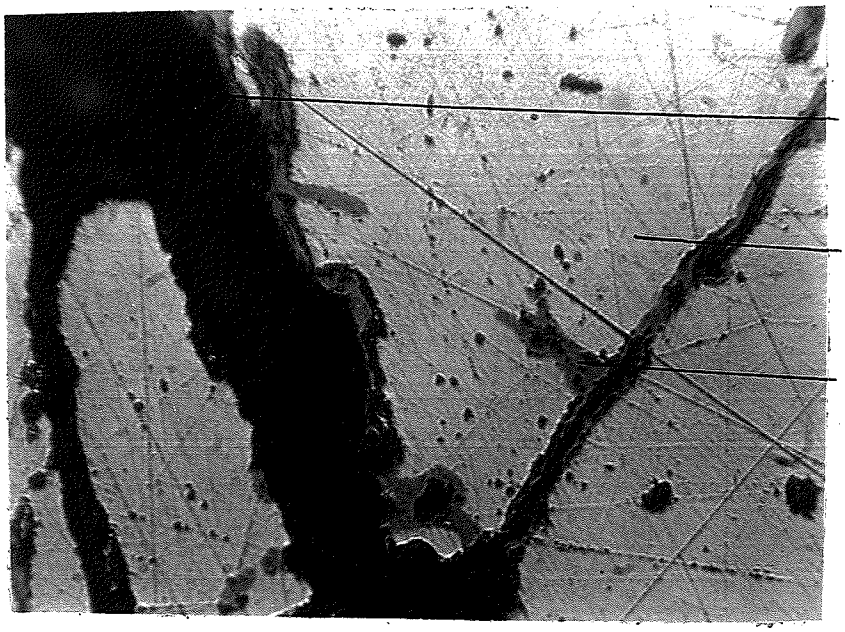

PLATE 23
Polished section photomicrograph of sphalerite veining pyrite. (1400X)

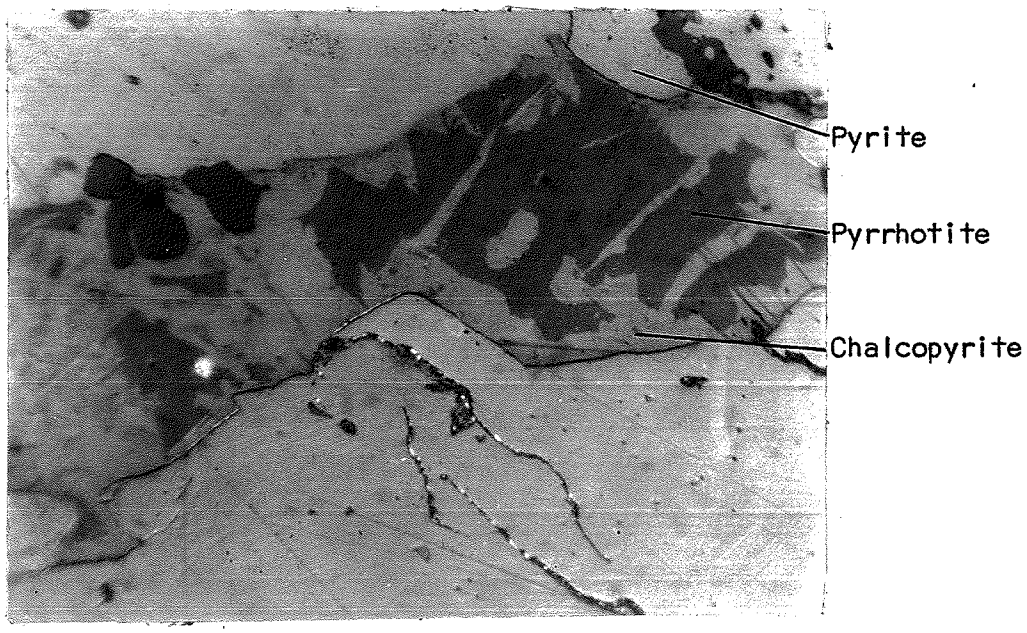

PLATE 24
Polished section photomicrograph of an inclusion of chalcopyrite (light grey) and pyrrhotite (dark grey) in pyrite. (1400X, polarized light)

PLATE 25
Polished section photomicrograph of chalcocite in quartz. (1400X)

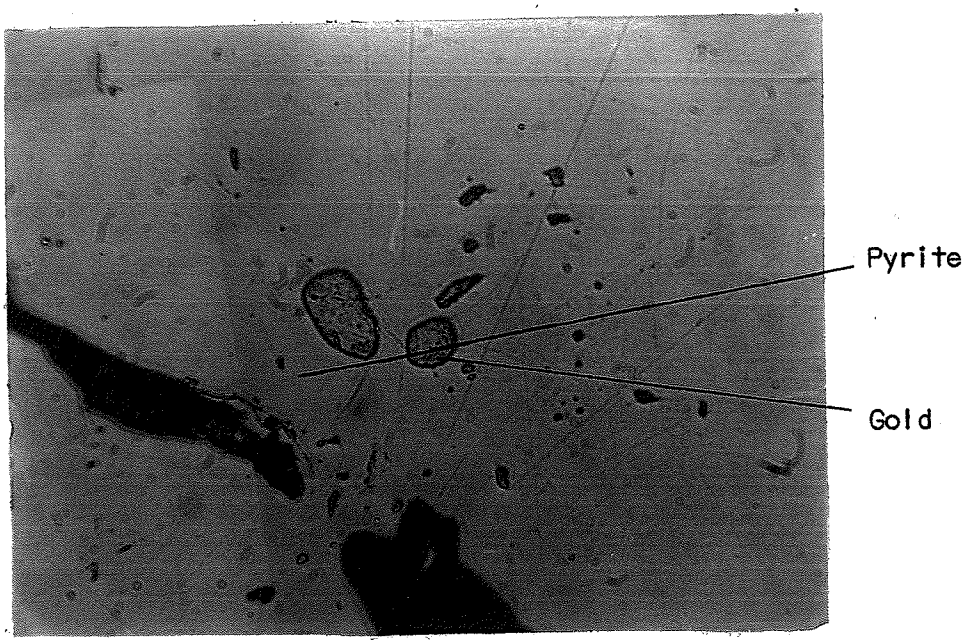

PLATE 26
Polished section photomicrograph of gold in pyrite. (1000X).

Ltd. The examination showed that pyrite is the major sulphide mineral; the other sulphide minerals constitute only one or two percent of the total sulphide content of the quartz veins. The pyrite is fractured and brecciated. Small veinlets of chalcopyrite, and occasionally sphalerite, occupy the tiny fractures in the pyrite (Figures 4a, e & f, and plates 21, 22 & 23, pages 42, 43, 44 & 45). The pyrite also contains many tiny blebs of chalcopyrite, sphalerite, pyrrhotite, and copper sulphides such as covellite, bornite, chalcocite and, possibly, tetrahedrite (Figures 4c, g & h and Plates 21, 22 & 24, pages 42,43, 44,45& 46). It is possible that these minerals, the metallic ions of which are compatible with the pyrite structure athigh temperatures, were exsolved from the pyrite structure during cooling and need not represent a second period of sulphide mineralization. Visible gold was observed only in one polished section, occurring in pyrite (Plate 26, page 47).

A positive identification of these sulphide minerals by chemical etch or hardness tests could not be made because of their small surface areas. Diffractograms and powder photographs of pyrite were made in an attempt to identify the minor sulphide minerals but, other than for pyrite, there were no identifiable patterns.

CHAPTER IV

STRUCTURAL GEOLOGY

IV. 1. Introduction

The Pilot-Smuggler shear zone is a north-northwesterly trending linear belt of steeply dipping sheared rocks that is approximately three miles long and an average of one hundred feet in width. The shear zone becomes diffuse and difficult to trace to the south and is terminated by a northwesterly trending shear zone to the north (Map 1).

This chapter outlines and describes the structural geology of the Pilot-Smuggler shear zone. The structural history of the shear zone, as indicated by the minor structural features, is quite complicated. The complexity of the internal structure of the shear zone was not fully realized at the time it was being mapped. The mapping that has been done and the structural data that has been collected serve to show the complexity of the structural geology but are not detailed enough to provide a good basis making any proper interpretation.

The orientations of planar and linear structural features of the shear zone were measured. A large percentage of the structural data that was collected comes from near the exploratory shafts of the Gold Lake Mines Company Limited, and this data has been plotted on Map 2. Structural data that was collected from the shear zone has also been plotted as stereographic diagrams.

The following section contains a description of the minor structural features, and the third section in this

chapter presents some possible interpretations of the structural geology of the shear zone.

IV. 2. Description of Minor Structural Features of the Pilot-Smuggler Shear Zone:

IV. 2A. Penetrative Planar Structures:

The varieties of penetrative planar structures are numerous. The penetrative planar surfaces are of two basic types. They may be a layering, where the surface is defined by compositional variation, or they may be a foliation, where the surface is defined by an internal fabric of the rock, usually the parallel orientation of platy and/or tabular minerals. A layering may be either a primary structure, that is formed at the same time as the rock, or it may be a secondary structure that was caused by later deformative forces. The penetrative planar structures encountered while mapping the Pilot-Smuggler shear zone structure are secondary features caused by deformation of the rocks. No primary structures were mapped in the volcanic rocks hosting the shear zone structure, and only in a few cases, within the shear zone structure, were thinly bedded silty sedimentary rocks found, and in these cases the primary layering was paralleled by secondary layering and foliation surfaces. Since the penetrative planar structures are formed by deformation of the rocks several varieties of penetrative planar surfaces may be formed by the equivalent deformative forces but may vary in type because of inhomogeneity of

of the rocks being deformed and because of local variations in the intensity of the deformative forces.

The description of the penetrative planar surfaces of the Pilot-Smuggler shear zone follows. It is presented in two parts. The first section briefly describes the varieties of penetrative planar surfaces into categories of surfaces, with similar orientations and age relationships, that were likely formed by the same set of deformative forces.

IV. 2A. (1) Varieties of Penetrative Planar Structures

(a) Layering:

bedding: This is a continuous layering, a few millimeters to a meter in width, observed in silty sedimentary rocks contained within the shear zone structure (Plate 28, page 52).

metamorphic layering: This is a discontinuous layering, a few millimeters in width, observed in rocks contained within the shear zone. This layering usually consists of alternating bands rich in sercite, chlorite and albite, and albite and chlorite (Plate 29, page 53).

transposed layering: This is a discontinuous layering resulting from the disruption and transposition of a prior layering into the movement plane of the disrupting forces. This variety of layering is found within the highly sheared rocks of the Pilot-Smuggler break.

(b) Foliation:

schistosity: This is a foliation defined by the parallel orientation of platy minerals. The volcanic rocks hosting the shear zone have a weak schistosity and the rocks contained within the shear zone have a well developed schistosity.

fracture and strain slip cleavage: The terms fracture and strain slip cleavage have been used in accordance with the definitions given by Turner and Weiss (1963). These are discrete surfaces of incipient transposition. The fracture cleavage is a parting independent of any planar preferred orientation of grain boundaries that

PLATE 27

Competent units (likely layers of sedimentary material) that have been folded and disjointed during formation of the shear zone.

PLATE 28

Minor 'S' folds, that characterize many portions of the Pilot-Smuggler shear zone, that deform sedimentary layering (1/2X)

PLATE 29
"Strain slip cleavage" that intersects
the shear zone schistosity

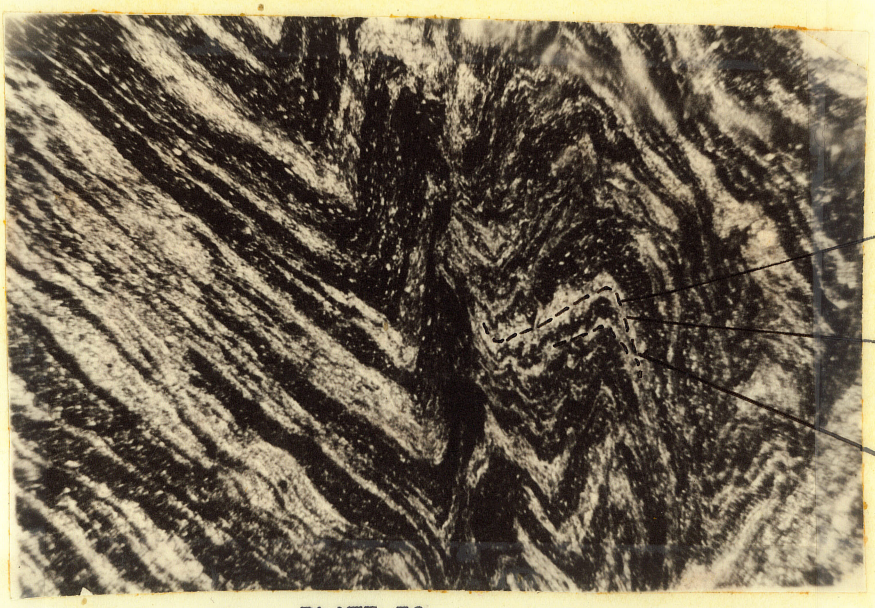

PLATE 30
Thin section photomicrograph of small chevron folds
that deform material composed of alternating layers
rich in chlorite-albite and sericite-albite
(10X, polarized light)

may exist in the rock while strain slip cleavage are surfaces of incipient transposition of pre-existing foliation surfaces in the rock (Plate 29, page 53). Two sets of fracture and strain slip cleavage are associated with the shear zone structure. One set occurs along the margins of the shear zone and the other within the central portions of the shear zone structure.

cataclastic foliation: The relatively more competent rocks, especially the quartz veins, have been finely brecciated by shearing movements and contain a well developed cataclastic foliation (Plates 13 to 15 inclusive, pages 34 & 35).

IV. 2A. (2) Categories of Penetrative Planar Structures

The penetrative planar structures have been grouped into categories on the basis of: (a) their orientations, and (b) their ages of formation, as suggested by crosscutting relationships. Three categories of s-surfaces have been distinguished, on the basis of these criteria, and have been designated as S_1, S_2 and S_3.*

S_1 This is a weak or incipient schistosity contained within the volcanic rocks that host the shear zone structure. This foliation, which is of regional extent, is the result of the parallelism of platy and tabular minerals, and, on a larger scale, of fragments of the volcanic rocks. The average orientation of S_1 is 305°/78°NE. This average orientation has been determined by taking the surface perpendicular to the density maxima of poles to S_1 as seen in Figure 5, page 55. The trend of the dacitic and rhyolitic units is parallel to this schistosity (Map 1).

* Note: A symbolic method of representing the structural features has been devised based upon that originated by Sanders (1950). The letters are coded as follows:

(S - penetrative planar structures
(F - minor fold axes
(L - linear structures
(A.P. - axial planes of folds
(J - joint surfaces

The numerals (example: S_1, S_2 and S_3) indicate the age of the indicated structure from earliest, S_1, to the most recent, S_3.

NOTE: Dots represent poles to s-surfaces

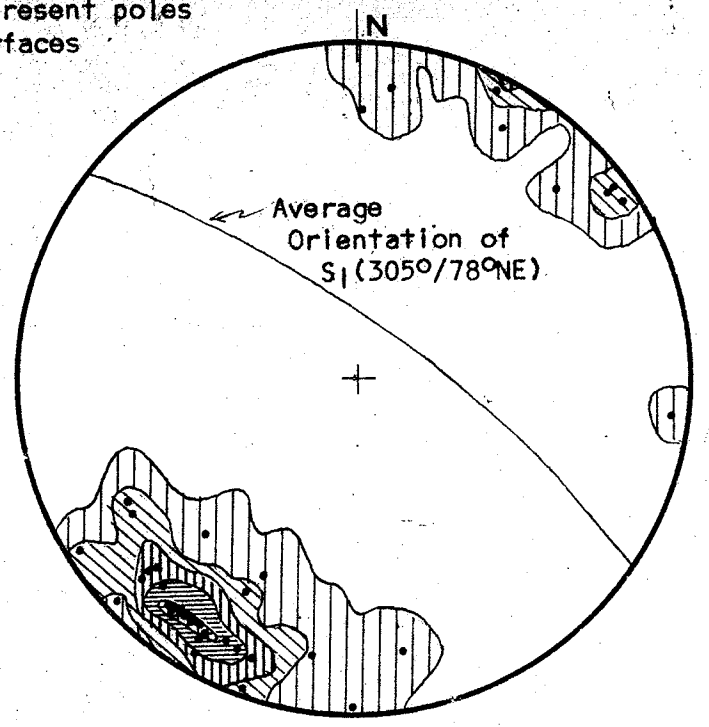

FIGURE 5
Contoured equal area stereographic plot of 41 poles S_1 (2-5-10-15-20% contours)

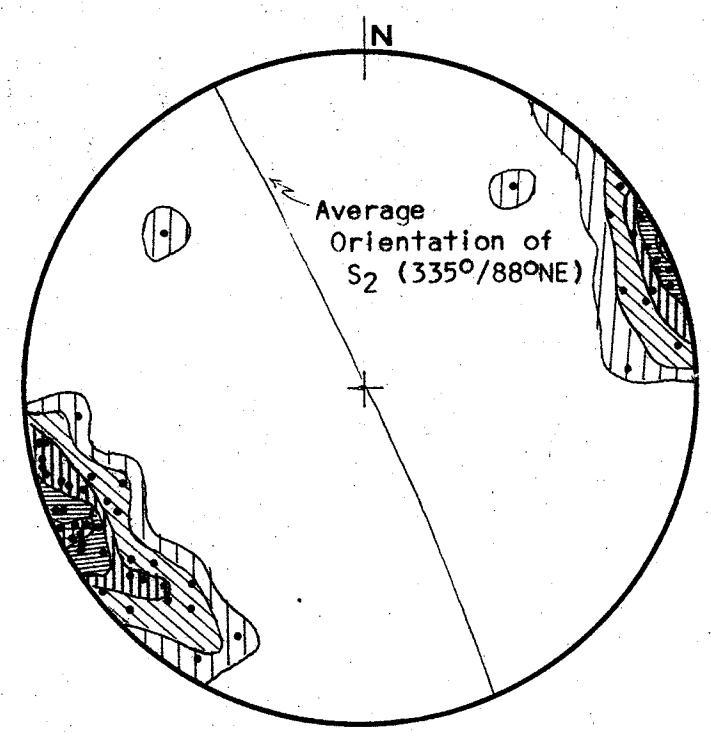

FIGURE 6
Contoured equal area stereographic plot of 59 poles to S_2 (2-5-10-15-25% contours)

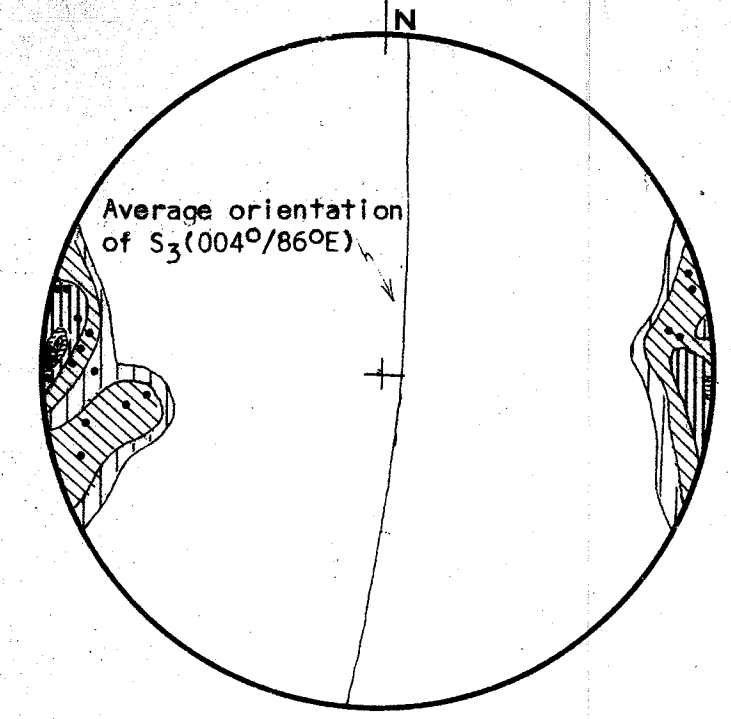

FIGURE 7
Contoured equal area stereographic plot of 18 poles to S_3(5-10-20-30-40% contours)

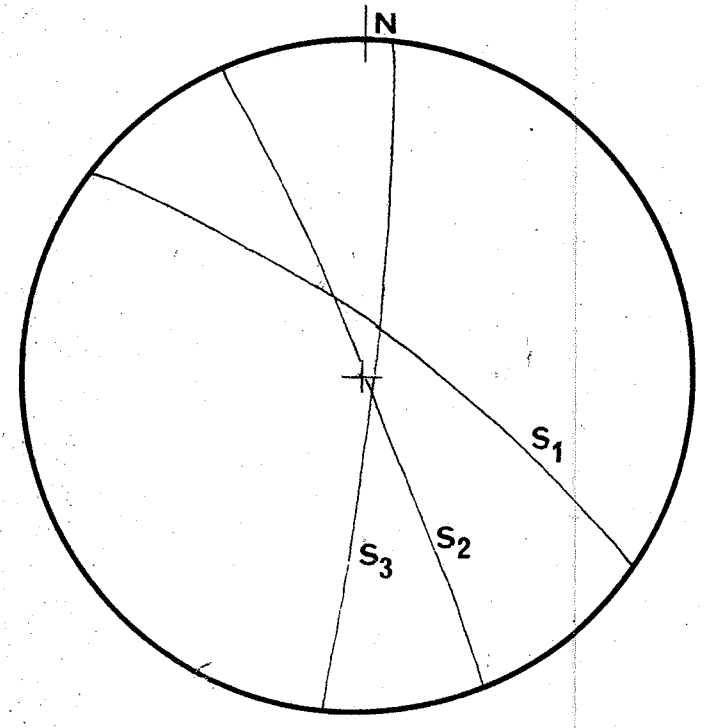

FIGURE 8
Synoptic stereographic plot of the average orientation of S_1, S_2, and S_3

FIGURES 5 - 8

STEREOGRAPHIC PLOTS OF S-SURFACES

S_2 — This is a well developed foliation and/or layering contained within, and approximately parallel to, the boundaries of the shear zone. It is often contorted by minor folds and kinks (Plate 30, page 53). S_2 cuts across and is therefore later than S_1. The average orientation of S_2 is 335°/88° NE. This orientation has been arrived at in the same manner as it was for S_1 (see Figure 6, page 55). Although by far the most typical S_2-surface is a schistosity, there are several other penetrative, planar surfaces that have been classed as S_2-surfaces; these include strain slip and fracture cleavage, cataclastic foliation, transposed layering and metamorphic layering. All these s-surfaces have been classed as S_2-surfaces because they have similar orientations, they often grade from one into the other both along and across strike, and beeause they all appear to have been the products of deformation relating tothe major movements or displacements along the shear zone structure. The S_2-surfaces, in the sedimentary rocks within the shear zone, have often formed parallel to the bedding planes but in other instances have cut and transposed this sedimentary layering.

S_3 — This is a surface of incipient transposition of S_2. It may be either a fracture or a strain slip cleavage. The fracture cleavage predominates in the relatively more massive rocks of the shear zone while the strain slip cleavage is restricted to the strongly foliated rocks. The S_3-surfaces occur within the strongly foliated rocks within the central portions of the shear zone. S_3 transects S_2 at a small angle. The average orientation of S_3 is 004°/86°E (Figure 7, page 55).

These three categories of s-surfaces have been distinguished largely on the basis of their orientation and their age of formation, as suggested by cross-cutting relationships. Each category of s-surfaces is also distinctive in its spatial relationship to the shear zone structure and in the varieties of penetrative surfaces that each category represents.

S_1 is a very weak foliation, that has been classed as a schistosity for lack of a better term, that is of

regional extent and occurs in the rocks outside the margins of the shear zone structure. This weak regional schistosity does not render the volcanic rocks fissile, except locally, and has an almost constant trend except near the shear zone where it swings in direction (Figure 9a, page 58) so that it approaches parallelism with the trend of the shear zone structure. It is as if the shear zone structure was initiated as a large kink of the S_1 schistosity which eventually ruptured along the s-surface, S_2. As the S_1 schistosity swings in direction near the margins of the shear zone it becomes more prominent, and better developed.

The surface, S_2, is confined to the shear zone structure. At the margins of the shear zone S_1 is cut by a strain slip and fracture cleavage, S_2, that develops into a strong schistosity towards the center of the shear zone. The strain slip cleavage, S_2, which disrupts S_1, is apparently a transitory stage in the development of the shear zone schistosity, S_2. Within the more competent rock units, such as the quartz veins, S_2 is typically a cataclastic foliation (Plates 14 and 15, page 35). A metamorphic layering is typical of the most strongly foliated rocks of the shear zone. In some cases, within the sedimentary rocks contained within the shear zone, the bedding has been transposed to form a new layering known as transposed bedding or transposed layering. The shear zone s-surfaces, S_2, make a small angle with the regional trend of the break (Figure 10). The poles to S_2-surfaces

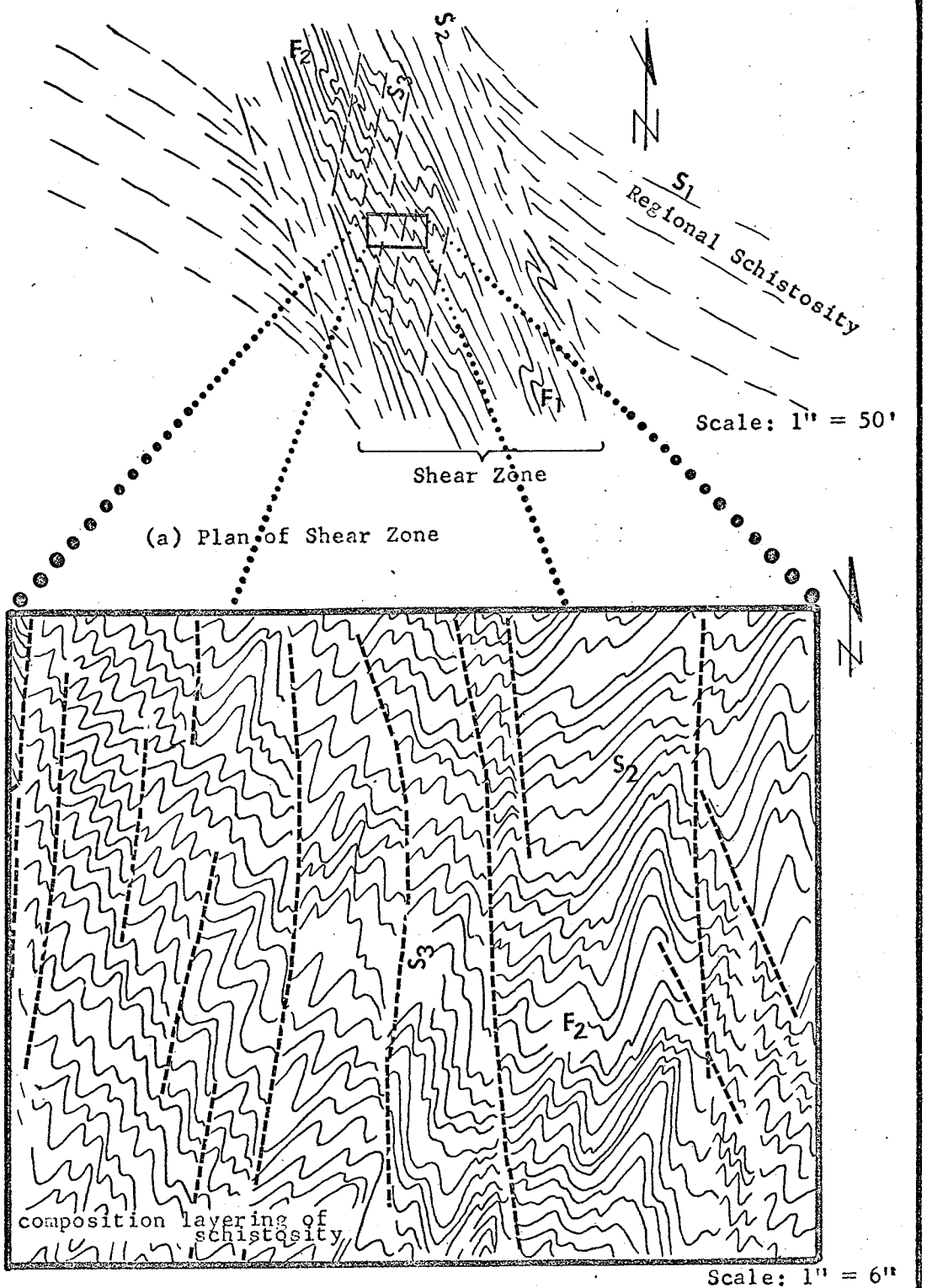

(b) Detailed Sketch of Steeply Plunging Minor Folds (F_2)

FIGURE 9

Steeply Plunging Minor Folds (F_2)

plot as a single maxima (Figure 6, page 55) which represents an average S_2-surface with a strike of 335° and a dip northeast of 88°, whereas the regional trend of the shear zone is more northerly than this average strike.

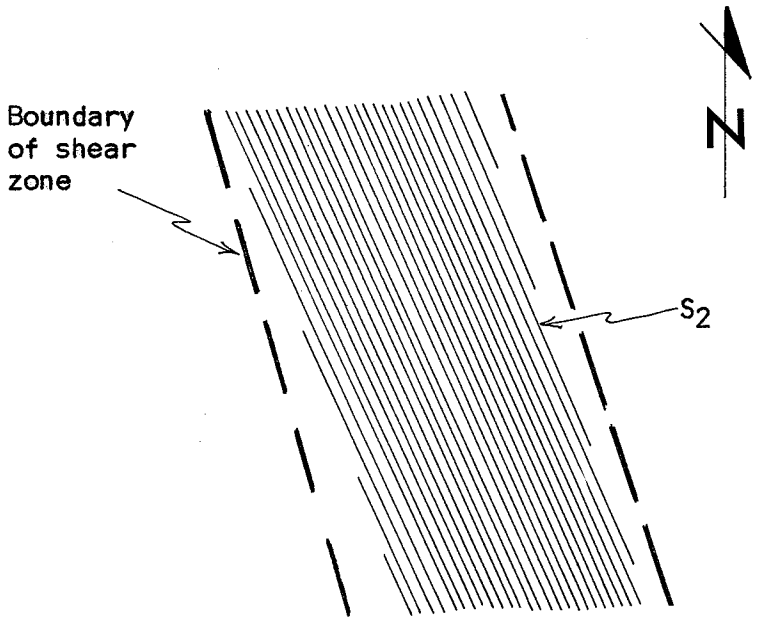

FIGURE 10

Diagramatic plan view showing trend of shear zone relative to strike of S_2.

The s-surface, S_3, is a surface of incipient transposition of S_2 (Plate 29, page 53). S_3, which is a surface of strain slip and fracture cleavage, is restricted to the strongly foliated rocks of the shear zone and is therefore found in the central portions of the shear zone. In this aspect especially it differs from the strain slip and fracture cleavage, S_2, which occurs only at the margins of the shear zone structure. The shear zone schistosity, S_2,

between the closely spaced partings of S_3, is crenulated. These crenulations are dominantly 'S' assymmetrical. (Figure 13f, page 62).

IV. 2B. Minor Folds and Linear Structures

The foliated rocks of the shear zone are deformed by many minor folds. The orientation of the axial planes and axes of these folds were measured and their style and geometrical symmetry noted. The assymmetrical folds have been described as either 'S' or 'Z' shaped. In the case of linear structures the plunge and azimuth were measured and the variety of the linear structure noted.

IV. 2B. (1) Minor Folds

The minor folds vary in size from small microcrenulations on schistosity surfaces to folds several feet in amplitude. The microcrenulations have been classed with the linear structures because only their linear element can be measured, however, their geometrical and genetic similarity to the larger fold structures is obvious.

There is considerable variation in types and orientations of folds contained within the shear zone structure. Based on their geometrical orientation, style and refolding relationships, the minor folds have been separated into two categories:

F_1 This is a group of shallow plunging tight 'Z' assymmetrical folds whose steeply dipping axial surfaces (which average 327°/72° NE - see Figure 11, page 61) are parallel to the trend of the shear zone schistosity (Figures 13a & b and Plate 31, pages 62 & 64). The F_1-folds are of the intrafolial variety. They have a tendency to become sheared parallel to their

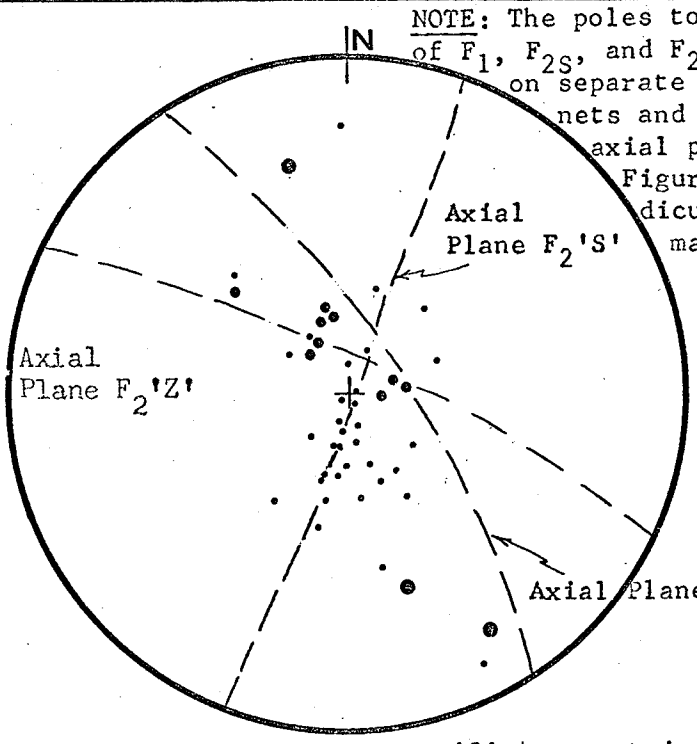

NOTE: The poles to the axial plane of F_1, F_{2S}, and F_{2Z} were plotted on separate stereographic nets and contoured. The axial planes shown on Figure 6 are perpendicular to the pole maxima.

FIGURE 11
A Stereographic Plot of Axes of Minor Folds.

- 'S' Assymmetrical Folds (F_2'S')
- 'Z' Assymmetrical Folds (F_2'Z')
- 'Z' Assymmetrical Folds (F_1) (shallow plunging)

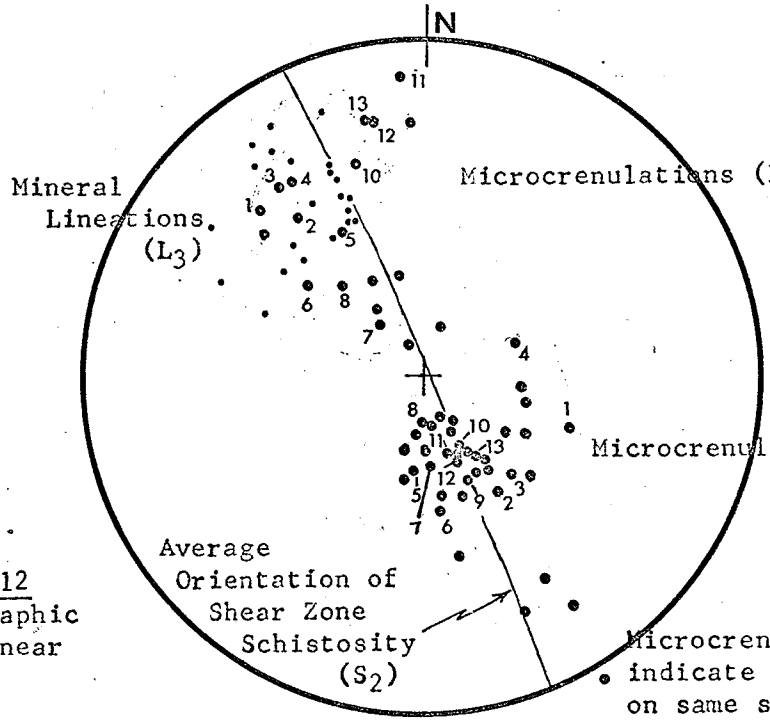

FIGURE 12
A Stereographic Plot of Linear Structures

- Microcrenulations (numbers indicate microcrenulations on same schistosity surface).
- Mineral lineations.

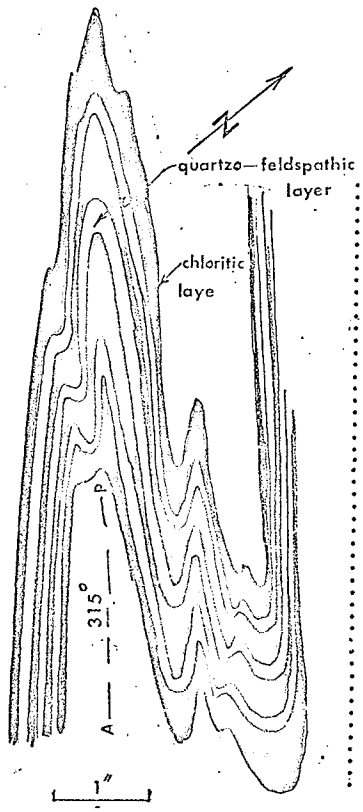

(a) A shallow plunging 'Z' assymmetrical fold (F_1) with alternating bands of chloritic and quartzo-feldspathic material.

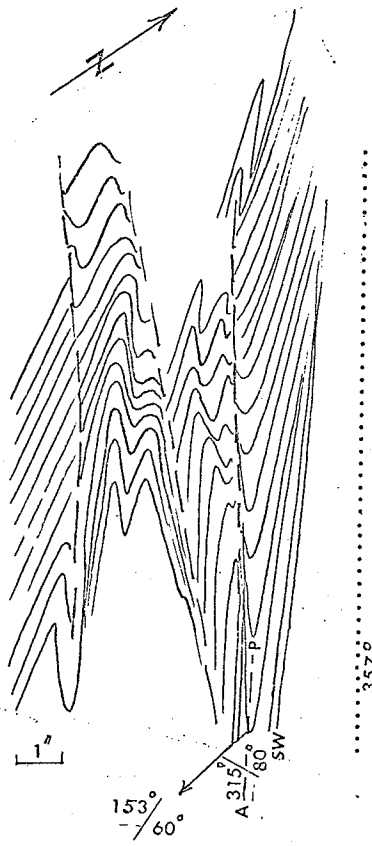

(b) A 'Z' assymmetrical fold (F_1).

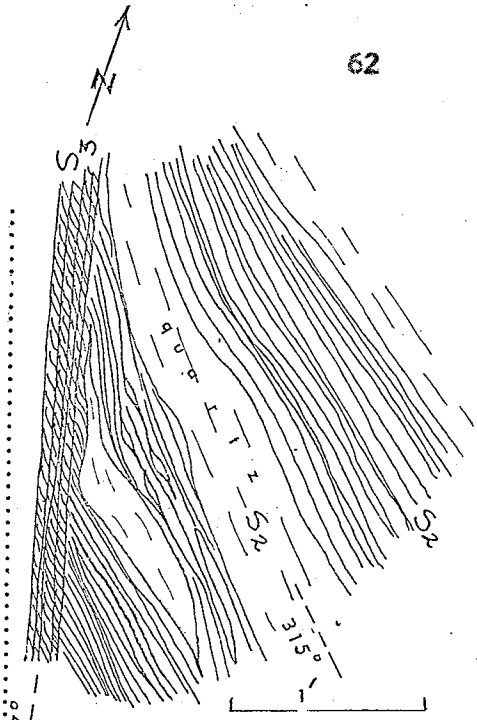

(c) Strain slip cleavage (S_3) transects and contorts shear zone schistosity (S_2) The quartz veins, which have a cataclastic foliation, are rotated by forces that caused strain slip cleavage.

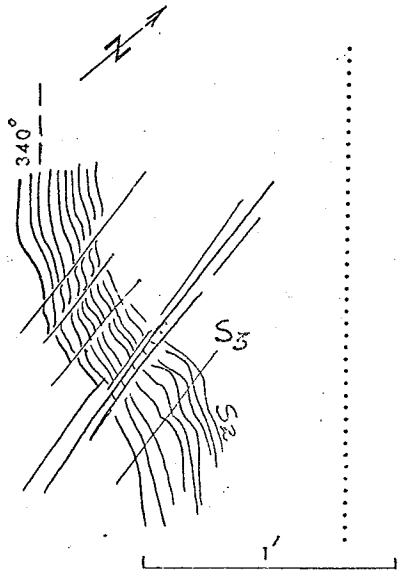

(d) Incipient strain slip cleavage (S_3) associated with minor 'S' folds (F_2).

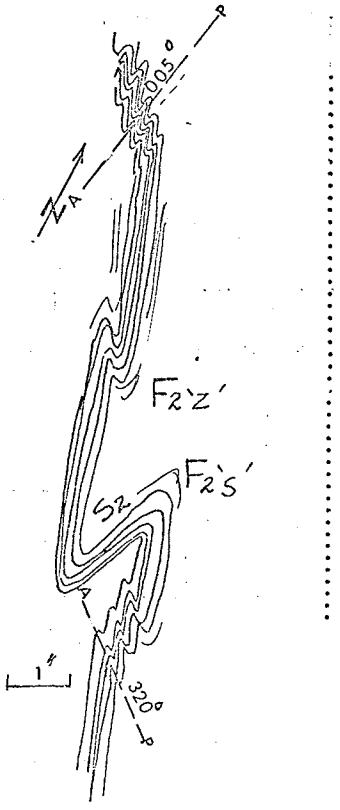

(e) A conjugate set of steeply plunging 'Z' and 'S' assymmetrical folds (F_2).

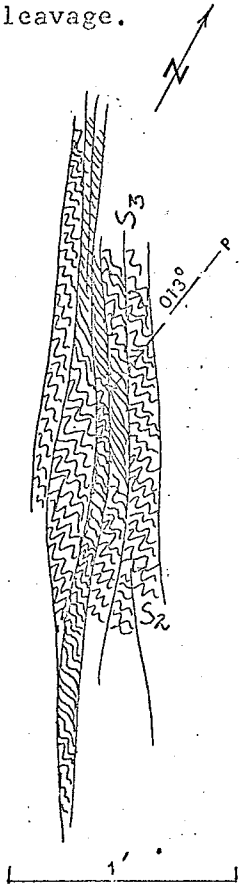

(f) Strain slip cleavage (S_3).

FIGURE 13 - MINOR FOLDS, PILOT-SNUGGLER SHEAR ZONE

axial planes. Folds of this group are generally found in the more competent rocks as they tend to become transposed and destroyed by movement along their axial planes in the less competent rocks.

F_2 This second group of folds deforms the surface, S_2, into kink, chevron, and conjugate folds. The F_2-folds are younger than the F_1-folds, which they refold. The F_2-folds include both 'S' and 'Z' assymmetrical folds, which belong to a conjugate set (Figure 13e and Plate 13, pages 62 & 34). Both sets of folds plunge steeply; the 'S' folds steeply south and the 'Z' folds usually steeply north. Most of the F_2-folds are 'S' assymmetrical with axial surfaces that have an average orientation of 019°/88° E. (Figures 9a and 11 and Plate 28, pages 58,61&52). The 'Z' folds have axial surfaces with an average orientation of 296°/78° N.

The F_1-folds are scarce and measurement of their orientation, especially their fold axes, is difficult as the fold hinges are rarely well exposed. Only three examples from this group of folds are plotted in Figure 11. The F_1-folds are most often found in the competent sedimentary layers. The F_2-folds, on the other hand, are very common. The 'S' and 'Z' folds of the conjugate fold system (F_2) both plunge steeply but their axes plot as two fairly distinct concentrations, as can be seen from Figure 11, page 61. The F_2-folds show a fairly wide range in orientation. Some of the F_2-folds plunge shallowly although most of them plunge steeply.

The F_2-folds are distinctly flexural in mechanism of formation. The F_2-folds may be kink, chevron and conjugate folds, which are typical of folds formed when strongly foliated rocks are deformed.

(a) A shallow plunging 'Z' assymmetrical fold (F_1) developed in a layer of quartzo-feldspathic sedimentary material.

(b) The sedimentary layer is contorted by many 'Z' assymmetrical folds. The lumbs of many of the folds are attenuated and the bedding becomes separated into structures similar to boudins.

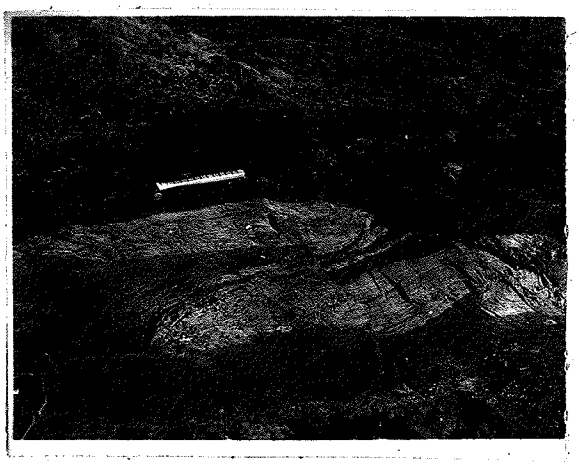

(c) The sedimentary layer has become transposed parallel to the axial plane of the fold until it is separated from the rest of the bed.

PLATE 31

A shallow plunging 'Z' assymmetrical fold (F_1) in a layer of sedimentary rock. (Photographs by H. Church)

IV. 2B. (2) Linear Structures

The linear structures found within the shear zone are of several types. The varieties of linear structures noted include mineral lineations, microcrenulations, intersection of s-surfaces, deformed clasts, and boudinage structures. Only the mineral lineations, an elongation or 'streaking out' of minerals in the plane of the schistosity (S_2), and the microcrenulations of the schistosity surface (S_2) were found in large numbers within the Pilot-Smuggler shear zone structure.

Three categories of linear structures have been distinguished. Two of these three categories are microcrenulations of the S_2-surface. Often on individual S_2-surfaces both of these categories of microcrenulations are present. The three categories of linear structures are:

L_1 — This is a group of microcrenulations that generally plunges shallowly to the north (average orientation is 324°/20°).* It is a very fine lineation that is often not more than a hairline on the schistosity surface, S_2.

L_2 — This is a second group of microcrenulations on the S_2-surface. These microcrenulations generally plunge steeply to the south (average orientation is 162°/62°). L_2 is generally a larger microcrenulation than L_1, and on surfaces where both lineations occur it is the more dominant of the two microcrenulations.

*Note: The L_1-lineations, as shown in Figure 12 (page 61), were density contoured and the maxima taken as the average orientation. This was also done to arrive at an average orientation for L_2.

PLATE 32

Thin section photomicrograph of minor folds (F_2). Light colored bands are sericite while darker bands consist of chlorite and albite.

(10X, polarized light)

L_3 This is a group of mineral lineations that plunges shallowly to the north (average orientation is $334^{o}/17^{o}$). These mineral lineations are always nearly perpendicular to L_2 on individual S_2-surfaces and appear to be the complementary 'a' lineations to L_2.

The microcrenulations cannot always be easily separated into the two groups, L_1 and L_2, because the orientations of the two groups of microcrenulations overlap somewhat. However if the microcrenulations L_1 and L_2 that have been measured from the same schistosity surface are plotted, as in Figure 12 (page 61), it is obvious the two groups of microcrenulations have quite distinctly different orientations with L_1-lineations generally plunging shallowly north while most of the L_2-lineations plunge steeply south.

The linear structures L_2 and L_3 are always very nearly perpendicular to one another on an individual S_2-surface, and as stated before the L_3-lineations appear to be 'a' lineations and the L_2-lineations appear to be 'b' lineations formed by the same set of deformative forces. The L_1 and L_2 lineations, on the other hand, which although their average orientations are perpendicular, are not always perpendicular on individual S_2-surfaces (Figure 12, page 61); nor do they bear any meaningful geometrical relationship to one another and therefore appear to be the products of two different stress systems.

Since the two microcrenulations, L_1 and L_2 are simply extremely small scale fold structures, they

should, and as expected do, bear geometrical and genetic similarity to the larger fold structures F_1 and F_2. The microcrenulations, L_1, and the minor folds, F_1, both plunge shallowly and are likely structural manifestations of the same system of deformative forces. This is difficult to substantiate properly since so few measurements of the F_1-folds, especially their axes, were taken that there is nothing to compare orientations of the L_1-lineations with. In the case of the L_2- and L_3-lineations, their geometrical and genetic connection to the F_2 fold structures is quite obvious. At each individual locality where structural measurements were taken, the L_2-lineations and the axes of the F_2-folds were coincident and the L_3-lineations were perpendicular to L_2 and F_2 within the plane of the folded S_2-surface. There is a continuous variation in size of the fold structures from the microcrenulations L_2 through to F_2-folds several feet in amplitude. The lineations, L_2, also show a similar distribution in orientations, as the F_2 ('S' and 'Z' assymmetrical) fold structures (Figures 11 and 12, page 61).

The much more limited occurence of L_1 than L_2 and the more variable orientation of L_1 than L_2 are taken as criteria indicating that L_1 was formed prior to the L_2-lineations. This is collaborated by the fact that the L_1-lineations are folded by the F_2-folds.

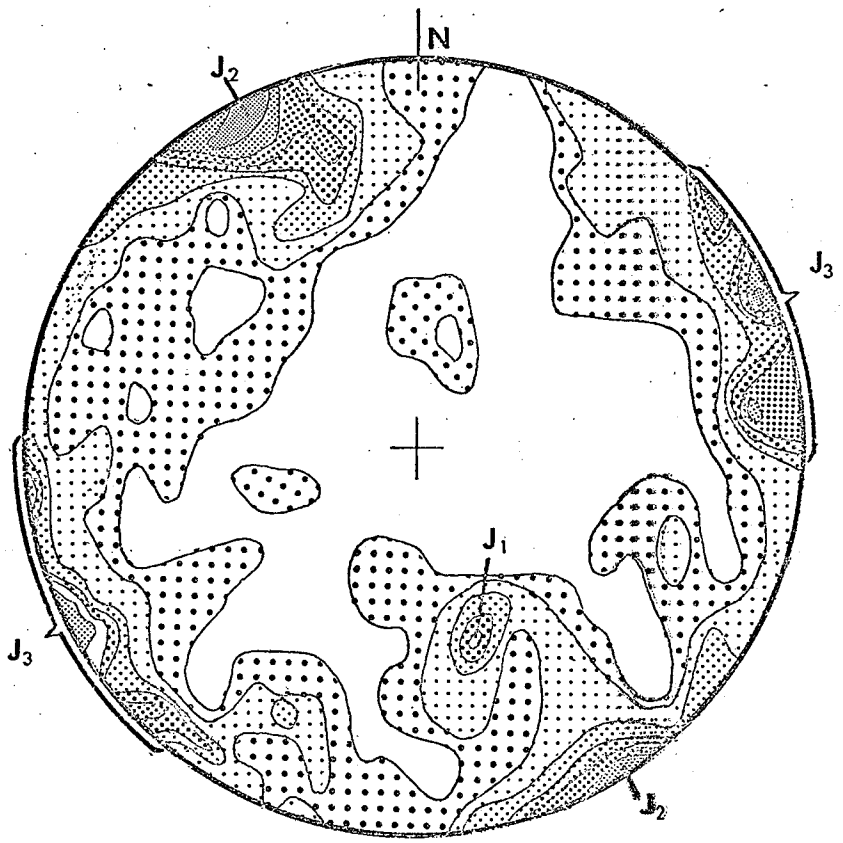

FIGURE 14

Contoured Equal Area Plot of Poles to 132 Joint Surfaces
(Contours of Percentage of Points per 1% Area)

½%	2½-3½%	5½-6½%
½-1½%	3½-4½%	6½%
1½-2½%	4½-5½%	

IV. 2C. Joints

Orientations and spacing intervals of joints within the shear zone and to a distance of several hundred feet on either side of the shear zone, were measured. On the assumption that the orientations and spacing intervals of joints would vary with their distance from the shear zone structure, the joints were plotted, with their spacing intervals indicated, for varying distances. However, no significant differences, with relation to distance from the shear zone, were evident and the joint surfaces have been plotted, regardless of their spacing or distance from the shear zone, and shown in Figure 14, page 69.

There are three distinct concentrations of poles to joint surfaces (Figure 14). Two sets of joints are perpendicular to the Pilot-Smuggler break; one set dips moderately to the north (J_1) and the other dips vertically (J_2). J_1 and J_2 are interpreted as being tension joints because they are perpendicular to the shear zone and the microcrenulations L_1 and L_2 are contained in the plane of the joints J_1 and J_2 respectively. The third system of joints consists of three closely grouped concentrations, that have been interpreted as being shear joints because they are subparallel to the shear zone structure.

IV. 3. Interpretation and Discussion of Structural Features of the Pilot-Smuggler Shear Zone:

It was stated at the beginning of this chapter that it is difficult to arrive at any well founded interpretations

of the structural history of the Pilot-Smuggler shear zone because there is not enough factual data. However, the remainder of this chapter outlines the most probable interpretation of the shear zone structure based on the limited data that is available. The interpetation given here is by no means considered proven. A more detailed structural study of this shear zone conbined with similar studies of other shear zones in the Rice Lake area should be done.

An interpretation of the structural history of the Pilot-Smuggler shear zone must be based on an understanding of the minor structural features that occur within the shear zone structure. The minor structural features, that were described in the previous section, can be separated into two categories on the basis of their orientations and age relationships:

1st category - S_2, F_1, L_1

2nd category - S_3, F_2 ('S' & 'Z'), L_2, L_3

These two groups of structural features can be interpreted as being the products of two, or possibly more, periods of deformation that have affected the Pilot-Smuggler shear zone. Within each of these groups, the structures bear a geometrical relationship that indicates they could be formed by the same set of deformative forces. The second category of structures are all later than those belonging to the first category; and as was evident from section IV. 2, the second category of structural features (S_3, F_2 ('S' & 'Z'), L_2, L_3) deform those belonging to the first category (S_2, F_1, L_1).

Figures 15A to 15C (pages73,74, &75) illustrate the possible mechanisms for the development of the Pilot-Smuggler shear zone. Each of the three figures includes a diagramatic plan view of the shear zone and also a stereographic plot that shows the average orientation of structural features shown in the diagramatic plan views. Figure 15A (page73) shows the Rice Lake series prior to formation of the shear zone. A schistosity, S_1, possibly related to an early period of folding of the Rice Lake series strikes west northwesterly.

Figure 15B, page 74, shows the shear zone structures following the development of the 1st category of minor structural features (S_2, F_1, L_1). The 1st category of minor structural features shown in the synoptic stereographic plot (Figure 15B) are outlined in red. These structures could be the products of the forces which initiated the Pilot-Smuggler shear zone and caused the major offsets on it. S_2 is a penetrative planar surface that has disrupted S_1. It is an s-surface that includes strain slip and fracture cleavage, schistosity, cataclastic foliation and layering, metamorphic layering and transposed layering; and it is a movement plane along which the major displacements of the shear zone structure took place. The joint surfaces J_1 and J_3 are tension and shear joints respectively formed by the shearing movements on the shear zone structure. The shallow plunging minor folds, F_1, and associated microcrenulations, L_1, have been formed by the movements on the shear zone. The F_1-folds are intrafolial folds that indicate an apparent horizontal right lateral movement has occurred;

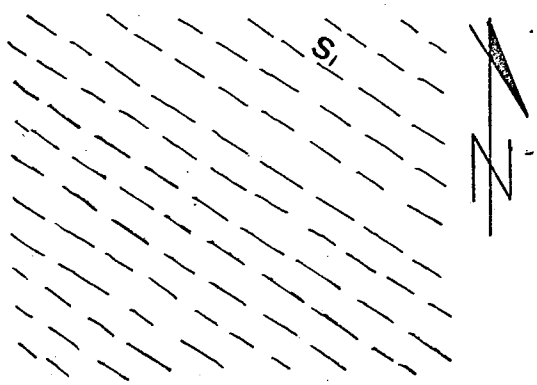

(a) Idealized Plan View of the Rice Lake series prior to rupture by the Pilot-Smuggler Shear zone.

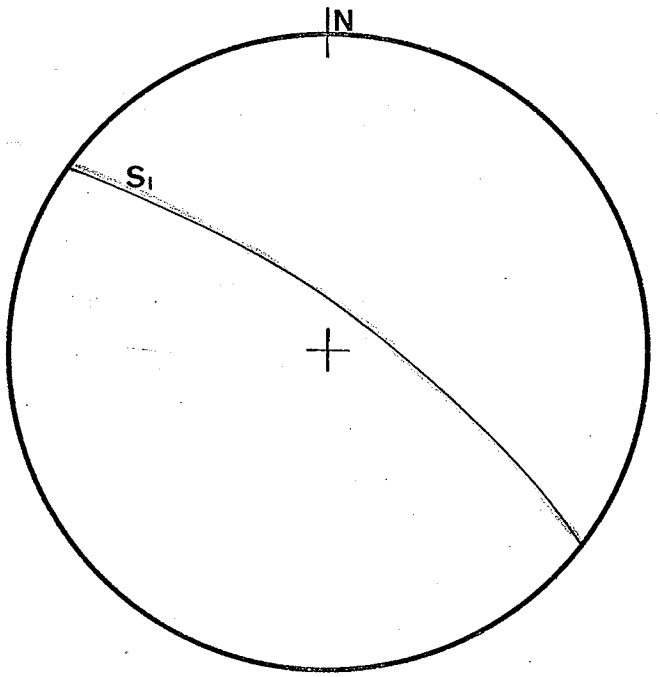

(b) Synoptic Stereographic Plot of Structural Features shown in (a)

FIGURE 15A
Idealized Evolution of Shear Zone Structures shown in Plan Views and Synoptic Stereographic Plots

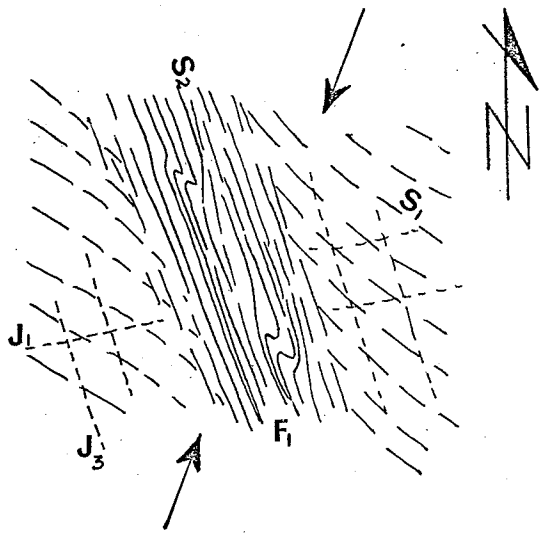

(a) Idealized plan view showing initial stage in development of the Pilot-Smuggler shear zone

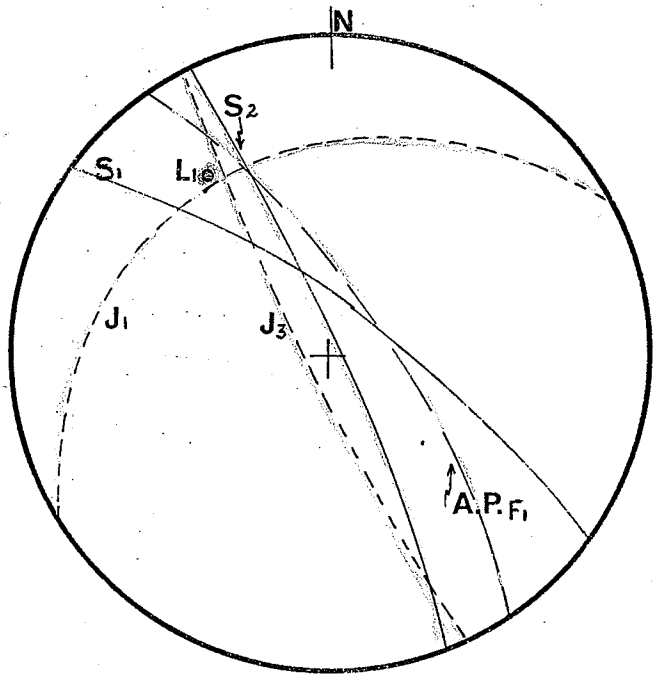

(b) Synoptic stereographic plot of structural features shown in (a)

FIGURE 15B

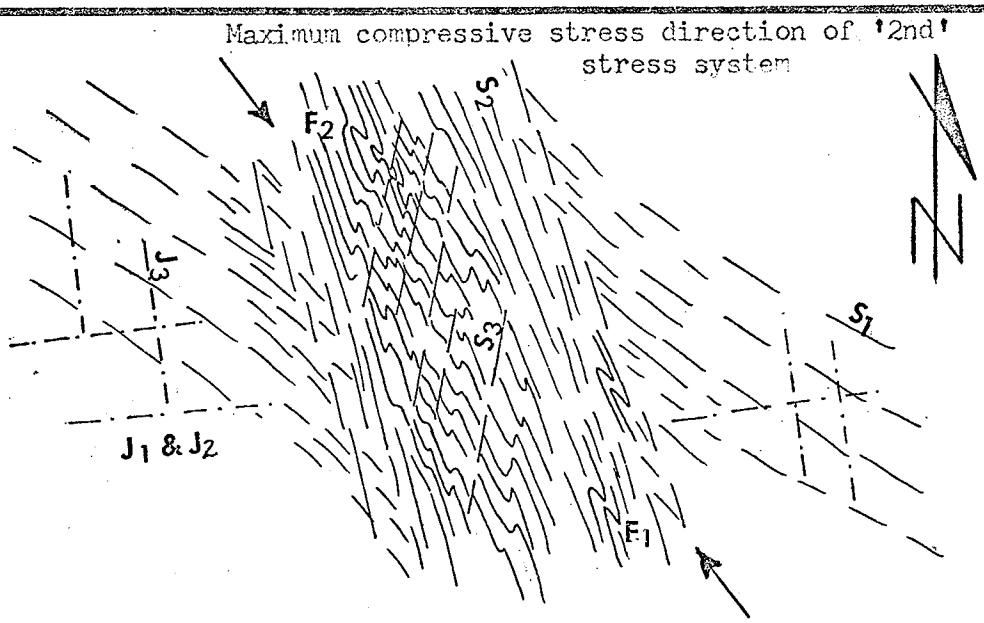

(a) Idealized Plan View of the Pilot-Smuggler Shear Zone Showing Structural Features

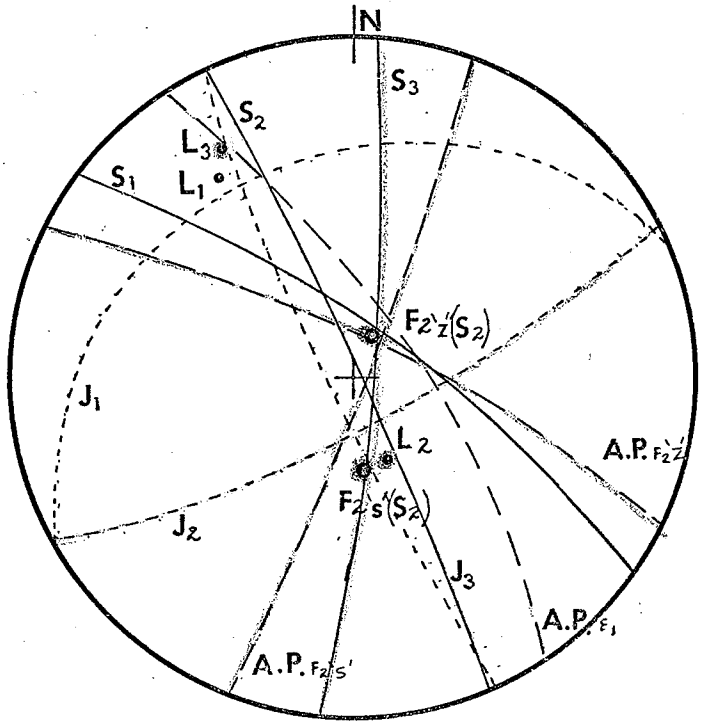

(b) Synoptic Stereographic Plot of Structural Features

FIGURE 15C

Average Orientations of Structural Features
Pilot-Smuggler Shear Zone

this is in agreement with the sense of movement indicated by geological features discussed in the latter part of Section III - 3.

The second category of structural features includes S_3, F_2, L_1 and L_3. These structural features, the most apparent being F_2 and S_3, contort the minor structures that belong to the first category and are therefore more recent than them. The second group of minor structures are closely related geometrically to one another (Figure 15C, page 75) and can be attributed to a single set of deformative forces. The s-surface, S_3, is a surface of incipient transposition of S_2 and intersects S_2 at a small angle. The schistosity, S_2, is crenulated into small 'S' assymmetrical folds between the surfaces of S_3 (Figure 13f, page 62). These small 'S' crenulations are part of a group of folded structures, F_2, that deform S_2 and range in size from microcrenulations, designated as L_2, to folds several feet in amplitude. The S_3-surface is generally parallel to the longer limbs of the 'S' assymmetrical folds, F_2, (Figure 9b, Page 58). The mineral lineation, which is perpendicular to L_2 and F_2('S') (Figure 15C, page 75) in the plane of the schistosity, S_2, represents the movement of 'a' strain axis of the folds, F_2.

The folds, F_2, which deform the shear zone schistosity vary in size and are both 'S' and 'Z' assymmetrical, although the 'S' folds predominate. The axes of the 'S' and 'Z' folds plunge in the plane of the S_3-surface, (the plane of incipient

transposition of S_2, Figure 15C, page 75); the 'S' folds plunge steeply south and the 'Z' folds steeply north. The 'S' and 'Z' folds are kink folds and conjugate kink folds (Figure 13e, page 62) which are similar to fold structures developed experimentally by Paterson and Weiss (1966) during the compression of highly schistose rocks parallel and subparallel to their schistosity (Figure 16, page 78). The schistose rocks of the shear zone may have been deformed in a manner similar to those in the experiments by Paterson and Weiss. Some of the conclusions reached by Paterson and Weiss during their experiments and which are relevant to the second category of minor structures of the Pilot-Smuggler shear zone are:

(1) The sharpness of a kink boundary depends upon the composition of the specimen. In very micaceous specimens the boundaries are sharp while in the more coarsely foliated, siliceous varieties boundaries are generally more diffuse and constitute a narrow zone of curvature.

(2) Where two kink bands of conjugate orientation approach each other, the foliation takes on the form of a conjugate fold (figure 16a, page 78).

(3) Specimens compressed parallel to their foliation tended to develop both sets of conjugate kinks, and consequently numerous conjugate folds, whereas specimens compressed subparallel to their foliation favored the development of one set of the conjugate kinks (Figure 16b, page 78).

FIGURE 16 Kinks and kink folds formed by compression subparallel to a previous foliation (after Paterson and Weiss, 1966)

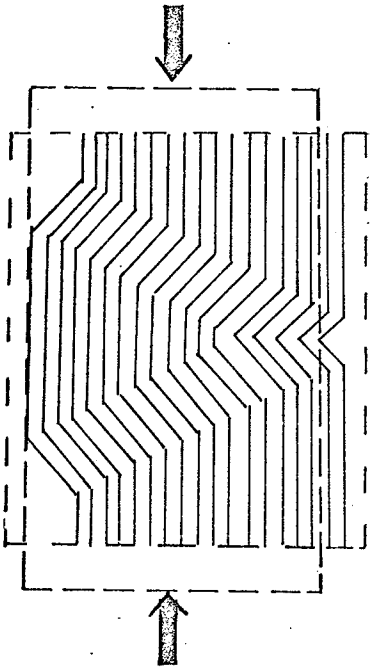

(a) Conjugate kinks formed by compression parallel to the foliation

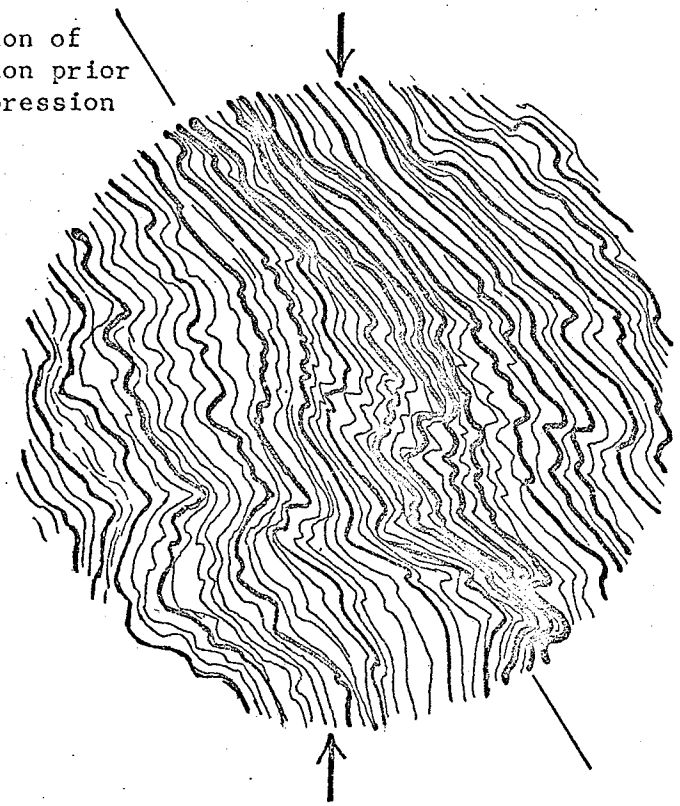

(b) Predominantly 'Z' assymmetrical kinks formed by compression subparallel to the foliation

(4) Specimens compressed at angles of 10 degree to their foliation deformed by kinking at compressive stresses lower than those compressed parallel to their foliation. These specimens preferably developed one set of kinks.

(5) Specimens compressed at angles greater than 25 degrees to their foliation deformed by planar gliding in preference to kinking. This angle appears to be the transition between deformation by planar gliding and kinking.

The kink and conjugate folds within the Pilot-Smuggler shear zone (Figures 9 & 13e, pages 58&62) are similar to the ideal kink folds and conjugate kink folds developed experimentally by Paterson and Weiss but are usually not as distinct and well developed because the rocks deformed are not always well foliated and are often siliceous. The 'S' assymmetrical kink folds by far predominate within the shear zone. This would suggest, by analogy to Figure 16b, page 78, a stress system with a shallow plunging principal compressive stress axis that is perpendicular to the axes of F_2 and L_2 and strikes between five and twenty degrees to the west of the north-northwesterly striking shear zone schistosity (see Figure 15a).

At least two periods of deformation have been indicated by the minor structural features. The emplacement of the gold-bearing quartz veins likely took place prior to the end of the first phase of deformation as many of the quartz veins have a strong cataclastic foliation, S_2 (Plates 14 & 15, page35), and definitely prior to the second phase of

deformation as many of them have been deformed into conjugate folds, F_2 (Plate 13, page 34).

To summarize, the Pilot-Smuggler shear zone has developed, as indicated by the interpretation of the minor structures, in two stages. During the initial stage the rupture and quartz veins were formed and during a second phase, possibly closely related to the first, the schistose rocks of the shear zone were kinked and folded by compression sub-parallel to the shear zone foliation, S_2.

IV. 4. General Discussion of Structure and Age Relationships of Geological Features of the Rice Lake area.

The Pilot-Smuggler shear zone structure is one of many such shear and fracture zones in the Rice Lake area. The shear and fracture zones and attendant gold-bearing quartz veins, are localized to the east and west of a large oval-shaped body of quartz diorite (Figure 2, page 4). The shear and fracture zones belong to two sets; one set strikes east-northeast and the other north-northwest. The east-northeast trending set dips steeply to the east. The apparent lateral horizontal offsets on the two groups of shear zones are in the opposite sense; the north-northwest set has a right lateral offset and the northeast trending set has an apparent horizontal left lateral offset (Stockwell, 1938 & Davies, 1953). The two sets appear to have developed contemporaneously, although over a considerable period of time, since the north-northwest set displaces the north-northeast set, and vice versa. Both C.H.Stockwell

1938 and J.F. Davies (1953) consider these two sets of shear zones to belong to a conjugate set that has resulted from a stress system with a north-northeast trending shallow plunging axis of principal compressive stress (Figure 17, page 82).

The quartz feldspar porphyry dikes, emanating from the quartz diorite intrusion, generally trend perpendicular to the shear zones. C.H.Stockwell (1938) has suggested that these porphyry dikes have been intruded along tension fractures perpendicular to the shear zones. If this is so, the shear zones are either older than, or contemporaneous with, the emplacement of the quartz diorite body. The porphyry dikes would appear to the author, however, to have been offset by, and therefore be older than, the shear zones.

The Rice Lake series of volcanic and sedimentary rocks to the east and west of, and adjacent to, the quartz diorite body, are essentially undeformed. These areas appear to be 'pressure shadows' that were protected from deformation by the competent quartz diorite. The Rice Lake series have been deformed since the intrusion of the quartz diorite body.

The Rice Lake series, east of the oval-shapped intrusion of quartz diorite, and the San Antonio formation west of the quartz diorite body, are folded in an east-southeasterly direction. (Stockwell, 1938). It is likely that this represents an east-southeasterly folding phase that deformed the whole Rice Lake series. Since the San Antonio formation is younger than the quartz diorite intrusion, this defor-

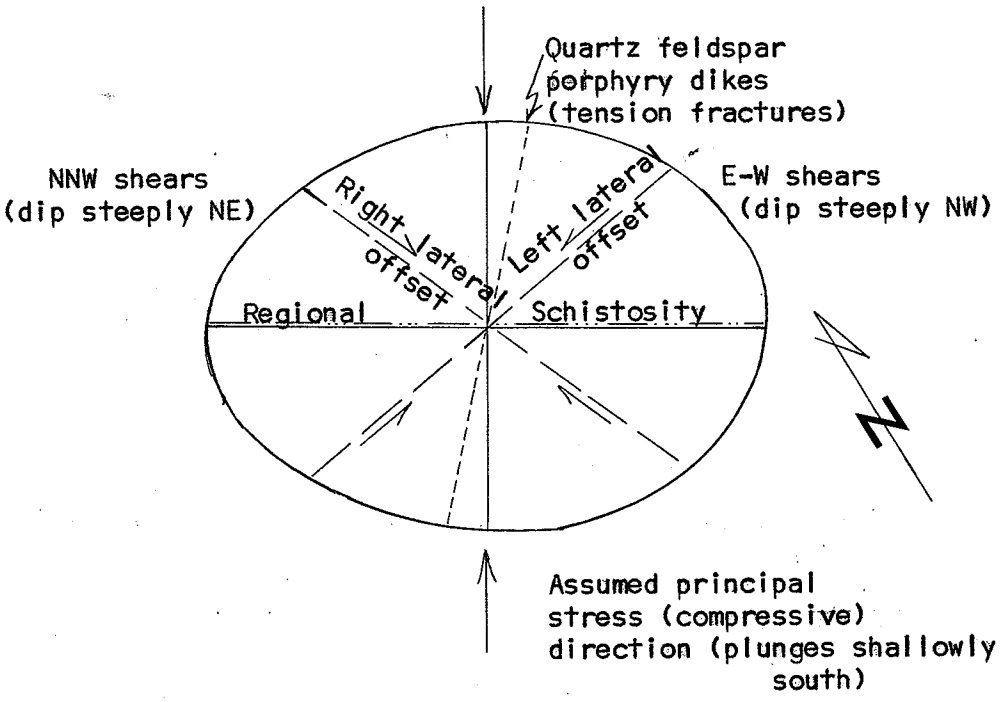

FIGURE 17

Representation of Structure South of Rice Lake by Strain Ellipsoid. (after Davies, 1953)

mation phase has occurred since the emplacement of the quartz diorite body. It is possible that the quartz diorite body acted as a buttress as was previously suggested, during this deformation and caused the shear and fracture zones to be localized nearby. If this is the case, the quartz diorite body, the most obvious source for magmatically derived hydrothermal solutions that could have deposited the gold-bearing quartz veins within the shear zones, must have been emplaced prior to the formation of these deposits and an alternative source for the gold has to be determined. An investigation of the structure and age of shear zones, as related to the quartz diorite, is a subject that deserves attention.

CHAPTER V.

GEOCHEMISTRY of the GOLD-BEARING QUARTZ VEINS

V. 1. Introduction

The quartz veins are one of the by-products of the tectonic forces that caused the formation of the shear zone structure. The quartz veins, as indicated in the discussion of the structural history of the shear zone, in the previous chapter, were emplaced during the deformation that initiated the shear zone and caused the major movements on the break. In order to better understand the mechanism of formation of the quartz vein deposits, the rocks hosting the quartz veins have been carefully examined in the field, studied in thin section and chemically analyzed.

The following three sections describe the alteration of the rocks hosting the quartz veins as determined in thin section, the distribution of the major and minor elements as related to the quartz veins and alteration zones, and, finally, a discussion of possible mechanisms of formation of the gold-bearing quartz veins.

V. 2. Description of Wall Rock Alteration

A suite of rock specimens were collected across the shear zone and attendant quartz veins along the grid line 3+50N (Map 2). These specimens along with specimens from other locations have been thin sectioned and chemically analyzed.

Chemical analysis of the volcanic rocks hosting the

shear zone, near the exploratory shafts of the Gold Lake Mine Company Ltd., indicates that they are ryhodacites and dacites (Table 2, page 31). These volcanic rocks are composed of a green fibrous amphibole (likely tremolite or actinolite), a fine feldspar matrix and plagioclase phenocrysts (oligoclase to andesine), accompanied by smaller proportions of brown biotite and dispersed alteration consisting of a mixture of epidote, chlorite, carbonate and sericite.

Table 4, page 86 shows a rough visual estimate of the percentages of constituent minerals, as determined in thin section, of the rock samples taken across the shear zone along the grid line 3+50N. Three zones of alteration are outlined that are related spatially to the quartz veins. The quartz veins are enveloped by the sericite-chlorite-carbonate schist of the shear zone. The volcanic host rocks flanking the shear zone structure are partially altered to the greenschist facies, while the volcanic rocks, unaffected by the altering processes associated with the shear zone, belong to the epidote-amphibolite facies.

A suggested sequence of steps of alteration of the volcanic rocks hosting the quartz veins is given by the Chemical equations shown below:

Epidote Amphibolite Facies: Greenschist Facies:

$$4CaAl_2Si_2O_8 + H_2O \rightleftharpoons 2Ca_2Al_3Si_3O_{12}(OH) + Al_2O_3 + 2SiO_2 + O_2$$
(plagioclase) (epidote)

$$Ca_2(Mg,Fe^2)_5Si_8O_{22}(OH)_2 \rightleftharpoons 6Ca_2Al_3Si_2O_{12}(OH) +$$
(tremolite) (epidote

$$+ 10CaAl_2Si_2O_8 + 6H_2O \quad (Mf,Fe)_5Al_2Si_3O_{10}(OH)_8 + 7SiO_2$$
(anorthite) (chlorite)

$$3Ca_2(Mg,Fe)_5Si_8O_{22}(OH)_2 \rightleftharpoons 3(Mg,Fe)_5Al_2Si_8O_{10}(OH)_8 + 10CaCO_3$$
(tremolite) (Chlorite)

$$+2Ca_2Al_3Si_3O_{12}(OH) + \quad + 21SiO_2$$
(epidote)

$$10CO_2 + 8H_2O$$

Greenschist Facies: Sericite-Chlorite-Carbonate Schist:

$$6Ca_2Al_3Si_3O_{12}(OH) + 3K_2 \rightleftharpoons 12CaCO_3 + 3K_2Al_4Si_6Al_2O_{20}(OH)_4 + 3H_2$$
(clinozoisite) (calcite) (muscovite)

$$+ 12CO_2 + 6H_2O$$

$$(Mg,Al,Fe)_{12}(Si,Al)_8O_{20}(OH)_{16} \rightleftharpoons K_2Al_4Si_6Al_2O_{20}(OH)_4 + 6H_2O$$
(chlorite) (muscovite)

$$+ 16CO_2 + K_2 + 8CaO + O_2 \quad + 8Ca(Mg,Fe)(O_3)_2$$
(ankerite)

The tremolite, biotite and plagioclase of the host volcanic rocks alter to chlorite, sericite, epidote and carbonate. Within the shear zone, these alterations are accompanied by the development of a strong schistose foliation composed of alternating bands of chlorite, sericite and fine-grained albite (Plates 30 & 32, pages 53&60).

The alteration reactions, as determined from thin sections, require an addition of H_2O, CO_2 and K_2O and are accompanied by the release of silica. An examination of the geological literature indicates that carbonate-sericite-chlorite alteration is almost always associated

TABLE 4

Mineralogy of the Alteration Zones, 3+50N Grid Line

Location	Alteration Zone	Mineralogy													Structure
		hornblende	fine (quartz) feldspar Matrix	brown biotite	feldspar phenocrysts	quartz	chlorite	sericite	epidote & leucocene	zoisite	apatite	calcite	opaques		
3+50E	epidote-amphibolite facies	30	55	-	-	-	10	trace	3	-	trace	1	1		---
2+50E		-	45	15	20	2	3	-	15	-	-	-	-		---
1+50E		65	25	-	1	-	5	-	2	-	½	3	1½		weak schistosity (S_1)
1+00E		-	55	-	-	-	10	30	-	-	-	-	5		weak schistosity (S_1)
0+77E	greenschist facies	-	20	-	-	5	25	45	-	4	-	-	1		---
0+67E		-	32	-	-	2	20	15	-	25	-	1	5		---
0+62E		-	30-35	-	-	-	20	30	-	5	-	5-10	5		---
0+44E	sericite-chlorite-carbonate schist	-	30	-	-	*4½	15	35	trace	-	-	15	½		strong schistosity (S_2)
0+40E		-	-	-	-	*40	20	30	-	-	-	5	5		strong schistosity (S_2)
0+32E		-	30	-	3	*15	15	30	1	-	-	4	2		strong schistosity (S_2)
0+25E		-	15	-	-	* 5	35	15	-	-	-	28	2		strong schistosity (S_2)
0+00B.L.	greenschist facies	-	30	-27-32		2	15-20	3	7	-	1	10	4		---
0+50W	epidote-amphibolite facies	10-15	26-31	7	25	5	2	3	5	-	1	4	3		---
1+00W		-	42	15	25	3	-	3	10	-	-	-	2		---
1+00W		35	23	-	-	-	15	5	15	2	-	4	1		---
2+00W		-	55	20	10	3	-	3	5	-	-	2	2		---

*includes vein quartz

TABLE 4

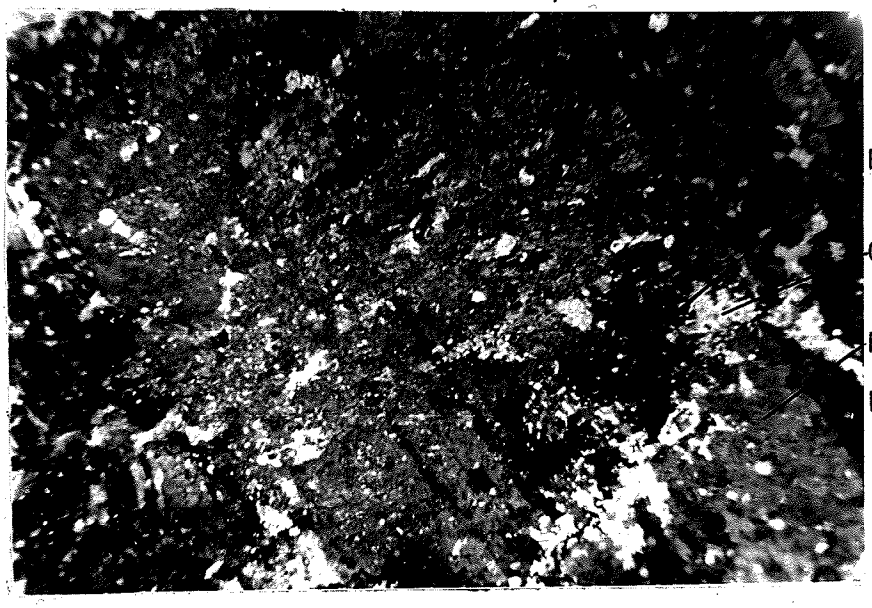

PLATE 33

A thin section photomicrograph of a feldspar phenocryst dappled by epidote, calcite, sericite alteration. (80X, polarized light)

PLATE 34

A thin section photomicrograph of a veinlet of epidote and calcite in a volcanic rock of the epidote-amphibolite facies. (90X, polarized light)

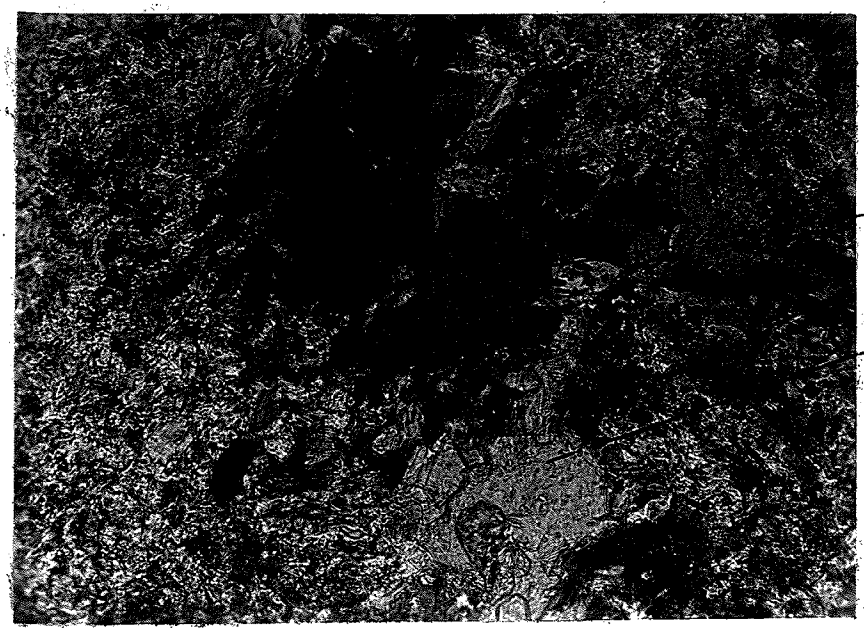

PLATE 33

A thin section photomicrograph of zoisite-calcite alteration in a volcanic rock of the greenschist facies. (200X, polarized light)

PLATE 36

A thin section photomicrograph of a carbonate, sericite, chlorite schist. The ferruginous carbonate is as stringers and patches. (20X, polarized light)

with gold deposits. Study of the processes that formed these alteration zones, therefore, may supply a clue as to what mechanism formed the gold-bearing quartz veins.

V. 3. Distribution of Elements in the Alteration Zones

Chemical analysis of a suite of samples collected from the 3+50N grid line, perpendicular to the direction of the shear zone, indicates a distribution of elements corresponding to that suggested by the chemical equations given in the previous section. The altered rocks, near the quartz veins, are enriched (relative to the host volcanic rocks) in the volatile and light elements - CO_2, S, K_2O and H_2O - and are depleted in silica. In Table 5, the increase and decrease of elements has been represented, relative to the unaltered volcanic rocks, as a weight percentage of the oxide as well as by the number of cations per unit cell, as determined by the method suggested by Barth (1948). The latter method is the more meaningful as it gives the number of cations that are introduced or removed from the rock and is not influenced by the weight of the element involved, as are the weight percentages. For instance, the standard cell calculations show that the introduction of the volatile elements, in particular H_2O, correlate most closely with the decrease in silica and play a major role in compensating the charge inbalance caused by the decrease in silica, while the weight percentages do not indicate this fact so clearly.

As the largest gold-bearing quartz veins occur where

TABLE 5

CHANGES IN CHEMICAL COMPOSITION OF ALTERATION ZONES

	Dacite (Epidote-Amphibolite Facies)		Greenschist Facies					Chlorite-Sericite-Carbonate Schist				
Constituents:	Wt. %:	Cations to 160 O,OH:	Wt. %:	Cations to 160 O,OH:	Gains & Losses of Cations:	% Gain & Loss of Cations:	Charge Gains & Losses:	Wt. %:	Cations to 160 O,OH:	Gains & Losses of Cations:	% Gain & Loss of Cations:	Charge Gains & Losses:
SiO_2	65.71	57.319	64.69	56.108	-1.211	-2.12	-4.844	52.59	46.296	-11.023	-19.60	-44.092
Al_2O_3	16.65	17.204	15.70	16.052	-1.152	-6.69	-3.456	15.50	16.086	- 1.118	- 6.85	- 3.354
Fe_2O_3	2.02	1.326	1.66	1.084	-0.242	-18.28	-0.726	2.46	1.630	+0.304	+22.95	+0.912
FeO	2.59	1.887	2.90	2.900	+0.318	+16.85	+0.636	7.71	5.292	+ 3.405	+181.00	+ 6.810
MgO	1.57	2.039	2.23	2.882	+0.843	+35.20	+1.686	4.79	6.286	+ 4.247	+208.10	+ 8.494
CaO	4.78	4.466	3.96	3.679	-0.782	-17.50	-1.564	3.40	3.207	- 1.259	-28.18	- 2.518
Na_2O	3.24	5.483	3.74	6.285	+0.802	+14.60	+0.802	2.83	4.836	-0.647	-11.81	- 0.647
K_2O	1.38	1.531	0.93	1.032	-0.499	-32.60	-0.499	1.76	1.979	+ 0.448	+29.20	+ 0.448
TiO_2	0.37	0.241	0.49	0.318	+0.077	+32.00	+0.308	0.68	0.450	+ 0.209	+86.60	+ 0.836
P_2O_5	0.15	0.136	0.14	0.136	-	-	-	0.15	0.148	+ 0.012	+ 8.24	+ 0.060
H_2O	1.44	(8.387)	2.28	(13.206)	+4.819	+57.40	+4.819	4.55	(26.754)	+18.367	+218.80	+18.367
CO_2	0.33	0.393	0.92	1.089	+0.694	+176.50	+2.776	3.04	3.656	+ 3.263	+829.00	+13.052
S	0.013	-	0.005	-	-	-	-	0.013	-	-	-	-
Total	100.34	92.025	99.64	90.771			-0.062		89.866			-1.632

(1) The chemical analyses given in this table are average chemical compositions for each alteration zone. The chemical analyses for samples taken across the shear zone are given in Appendix III.

(2) The gains and losses of cations in the greenschist facies and the chlorite-sericite-carbonate schist are relative to the unaltered host dacites.

the 3+50N grid cuts across the shear zone (Map 2), samples for chemical analysis were collected from along this grid line. A factor complicating the interpretation of the distribution of elements in the shear zone is the chlorite-carbonate schist, as shown in the geological profile of Figure 18 (page 92). This chlorite-carbonate schist is a dark green, rough weathered rock that has been interpreted by the author as the schistose equivalent of a diabase dike (Map 2). This 'sheared diabase' coincides with the decrease in silica (Figure 18, page 92) and the increase in ferromagnesian elements (Figure 19, page 93). The problem is whether to attribute the present distribution of elements in the shear zone to alteration processes or to differences in the original composition of these rocks. The following factors tend to favor that the present distribution of elements is predominantly a result of alteration processes:

(1) The increases in volatile content (H_2O, CO_2 & S) correlate with decrease of silica and increase of ferromagnesian elements (Figures 18 & 19, pages 92&93).

(2) The chemical analyses of a sample of quartz feldspar porphyry, and its sheared equivalent, indicate that silica has decreased markedly in the sheared specimen with an attendant increase in volatile constituents (Table 2, page 31).

(3) The unsheared diabase contains approximately 49% silica, (Table 2, page 31), while the sheared chlorite-carbonate-sericite schist

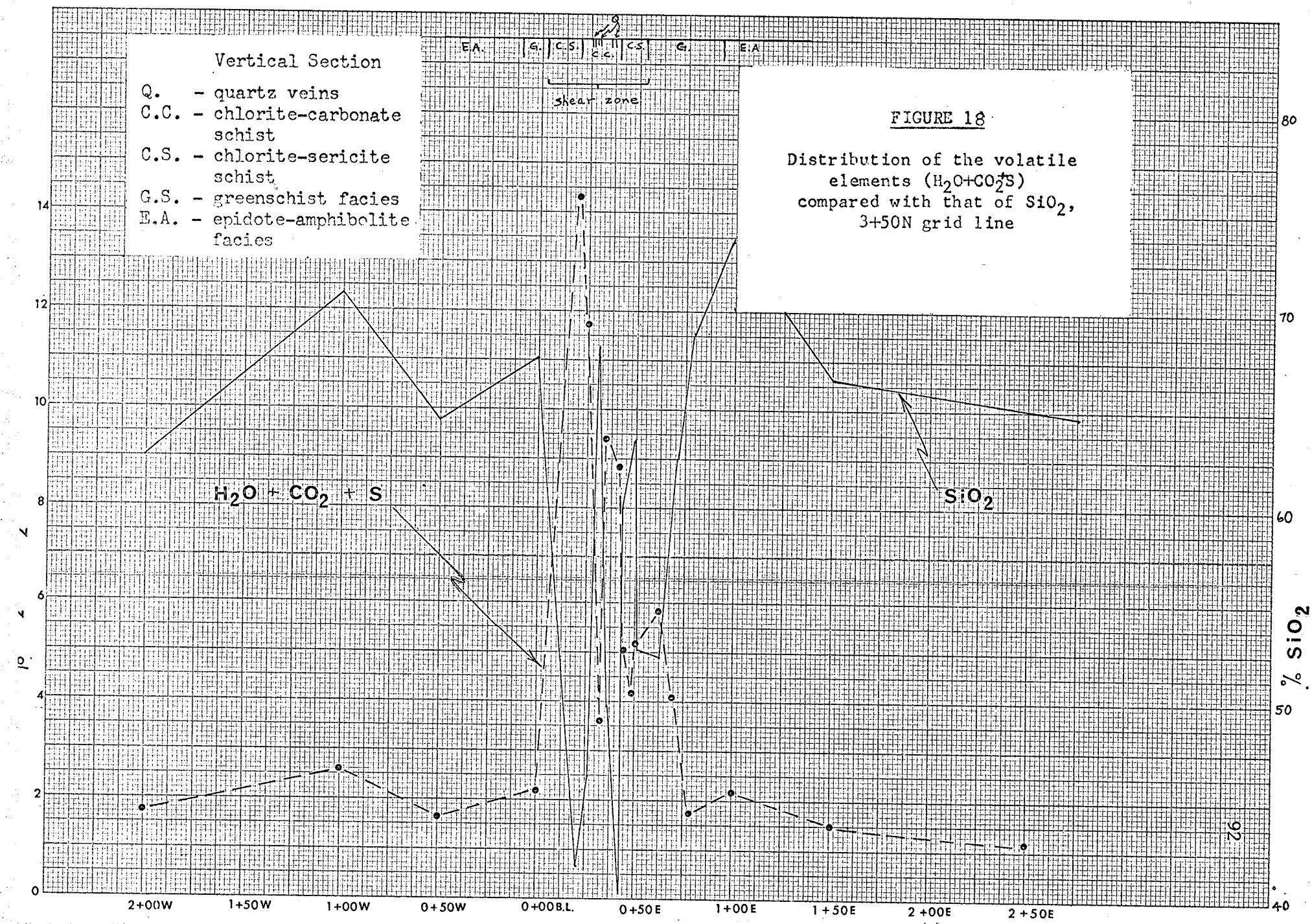

FIGURE 18

Distribution of the volatile elements (H_2O+CO_2+S) compared with that of SiO_2, 3+50N grid line

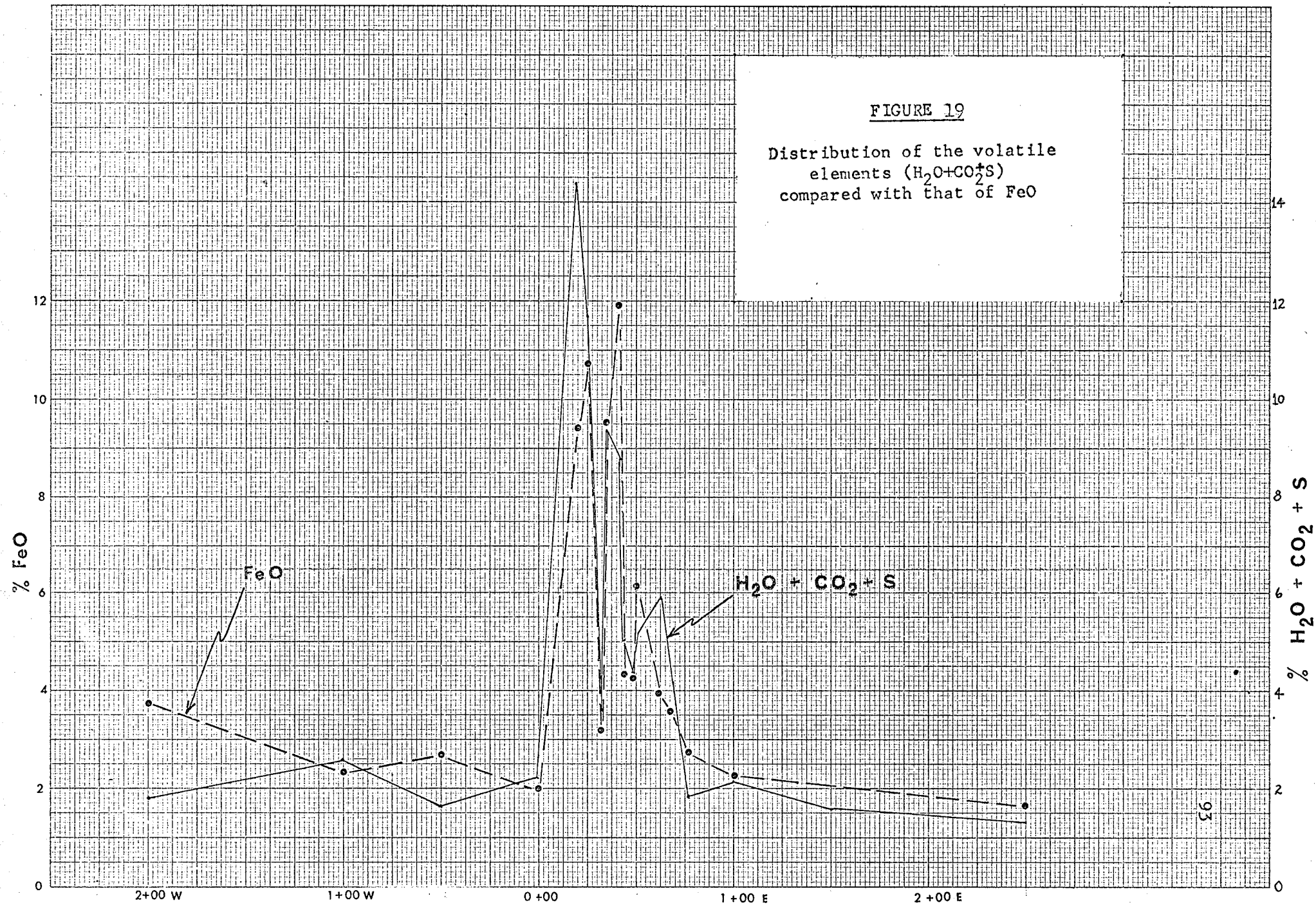
FIGURE 19
Distribution of the volatile elements (H_2O+CO_2+S) compared with that of FeO
% FeO
% $H_2O + CO_2 + S$
FeO
$H_2O + CO_2 + S$
0
2
4
6
8
10
12
14
2+00 W
1+00 W
0 +00
1+00 E
2 +00 E

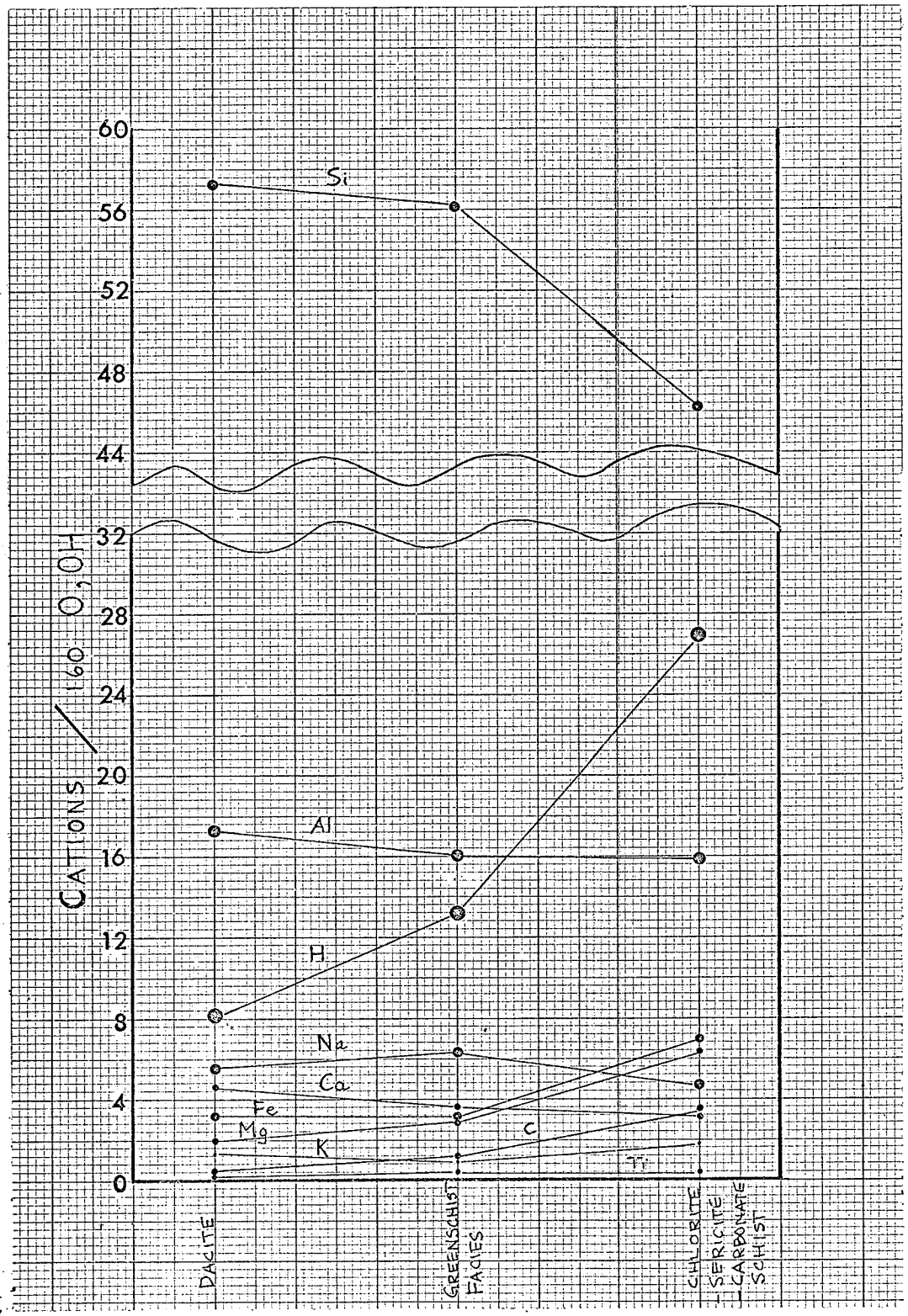

Figure 20

Distribution of Cations in Alteration Zones.

near the quartz vein contains as low as 40% silica.

V. 4. Origin of the Gold-Bearing Quartz Veins of the Pilot-Smuggler Shear Zone

The distribution of elements in the alteration zones associated with the gold-bearing quartz veins of the Pilot-Smuggler shear zone appears to be dominantly a redistribution of the elements originally contained within the rocks, rather than an introduction of elements from an external source. Although there is a possibility that some of the elements, expecially H_2O, CO_2 and S, could have been introduced from an external source, there is no overriding evidence in support of this. All of the elements presently contained in the alteration zones and quartz veins, including the gold, could have been released during alteration of the minerals in the volcanic rocks.

A study of the gold content of the minerals and rocks of the Skaergaard intrusion by Vincent and Crocket (1960) showed that these rocks contain traces of gold.

TABLE 6

Gold in Minerals of the Skaergaard Differentiated Intrusion

Mineral:	Au ppm in mineral:
Plagioclase (An_{40})	0.0029
Pyroxene ($Ca_{35}Mg_{34}Fe_{31}$)	0.0021
Titaniferous Magnetite	0.0043
Ilmenite	0.0029

(after Vincent & Crocket - 1960)

Similar minerals are contained in the host rocks of the Pilot-Smuggler shear zone. During alteration of these minerals, it is possible that gold was released from their structures and freed to migrate. Vincent and Crocket also found that the more basic fractions of the Skaergaard intrusion are richer in gold than are the acid differentiates. The more important gold deposits of the Rice Lake area are hosted by the basic volcanic and intrusive rocks (Davies 1962). This could be a result of the higher gold content, and easier susceptibility to retrograde alteration, of the more basic rocks.

If the elements of the alteration zones, associated with the quartz veins, have been mobilized during the mineralizing process, as postulated, it is most likely that these elements migrated by intergranular diffusion. The shearing movements, that cause numerous intergranular openings and fractures, therefore, are an integral part of the alteration and mineralizing process.

This study of the gold-bearing quartz veins of the Pilot-Smuggler shear zone suggests a similarity in origin with that of the Yellowknife deposits, as envisaged by Boyle (1961). The Yellowknife greenstone belt is composed of a similar assemblage of rocks as those of the Rice Lake area. The gold ore bodies are associated with shear zones and have a similar occurrence and mineralogy as the deposits of the Rice Lake area. The gold-bearing quartz lenses are enveloped by carbonate-sericite-pyrite-

arsenopyrite alteration zones which grade imperceptibly into chlorite-albite-carbonate schist of the shear zones. Boyle has concluded, as a result of his study, that all the elements present in the ore bodies have been derived from the country rocks in which the deposits occur. According to Boyle, the major factor causing these elements to migrate into the veins is a pressure gradient caused by dilatent zones that were set up during movement along the shear zones. The mobile elements such as water, carbon dioxide, sulphur arsenic, antimony, copper, lead, zinc, gold, silver and silica are thought by Boyle to migrate towards the dilatent zones by ionic diffusion through a nearly static flux of water vapor.

A distinct possibility exists that the Pilot-Smuggler gold-bearing quartz veins have formed in a manner similar to that postulated by Boyle for the Yellowknife area deposits; although magmatic hydrothermal, or hydrothermal solutions of other origin, cannot be overlooked as possible agents in the process of vein formation.

The formation of the shear zone and the formation of the gold-bearing quartz veins are intimately interrelated. It is the shear zone structure that has supplied a channel-way into which the mobile elements, H_2O, CO_2 and S, have migrated. The source of these solutions is not known but could be magmatitic or derived through metamorphic processes. The influence of these volatile constituents and the temperature and pressure conditions prevailing in the shear

zone cause the retrograde alteration of the shear zone rocks. It is this retrograde alteration of the shear zone rocks that has released the elements necessary for the formation of the gold-bearing quartz veins. The quartz veins are formed as a result of the formation of the shear zone structure.

If the gold deposits have formed by lateral secretion of the constituents from their altered host rocks, as has been postulated, then the structural breaks in basic intrusive and extrusive rocks should be prime target areas for exploration for gold deposits; and large carbonate-chlorite-sericite alteration halos should be considered good indicators of mineralized zones.

CHAPTER VI

SUMMARY AND CONCLUSIONS

The Rice Lake area contains many gold-bearing quartz veins that occur within shear and fracture zones. The shear and fracture zones are concentrated to the east and west of a large oval shaped intrusion of quartz-diorite. It is apparently the buttress action of this quartz diorite body, which was emplaced prior to the formation of the shear and fracture zones, which caused the shear and fracture zones to be formed nearby. For this reason the gold mineralization cannot be attributed to the quartz diorite body as it has often been because of its association with this igneous body. According to the results of this study the gold-bearing quartz veins have been formed by alteration of the rocks during the formation of the shear zone. The material necessary to form the quartz veins has been derived from release of constituents from the altered rocks and a migration of this material into vein sites.

The information used to arrive at this hypothesis has resulted from a detailed geological examination of the Pilot-Smuggler shear zone, and attendant gold-bearing quartz veins, which is a typical gold vein-bearing shear zone structure of the Rice Lake area. This study includes a description of the structure, the petrology and alteration of the rocks hosting the veins, and the mineralization and geochemistry of the shear zone.

The gold-bearing quartz veins occur as small discontin-

uous lenses which are aligned approximately parallel to the trend of the shear zone. The quartz veins are fractured and disjointed and contain brecciated patches and stringers of sulphide and carbonate minerals. Pyrite, the dominant sulphide mineral, contains traces of spalerite, pyrrhotite, chalcopyrite and other copper sulphides as small inclusions and veinlets that have likely been exsolved from the pyrite structure. The gold assays of the quartz veins are proportional to their sulphide content.

The interpretation of the minor structural features indicates that the Pilot-Smuggler break has been affected by two stages of deformation. During the first stage the rupture was initiated and the major offsets across the break occurred. The second period of deformation, caused by compression subparallel to the schistose rocks of the shear zone, caused them to be deformed into numerous kink, chevron and conjugate folds. The quartz veins, and the associated mineralization were emplaced during the first stage of deformation.

The alteration processes, as determined from studies of thin sections and chemical analyses of specimens of altered rocks, suggest an influx of the volatile elements, H_2O, CO_2 and S, has caused the host dacites to be altered to sericite-chlorite-carbonate schist. The breakdown of the dacites is accompanied by the release of many elements not required for the formation of the new minerals, sericite and chlorite. The distribution of elements in the

alteration zones suggests that the constituents of the mineralized quartz veins could be derived from the adjacent altered rocks. The shearing has played an important role in providing access for the altering solutions and in providing localities for the emplacement of the gold-bearing veins and is, in fact, an integral part of the mineralizing process.

LIST OF REFERENCES

Armstrong, H.S.
1943 Gold ores of the Little Long Lac area, Ontario; Econ. Geol., vol. 38, p.p. 204-252.

Bateman, J.D.
1940 Rock alteration in the Uchi gold area; Econ. Geol., vol. 35, p.p. 382-404.

Barth, T.F.W.
1948 Oxygens in rocks: a basis for petrographic calculations; Jour. Geol., vol. 56.

Boyle, R.W.
1953 The mineralization of the Yellowknife gold belt with special reference to the factors which controlled its localization; PH.D. Thesis, Univ. of Toronto, 257 pgs.

1959 The geochemistry, origin, and role of carbon dioxide, water, sulpher, and boron in the Yellowknife gold deposits, Northwest Territories, Canada; Econ. Geol., vol. 54, p.p. 1506-1524.

1961 The geology, geochemistry, and origin of the gold deposits of the Yellowknife district; Geol. Surv. Can., Mem. 310, 193 pgs.

Byers, A.R.
1940 Geology of the Nighthawk Peninsular gold mine; Econ. Geol., vol. 35, p.p. 996-1011.

Clark, E. & Ellis, H.A.
1939 Metasomatism of country near ore-bodies and its possible economic significance; Econ. Geol., vol. 34, p.p. 777-789.

Coleman, L.C.
1957 Mineralogy of the Giant Yellowknife Gold Mine, Yellowknife, N.W.T.; Econ. Geol., vol. 52, p.p. 400-425.

Cooke, H.C.
1922 Geology and mineral resources of Rice Lake and Oiseau River areas, Manitoba; Geol.Surv. Can., Sum. Rept., 1921, Pt. C, 36 pgs.

Cooke, H.D.
1946 Canadian lode gold areas (summary account); Geol. Surv. Can., Econ. Geol. Ser., No. 15, 86 pgs.

Cooke, H.R.
1947 The original Sixteen to One gold vein, Alleghany California; Econ. Geol., vol. 42, p.p. 211-250.

Davies, J.F.
1953 Geology and gold deposits of Southern Rice Lake area; Man. Mines Branch, Publication 52-1, 41 pgs.

1962 Geology and mineral resources of Manitoba; Manitoba Dept. of Mines and Nat. Res., p.p. 47-52.

1963 Geology and gold deposits of the Rice Lake-Wanipigow River area, Manitoba; Ph.D. Thesis, Univ. of Toronto, 142 pgs.

Delury, J.S.
1921 Mineral prospects in Southeastern Manitoba (Rice Lake, Maskwa River and Boundary Districts); Man. Govt. Bull., Commissioner of Northern Manitoba, 55 pgs.

Dougherty, E.Y.
1935 Geologic problems of the Canadian Pre-Cambrian gold fields; Econ. Geol., vol. 30, p.p. 879-889.

Emens, W.H.
1936 Gold Lake Mines Ltd., Rice Lake District, Manitoba; Man. Mines Branch, Cancelled Assessment Files.

Gallagher, G.M.
1940 Albite and gold; Econ. Geol., vol. 35, p.p. 698-736.

Gunning, H.C.
1937 Cadillac area, Quebec; Can. Dept. Mines and Res., Geol. Survey, Mem. 206.

Hurst, M.E.
1935 Vein formation at Porcupine, Ontario; Econ. Geol., Vol. 30, p.p. 103-127.

Knopf, A.
1929 The Mother Lode System of California; U.S. Geol. Surv., Prof. Paper, No. 157, 85 pgs.

Lindgren, W.
1905-6 Metasomatic processes in gold deposits of Western Australia; Econ. Geol., vol. 1, p.p. 530-544.

Manitoba Mines Branch
Cancelled Assessment Files, Rice Lake Area.

Moore, E.S.
1912 Hydrothermal alterations of granite and the source of vein quartz at the St. Antony Mine; Econ. Geol., Vol. 7, p.p. 751-761.

Moorhouse, W.W.
1959 The Study of Rocks in Thin Section; Harper and Brothers, New York, 514 pgs.

Pardie, J.T. & Park, C.F. Jr.
1948 Gold deposits of the Southern Piedmont; US. Geol. Surv., Prof. Paper., No. 213

Paterson, M.S. & Weiss, L.E.
1966 Experimental deformation and folding in phyllite; Geol. Soc. Am. Bull., vol. 77, p.p. 343-374.

Sander, B.
1950 Einfuhrung in die Gefugekunde der geologischen Korper, I & II; Springer Verlag, Vienna

Schmitt, H.
1954 The origin of silica of the bedrock hypogene ore deposits; Econ, Geol., vol. 49, p.p. 877-890.

Scherbakov, Yu.G. & Perezhogin, G.A.
1963 Geochemical relation between gold mineralization, intrusives, and the enclosing rocks in Western Siberia; Geochemistry, No. 9, p.p. 882-890.

Stockwell, C.H.
1935 Gold deposits of Elbow-Morton area, Manitoba; Geol. Surv. Can., Mem. 186, p.p. 12-15.

1937 Gold deposits of Herb Lake area, Northern Manitoba; Geol. Surv. Can., Mem. 208, p.p. 13-17.

1938 Rice Lake-Gold Lake area, Southeastern Manitoba; Geol. Surv. Can., Mem. 210, 79 pgs.

Turner, F.J. & Weiss, L.E.
1963 Structural Analysis of Metamorphic Tectonites; McGraw-Hill Book Co., 545 pgs.

Vincent, E.A. & Crocket, J.H.
1960 Studies in the geochemistry of Gold-I, The distribution of gold in rocks and minerals of the Skaergaard intrusion, East Greenland; Geochem. et Cosmo. Acta., Vol. 18, p.p. 130-142.

Warren, H.V., et al
1966 Some observations on the geochemistry of mercury as applied to prospecting; Econ. Geol., vol. 61, p.p. 1010-1028.

White, W.H.
1943 Mechanism and environment of gold deposition; Econ. Geol., vol. 38, p.p. 512-532.

Wright, J.F.
1932 Geology and mineral resources of a part of Southeastern Manitoba; Geol. Surv. Can., Mem. 169.

APPENDIX I

Mercury Vapor Analysis

Rock samples collected across the Pilot-Smuggler shear zone, along the surveyed grid lines (Map 2), were analyzed for their mercury content. A type SVI mercury detector, manufactured by the Lemaire Instrument Corporation, was used for analyzing the samples. The mercury analyzer is based on the principle of adsorption of specific frequencies of radiation by mercury.

Mercury vapor is volatilized and removed from heated rock samples. The mercury-rich vapor is then drawn off the heated rock sample and diluted in a specific volume of air in a pump. The vapor is transferred from the pump into another chamber at a specified rate. Through this chamber is directed a filtered beam of ultraviolet radiation of a frequency that is adsorbed by mercury. A radiation-sensitive detector at the opposite end of the chamber measures the radiation and converts it to a mercury concentration of the atmosphere of the detector chamber. Ideally this is converted to the mercury concentration of the original rock sample by the following formula:

$$\text{P.P.M. mercury (rock sample)} = \frac{\text{instrument reading (micrograms/litre)} \times \text{pump size (litres)}}{\text{rock sample size (gms.)}}$$

It was found that the size of the sample and also the size of pump used, affected the results of the analysis. An attempt was made to empiracally calibrate the detection procedure but samples with known mercury contents could not

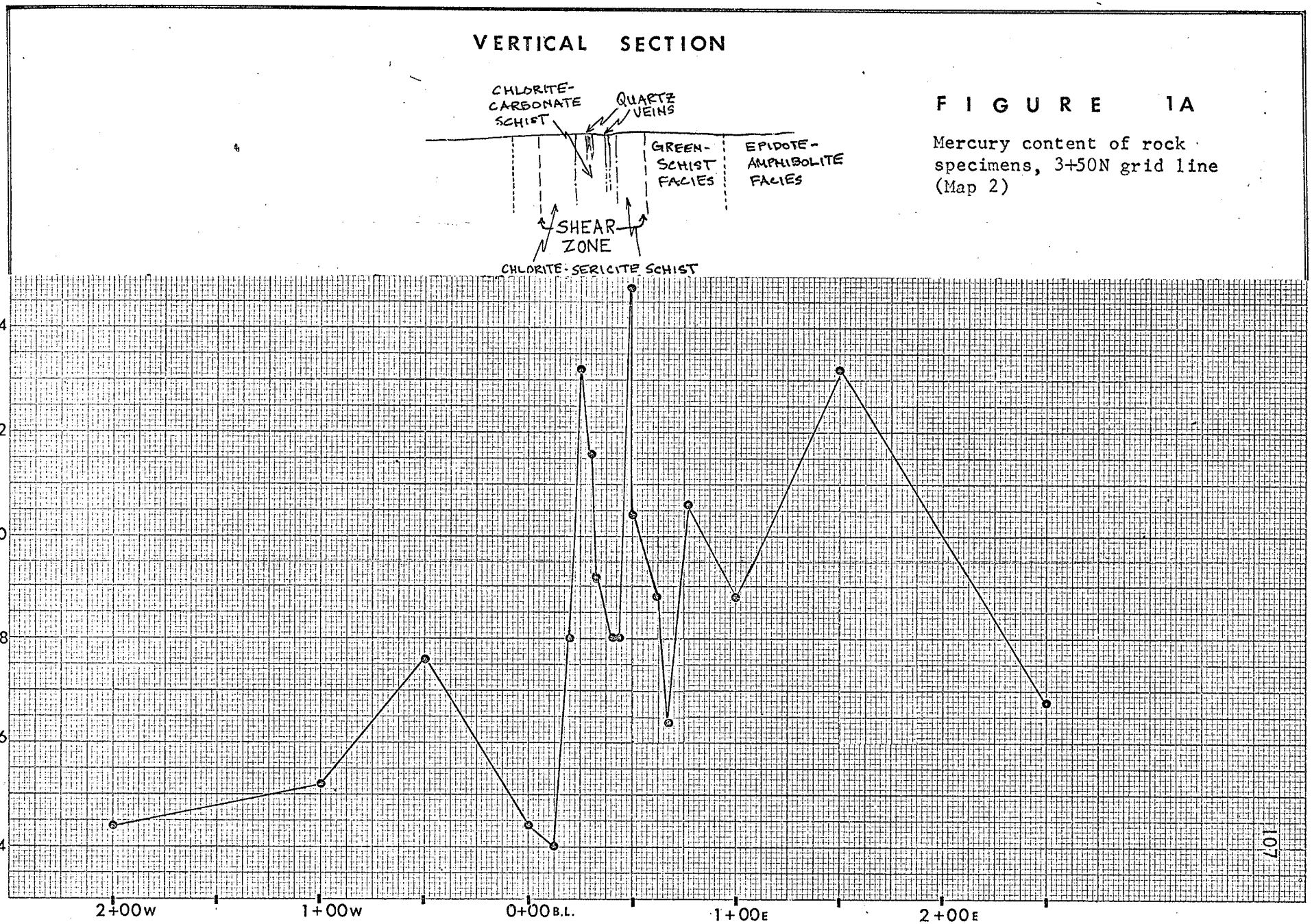

FIGURE 1A

Mercury content of rock specimens, 3+50N grid line (Map 2)

be prepared. The mercury values of samples analyzed have been expressed as parts per million in Figure 1A.

The mercury vapor analyses of samples across the Pilot-Smuggler shear zone were made to determine if noticeable mercury anomalies are associated with the gold deposits of the Rice Lake area. Warren (et al., 1966) found mercury values in vegetation and soil samples to be directly related to Pb, Zn, and Au concentrations in bedrock samples. However, the mercury contentnof samples associated with the Pilot-Smuggler gold-bearing deposits was found to be too low to be properly detected by the SVI detector. A small increase in the mercury content of the rocks next to the gold-bearing quartz veins was found but mercury vapor analysis of rock samples would not be of any value as an exporation tool for gold ore bodies of the type found in the Rice Lake area.

APPENDIX II

Gamma Ray Spectrometer Survey

A gamma ray spectrometer survey using a portable instrument with potassium, thorium, and uranium channels, was done on the surveyed grid near the Gold Lake Mine shafts on the Pilot-Smuggler break. Each of the rocks' units showed a distinctive value of K gamma counts per minute:

Volcanics (dacites)	X = 98.25	counts/min.
Sheared volcanics	X = 151.8	" "
Diabase	X = 51.1	" "
Sheared diabase	X = 89.7	" "
Quartz feldspar porphyry	X = 108.6	" "

Sheared rocks showed a marked increase in potassium content, as indicated by their increased counts per minute. The potassium has likely migrated into the shear zone during the alteration processes associated with the formation of the gold quartz veins.

The volcanic units that are cut by the Pilot-Smuggler shear zones are very similar in composition. It was thought that units could be outlined by their potassium gamma counts. A statistical treatment of the potassium gamma counts per minute for the unsheared volcanic rocks showed they plot as a normal curve with mean 98.25 counts per minute, and a standard deviation of 17 counts per minute (Figure 2A). Using standard deviations as contour intervals, the potassium gamma counts per minute for the volcanic rocks of the surveyed grid area, were contoured. (Map 3). Areas of volcanics with definitely high, and

Leaf 110 omitted in page numbering.

others with low K gamma counts, could be outlined. In many cases the contours appear to outline volcanic units trending in the same direction as the regional schistosity (S_1).

APPENDIX III

Chemical Analyses

A suite of specimens was collected along the 3+50N grid line of the area of the detailed study near the exploratory shafts of the Gold Lake Mine Company Ltd. (Map 1). Chemical analyses of the rock samples were provided by K. Ramlal. The purpose of the chemical analyses was to determine the distribution of the major elements in the alteration halos associated with the gold-bearing veins. The following figures graphically illustrate the distribution of elements as related to the gold-bearing quartz veins:

TABLE 1A

CHEMICAL ANALYSES OF ROCK SPECIMENS, 3+50N GRID LINE

	2+00W	1+00W	0+50W	0+00BL	0+20E	0+25E	0+32E	0+34E	0+40E	0+44E	0+49E	0+50E	0+62E	0+67E	0+77E	1+00E	1+50E	2+50E
SiO_2	62.30	70.95	64.55	67.55	41.50	46.10	67.95	49.55	40.20	59.90	63.15	52.50	52.05	62.40	68.65	73.35	66.35	64.40
Al_2O_3	15.70	15.89	16.26	15.14	12.05	14.20	12.82	13.18	20.80	16.90	15.26	19.30	20.40	15.06	15.52	12.40	15.16	20.25
Fe_2O_3	3.05	1.64	2.19	2.04	2.06	3.51	0.85	3.53	4.29	1.89	1.17	2.42	1.45	2.52	1.25	1.05	4.74	1.20
FeO	3.72	2.32	2.68	2.00	9.40	10.72	3.20	9.52	11.92	4.32	4.28	6.16	3.96	3.56	2.72	2.28		1.64
MgO	2.68	1.20	1.68	1.12	6.45	6.10	1.84	6.33	7.56	2.80	2.60	4.47	3.19	3.80	1.57	1.60	1.15	0.15
TiO_2	0.52	0.42	0.46	0.44	0.81	-	0.42	0.92	1.60	0.55	0.48	0.68	0.67	0.44	0.44	0.44	0.46	-
CaO	5.12	3.98	4.77	3.84	10.20	5.36	2.56	4.02	0.81	2.08	2.02	1.18	3.84	5.01	3.84	3.30	6.42	3.64
Na_2O	3.32	0.16	4.44	5.02	1.32	1.08	4.29	1.60	0.45	2.97	5.42	5.64	6.66	2.62	2.86	1.54	3.25	5.02
K_2O	1.82	1.22	1.22	0.48	1.50	1.28	1.15	0.67	3.48	3.32	0.94	1.77	1.36	0.60	0.48	1.80	0.55	2.10
H_2O	1.59	2.04	0.93	1.52	4.14	6.04	2.42	5.47	7.43	3.85	2.51	4.52	3.25	2.72	1.75	2.15	1.22	1.18
CO_2	0.11	0.56	0.69	0.66	10.11	5.06	1.10	3.74	0.79	1.18	1.65	0.66	2.60	1.35	-	-	0.27	-
P_2O_5	0.21	0.14	0.21	0.13	0.10	0.20	0.13	0.13	0.16	0.14	0.14	0.20	0.17	0.11	0.16	0.13	-	0.17
S	.025	0.004	0.035	0.004	0.055	0.560	0.089	0.192	0.63	0.001	0.003	0.002	0.008	0.003	0.005	0.004	-	-
Total	100.17	100.52	100.12	99.94	99.70	100.21	98.82	98.85	100.12	99.90	99.62	99.90	99.61	100.18	99.25	100.04	98.67	99.75

Analyses by K. Ramlal,
Chemist, Dept. of Geology,
University of Manitoba

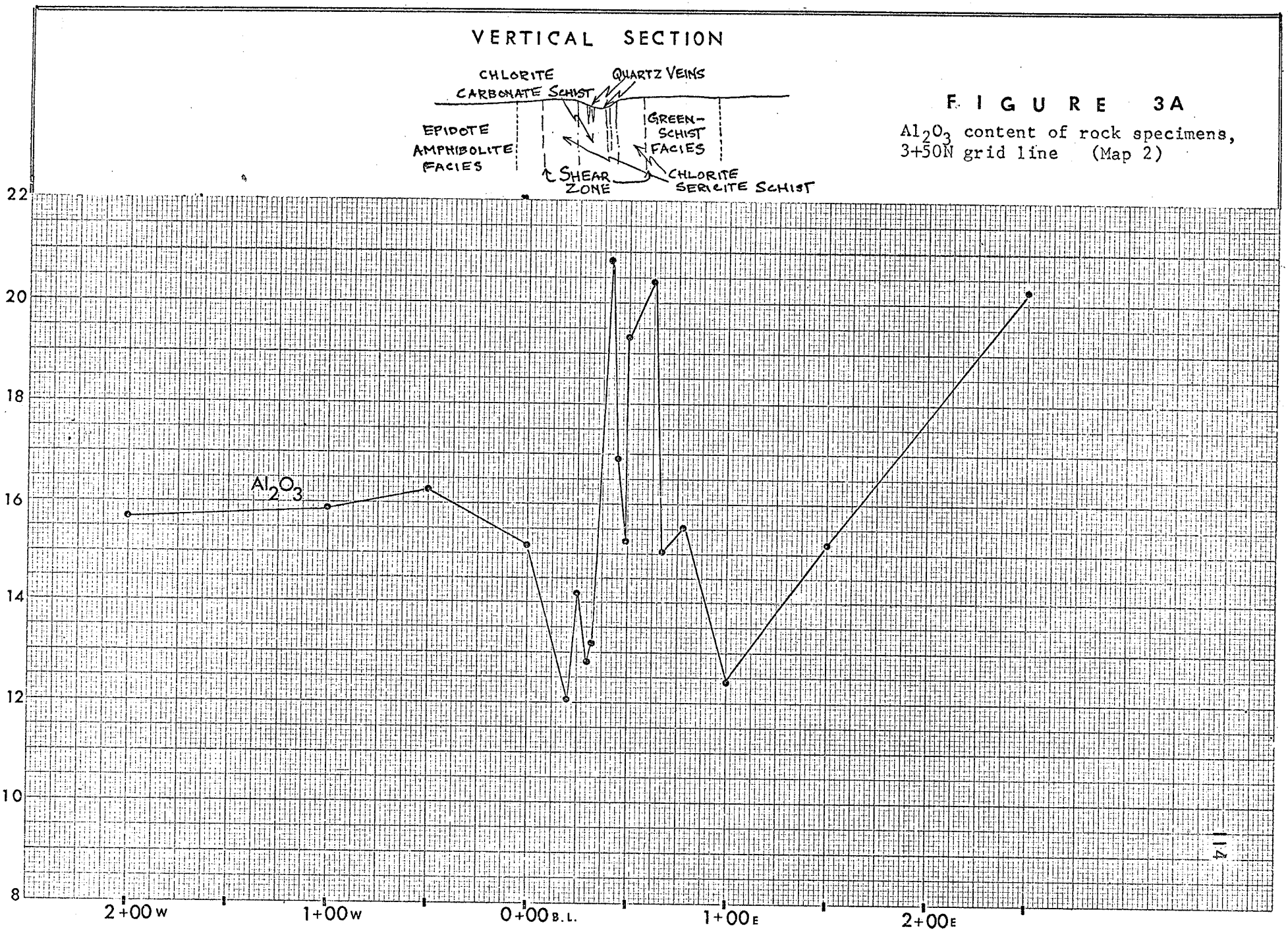

FIGURE 3A

Al_2O_3 content of rock specimens, 3+50N grid line (Map 2)

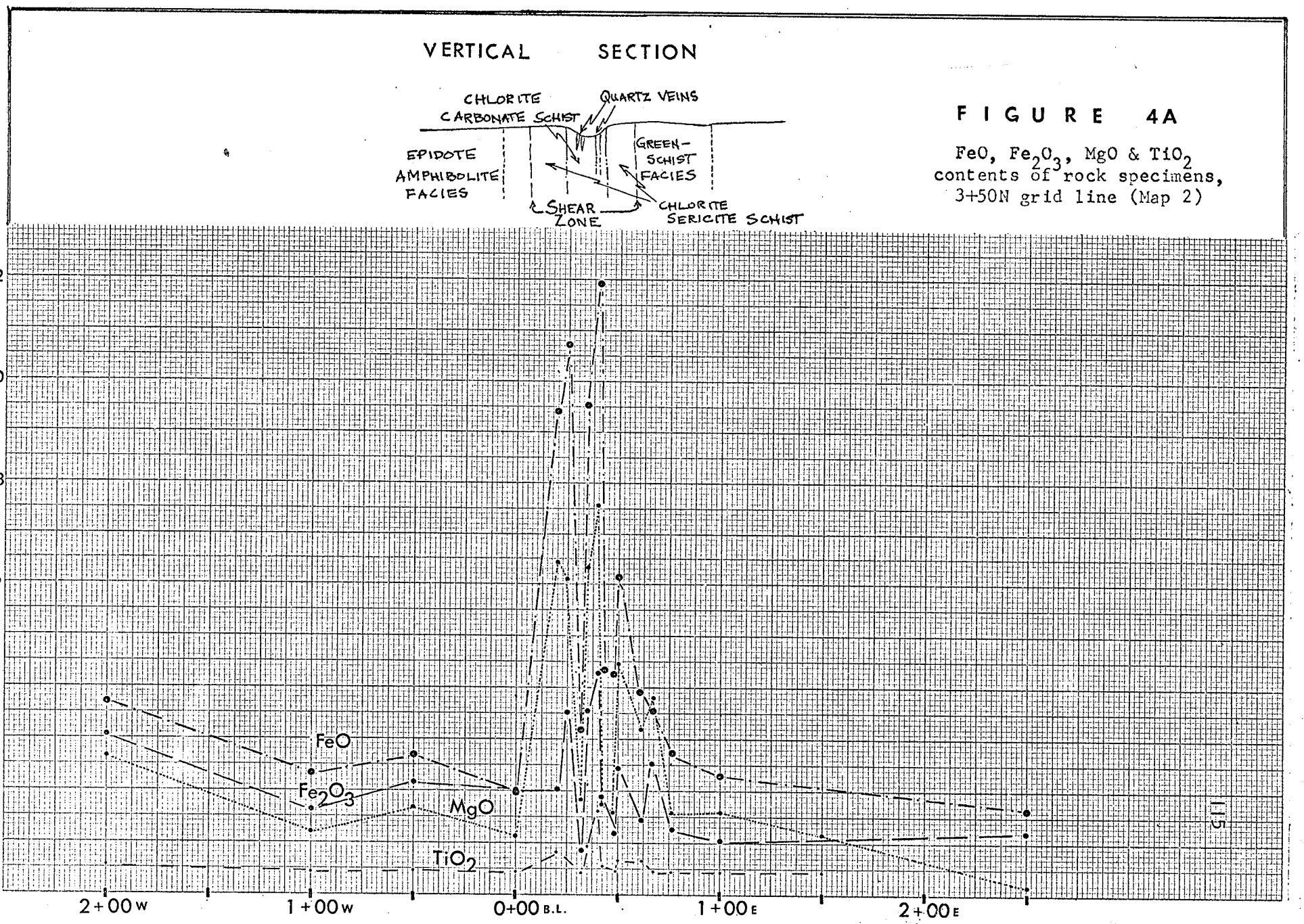

FIGURE 4A

FeO, Fe_2O_3, MgO & TiO_2 contents of rock specimens, 3+50N grid line (Map 2)

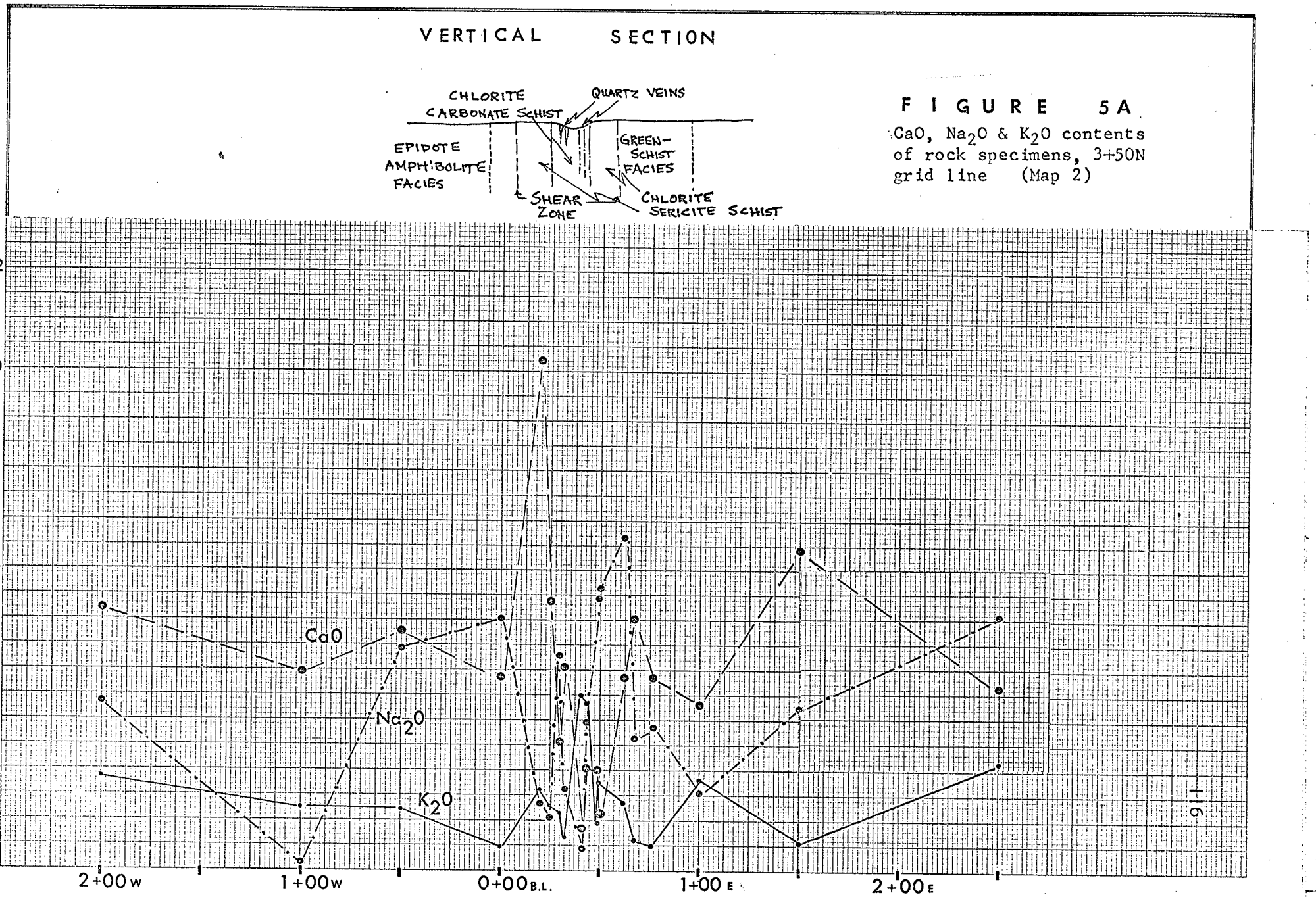

FIGURE 5A

CaO, Na_2O & K_2O contents of rock specimens, 3+50N grid line (Map 2)

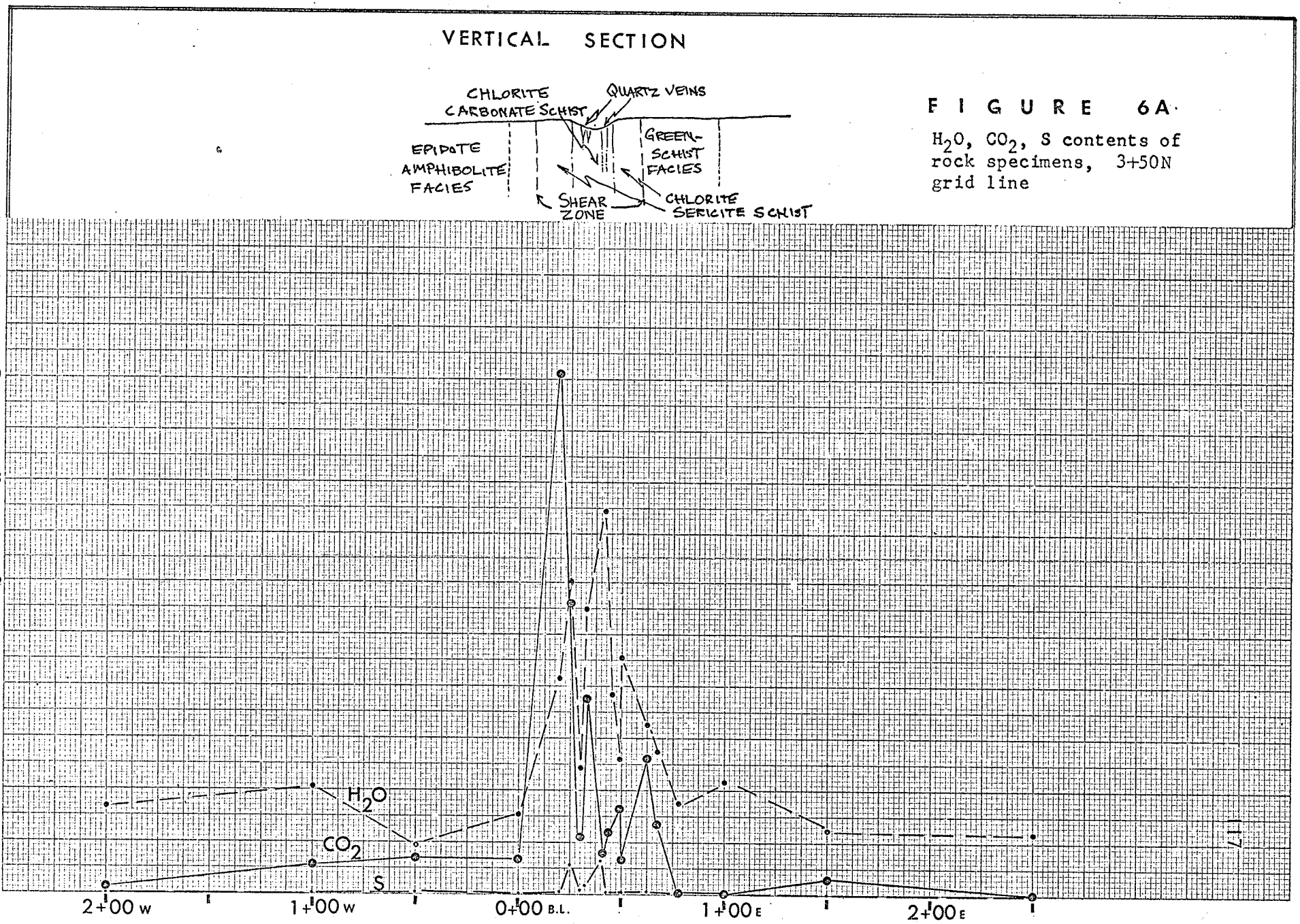

F I G U R E 6A.

H_2O, CO_2, S contents of rock specimens, 3+50N grid line

MAP 1

GEOLOGICAL MAP OF THE

PILOT-SMUGGLER SHEAR ZONE

1" = ½ mile

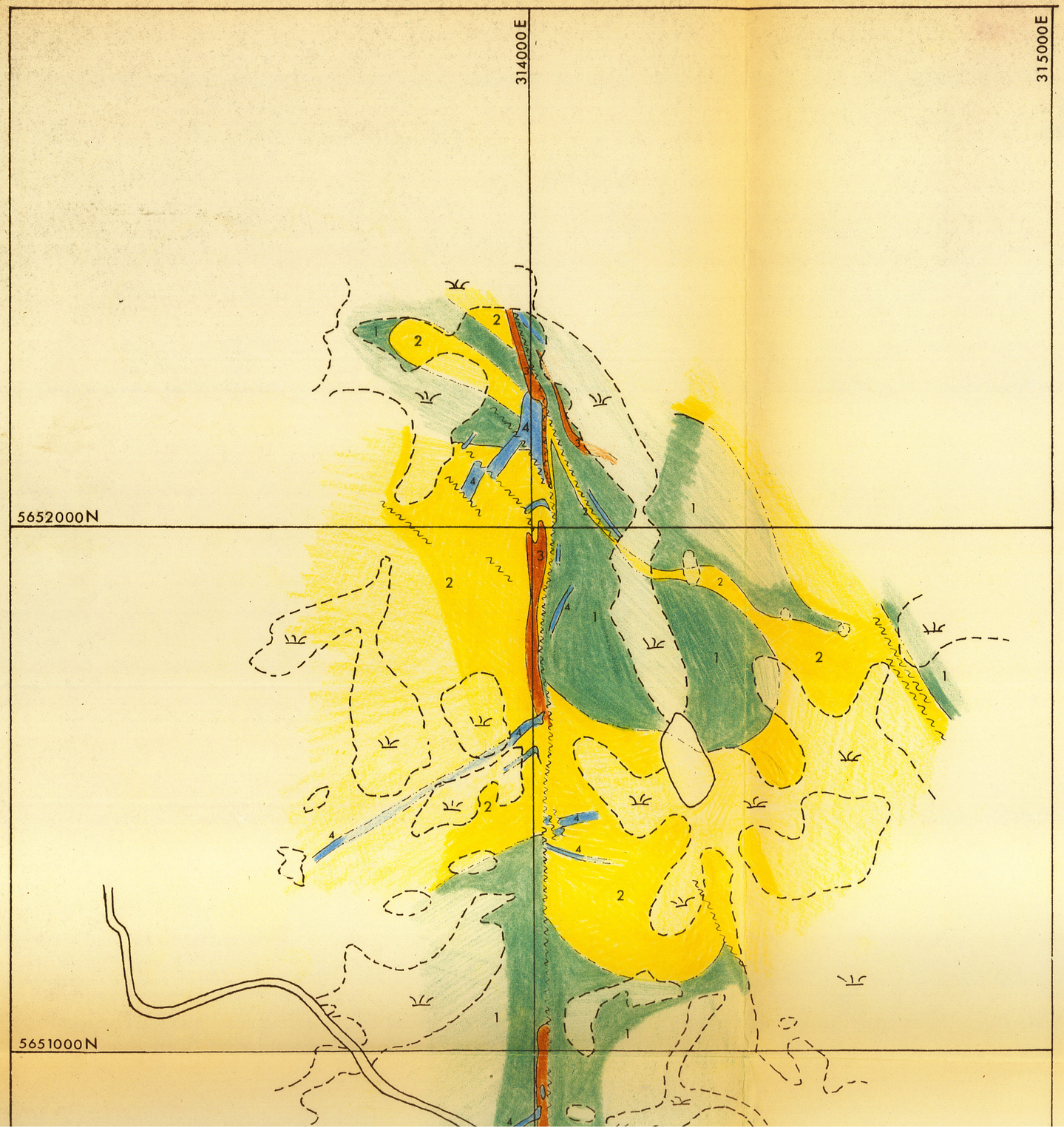

LEGEND

1 ..... FRAGMENTAL DACITE

2 ..... FRAGMENTAL RHYOLITE

3 ..... DIABASE

4 ..... QUARTZ FELDSPAR PORPHYRY

..... GEOLOGICAL CONTACT

..... known

..... gradational, difficult to define

..... assummed

..... SHEAR ZONE

..... SWAMP

..... ROAD

GRID IN U.T.M. COORDINATES

5651000N

5650000N

5649000N

GRID IN U.T.M. COORDINATES

0 660' 1320' 1980' 2640'

SCALE

1 INCH = 1/8 MILE

5+00 **E**

4+50 **E**

4+00 **E**

3+50 **E**

3+00 **E**

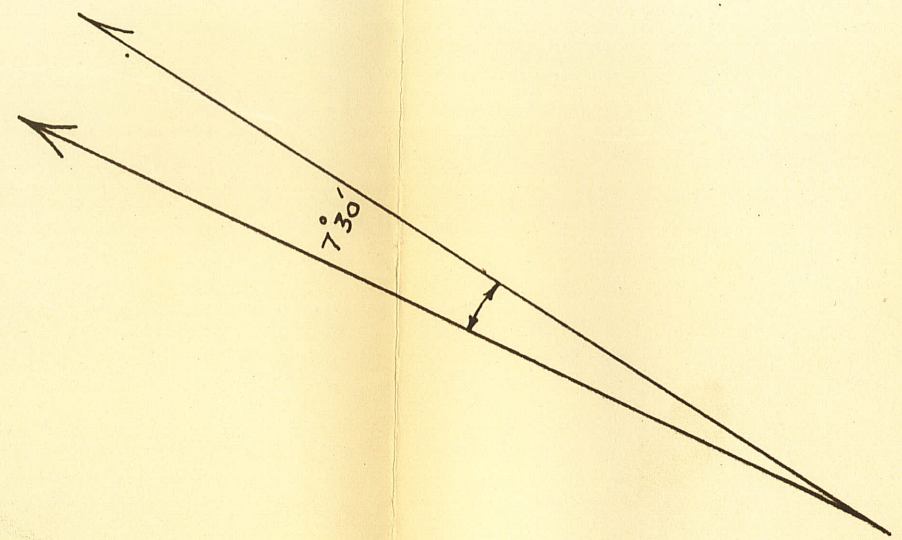

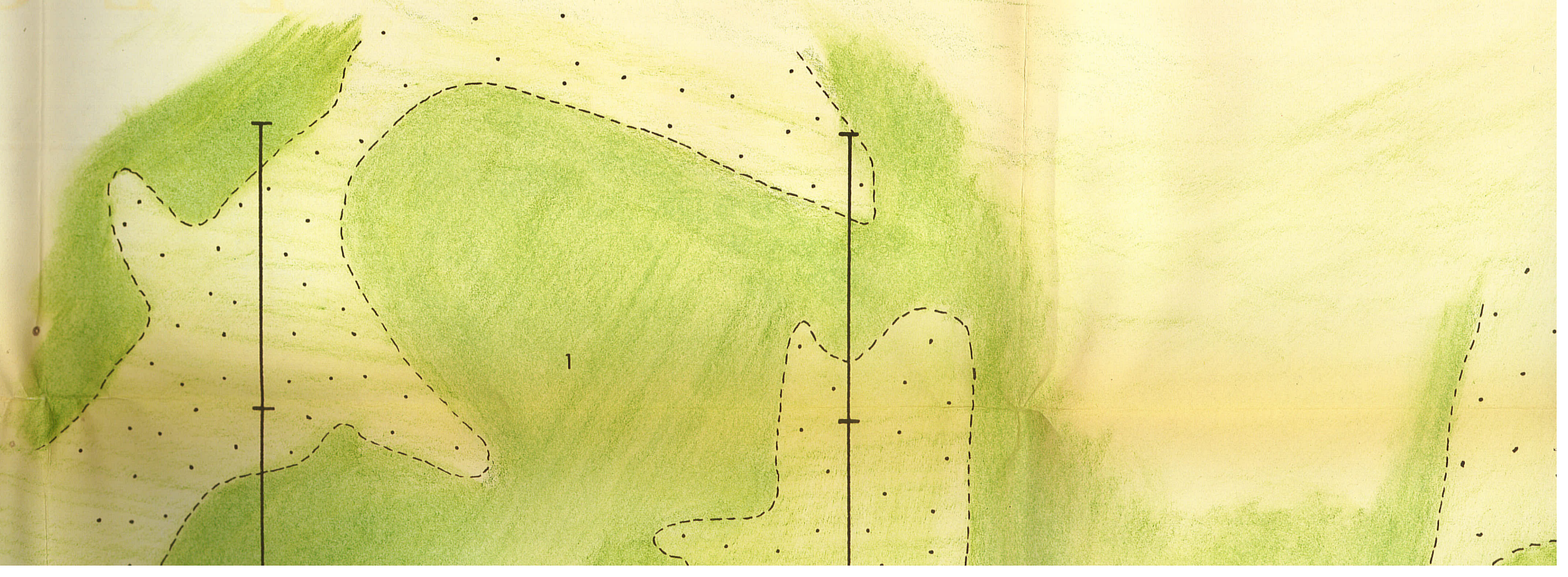

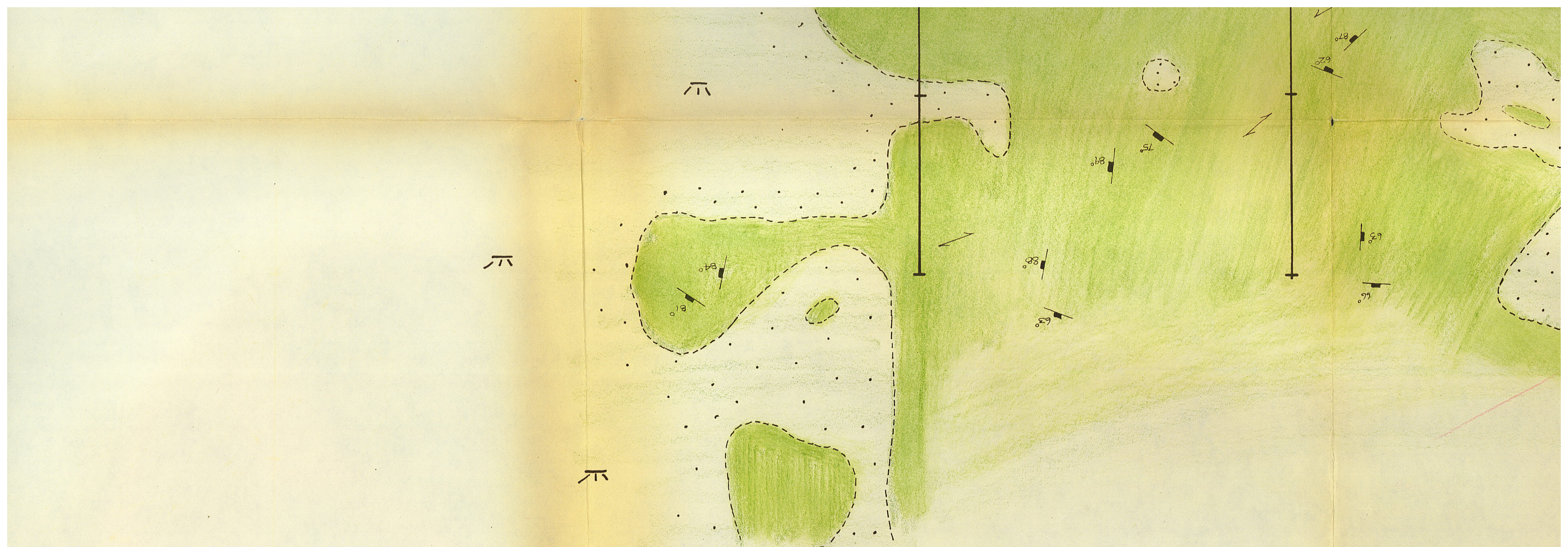

L E G

GEOLOGI

VOLCAN

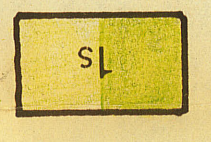

SERICIT

DIABAS

L E G E N D

GEOLOGICAL UNITS

1	VOLCANICS, fragmental porphyritic dacites and andesites
1s	SERICITE CHLORITE SCHIST

2+50 E

2+00 E

1+50 E

1+00 E

0+50 E

0+00 B.L.

1s

4

1s

2s

3s

2

1

3A

3A

82°

87°

57°

37°

86°

82°

14°

85°

28°

52°

35°

83°

58°

76°

85°

74°

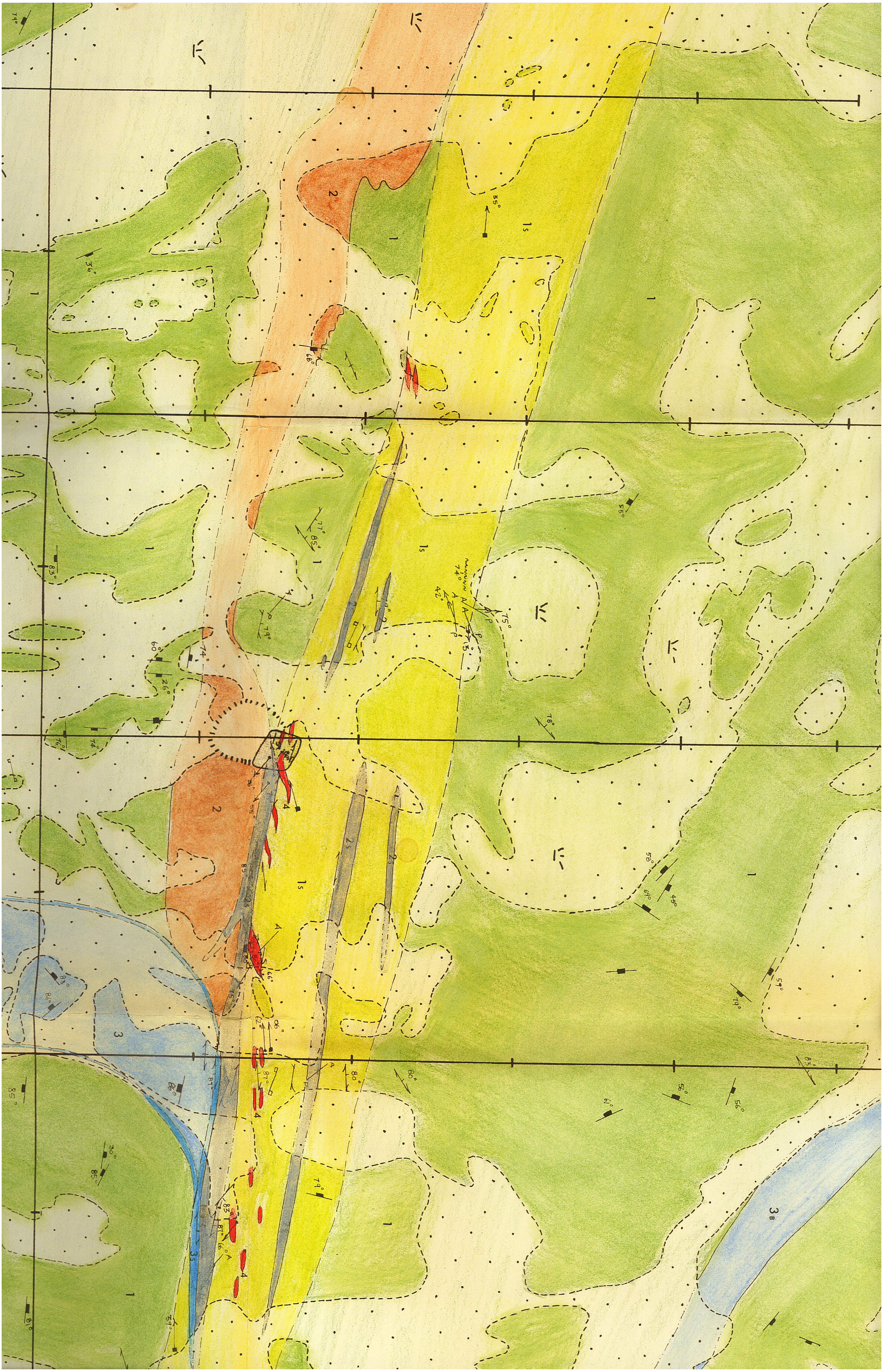

1
1s
2
2s
3
3B
3s
4
A
P
85°
36°
68°
55°
77°
85°
74°
42°
75°
79°
60°
26°
83°
76°
78°
58°
45°
69°
59°
79°
83°
61°
56°
80°
87°
62°
66°
30°
81°
86°
39°

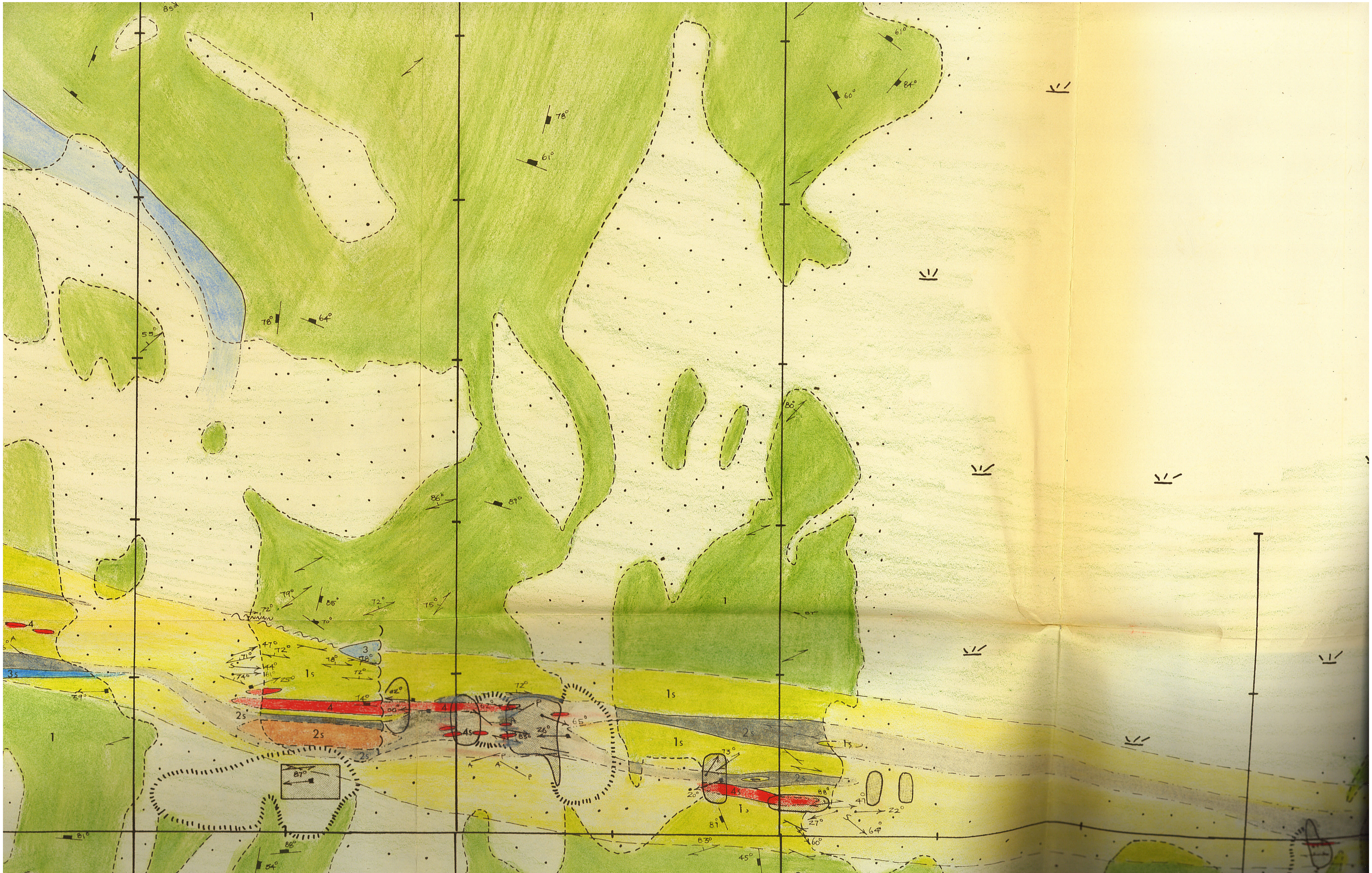
1
1s
2s
3
3s
4
4s
P
A

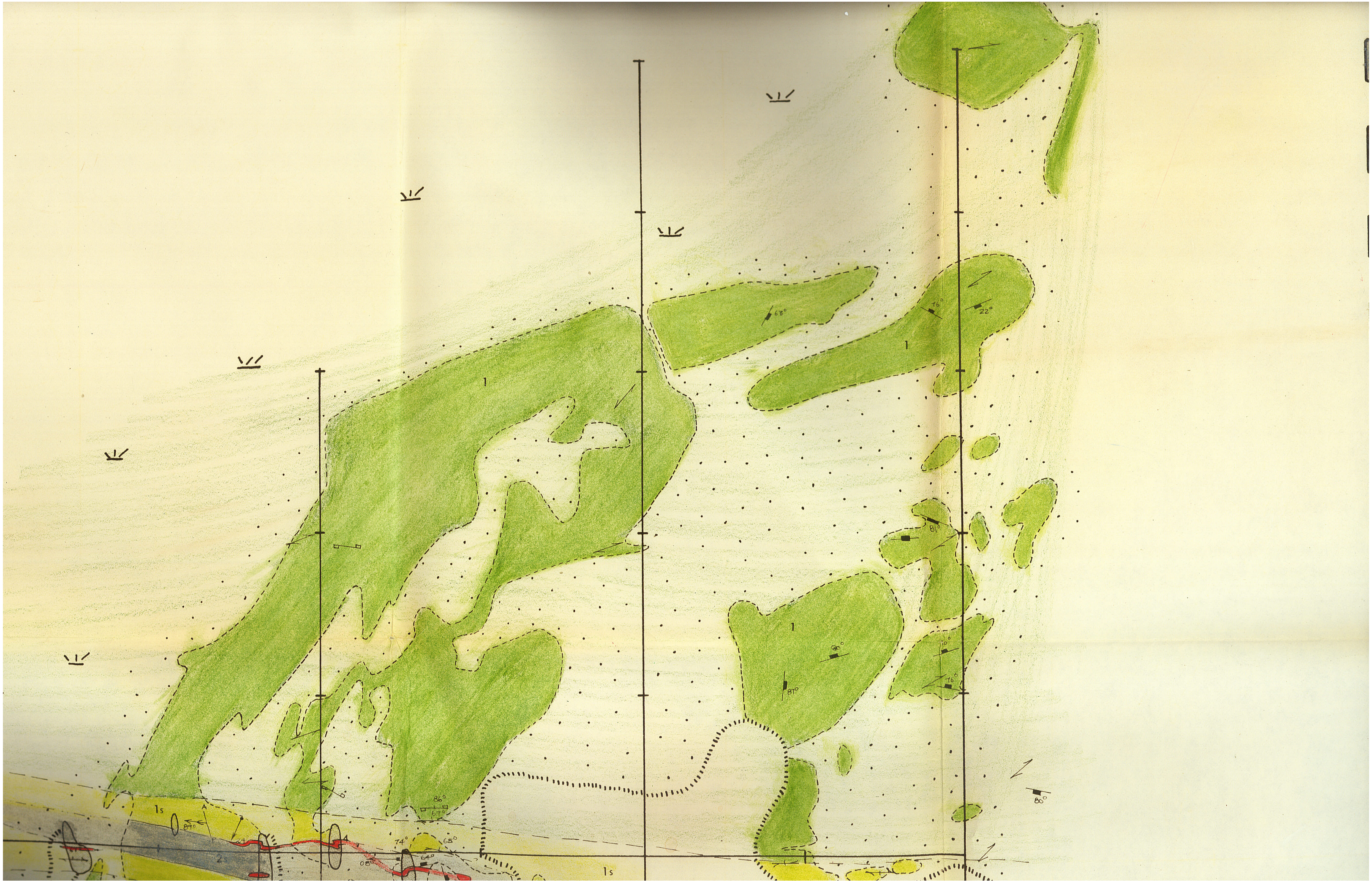
1
1
1
1
1s
1s
2
A
A
63°
76°
22°
86°
67°
74°
65°
64°
68°
81°
87°
80°

2s — CHLORITE SCHIST

3 A&B — QUARTZ FELDSPAR PORPHYRY, (a) coarse grained light coloured matrix, (b) fine grained dark matrix

3s — SERICITE CHLORITE SCHIST, with quartz eyes

4 — QUARTZ VEIN

GEOLOGICAL SYMBOLS

SCHISTOSITY, vertical, dipping

STRAIN SLIP CLEAVAGE, vertical, dipping, with plunge of small folded increments

FRACTURE CLEAVAGE, vertical, dipping

JOINT, vertical, dipping

LINEATION, microcrenulation, mineral

MINOR FOLD (plunge & trend of axis), Z & S assymetrical, symmetrical, with axial plane

FAULT, apparent horizontal displacement

CATACLASTIC FOLIATION

GEOLGICAL CONTACT, known, assummed

BOUNDARY OF SHEAR ZONE

0+50W

1+00W

1+50W

2+00W

2+50W

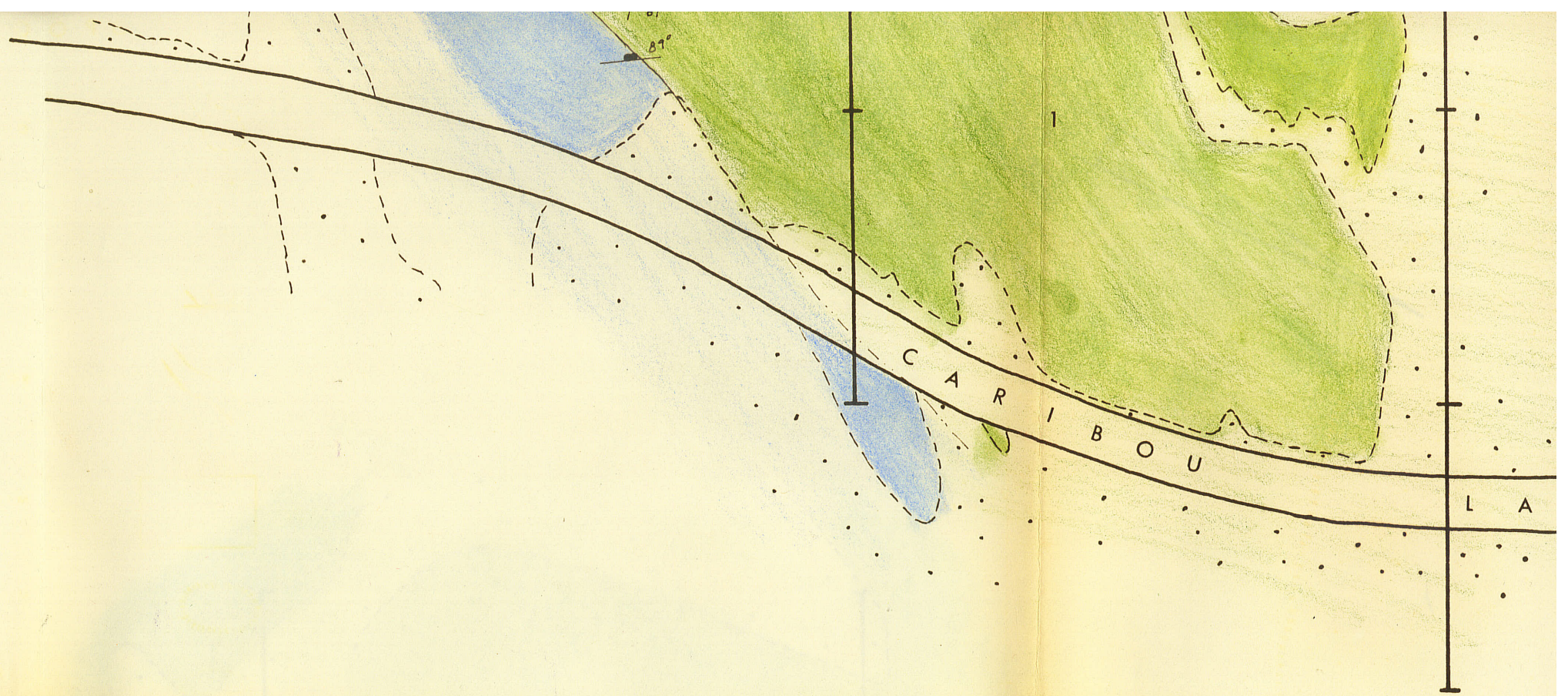

50N

50N

0N

50N

LAKE ROAD

54°

74°

74°

74°

77°

67°

1

57°

87°

3

77°

81°

75°

87°

85°

1

75°

GOLD LAKE MINE

N

N

N

S00+

S00

N00

ROAD

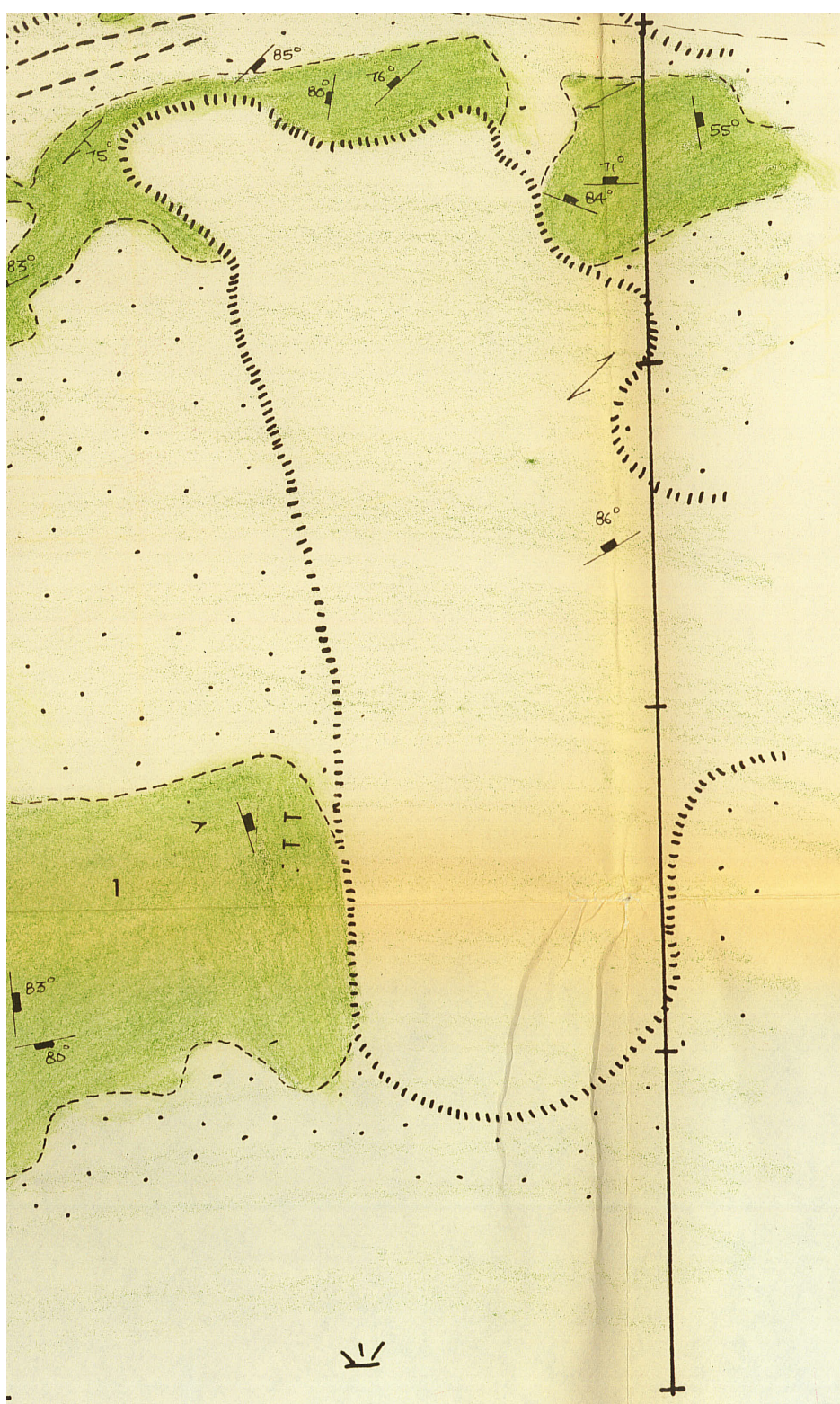

OUTCROP

LIGHT OVERBURDEN

SWAMP

ROAD

MINE SHAFT

MINE TAILINGS

TRENCH

25′ 0 25′ 50′ 100′ 150′

S C A L E

1 INCH = 25 FEET

MAP 3

GAMMA RAY SPECTROMETER SURVEY

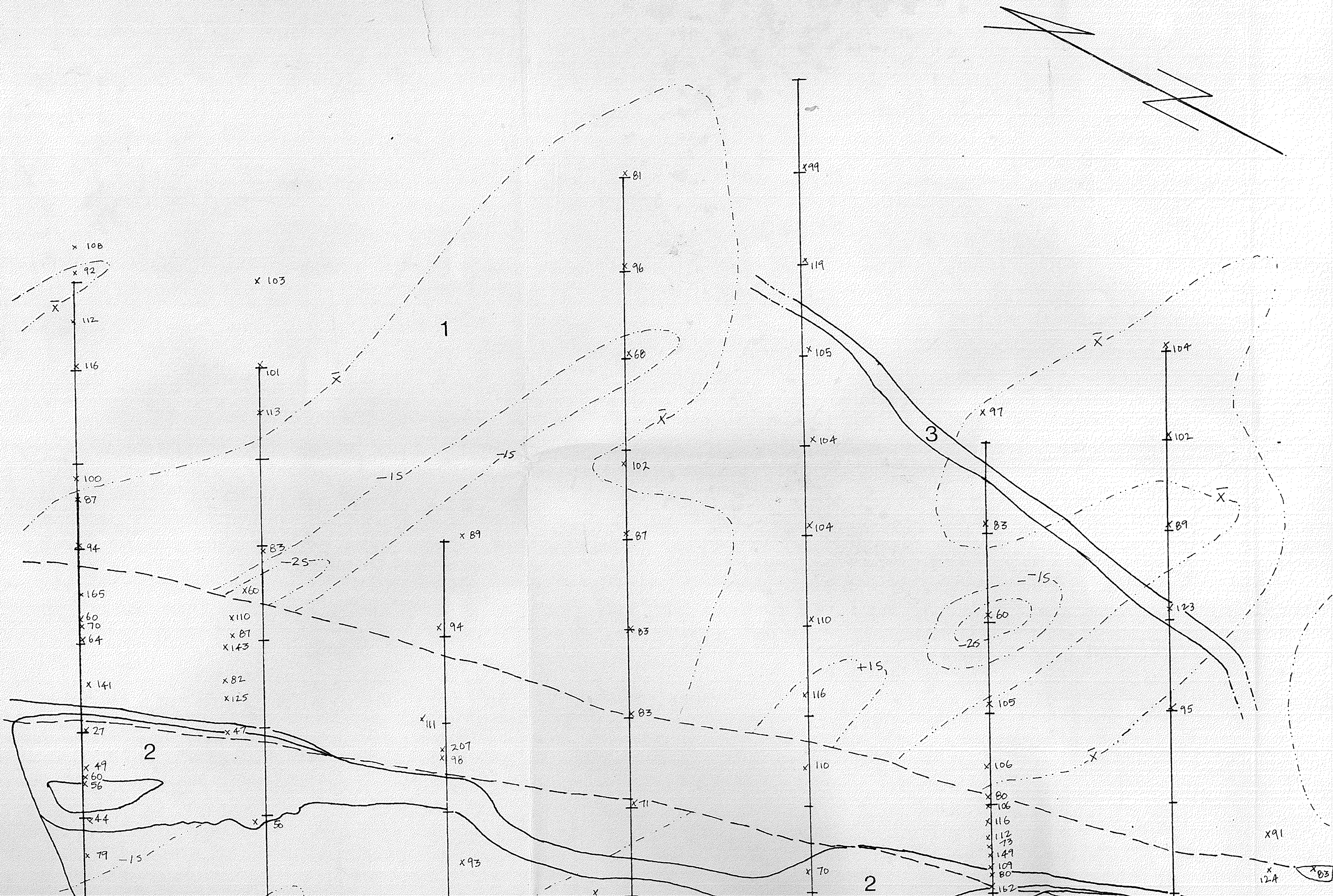
1
2
3
2
x 108
x 92
X
x 112
x 116
x 103
x 101
x 113
x 100
x 87
x 94
x 165
x 60
x 70
x 64
x 141
x 27
x 49
x 60
x 56
x 44
x 79
-15
x 83
-25
x 60
x 110
x 87
x 143
x 82
x 125
x 47
x 56
-15
-15
x 89
x 94
x 111
x 207
x 98
x 93
x 81
x 96
x 68
X
x 102
x 87
x 83
x 83
x 71
x 99
x 119
x 105
x 104
x 104
x 110
x 116
x 110
x 70
+15
x 97
x 83
-15
x 60
-25
x 105
x 106
x 80
x 106
x 116
x 112
x 73
x 149
x 109
x 80
x 162
X
x 104
x 102
x 89
x 123
x 95
x 91
x 124
x 83

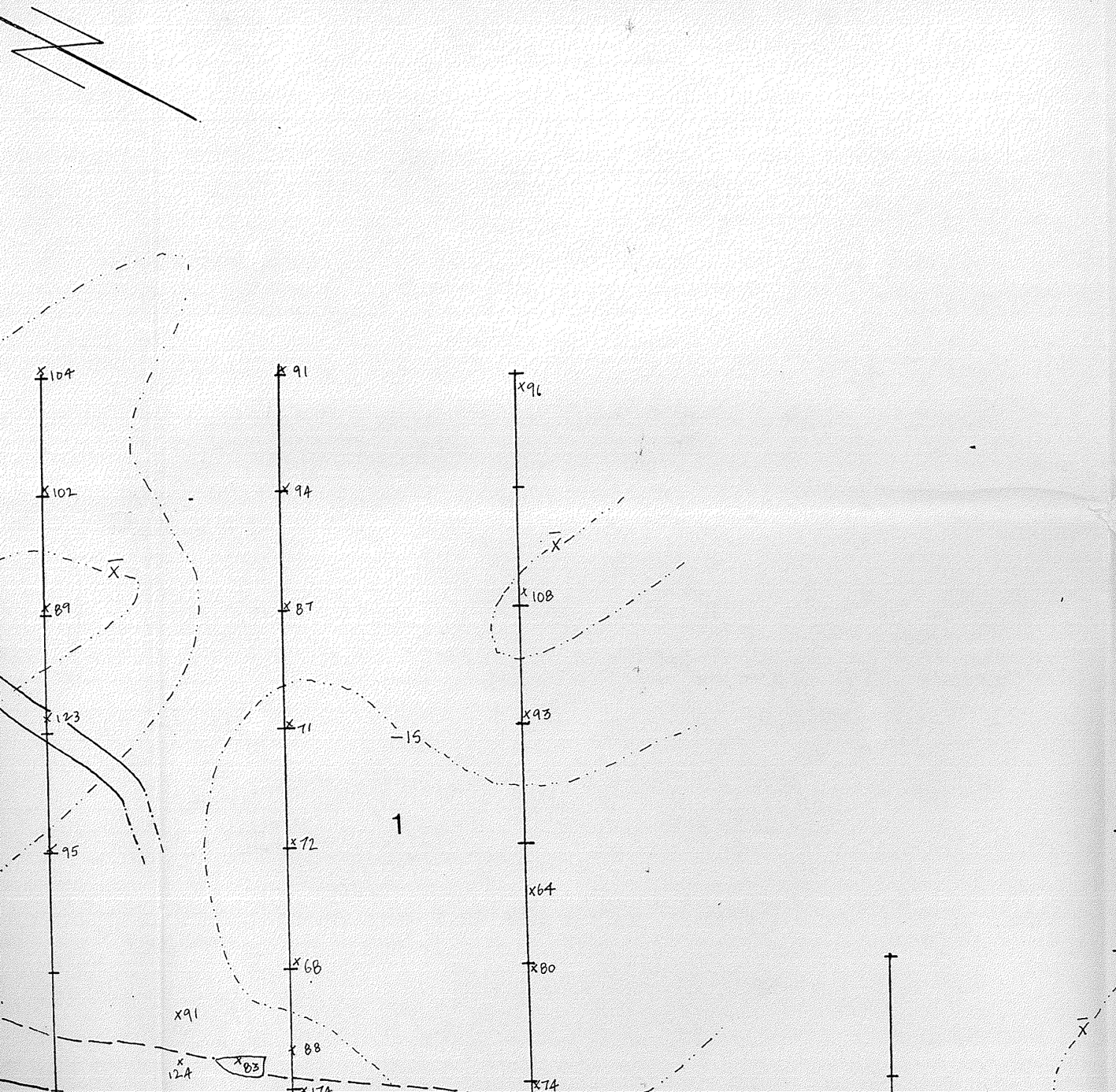
104
91
96
102
94
89
87
108
123
71
93
15
95
72
64
68
80
91
88
83
12A
74
112
91
107
103
15
72
137
+15
+25
97
121
5+00 E
4+50 E
4+00 E
3+50 E
3+00 E
2+50 E
2+00 E
1+50 E
1+00 E
0+50 E

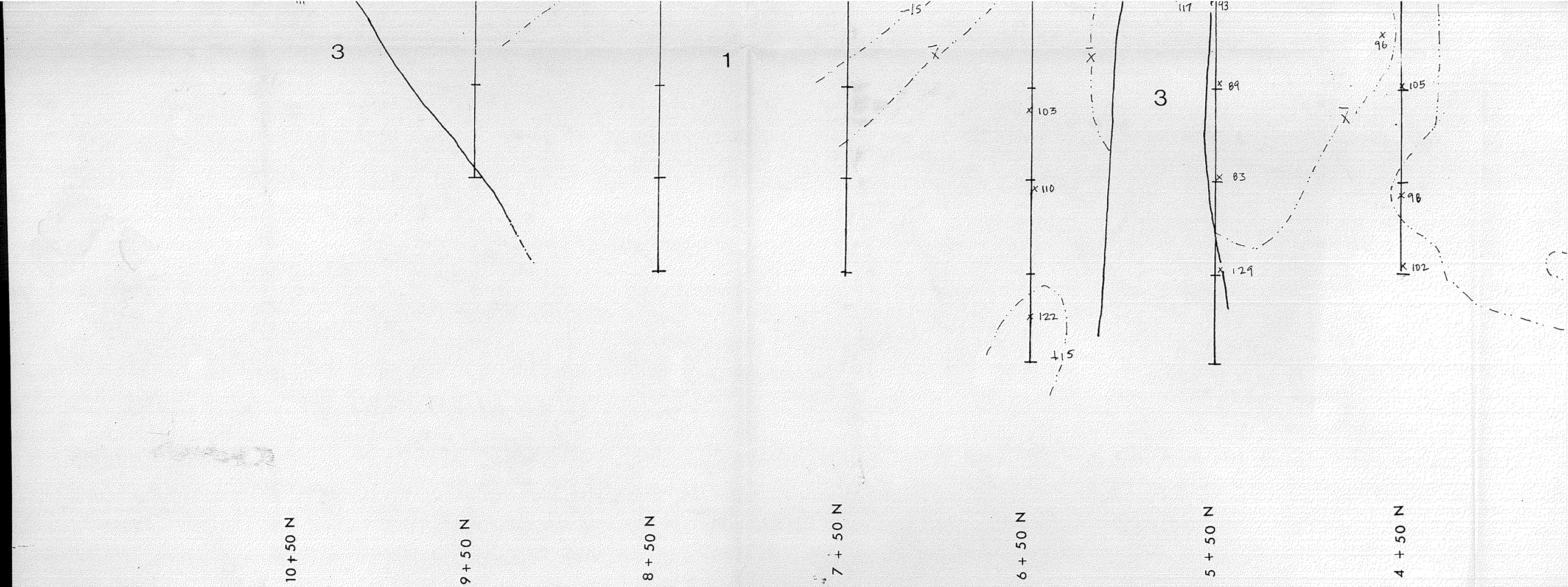

L E G E M D

1 ..... DACITE

2 ..... DIABASE

3 ..... Quartz Feldspar Porphyry

..... Geological Contact

..... Shear Zone

..... Contours K gamma counts/min.

50' 0 50' 100' 150' 200' 250'

$\bar{x}$ = 9

s = 1

+1s = 1

+2s = 1

−1s = 8

−2s =

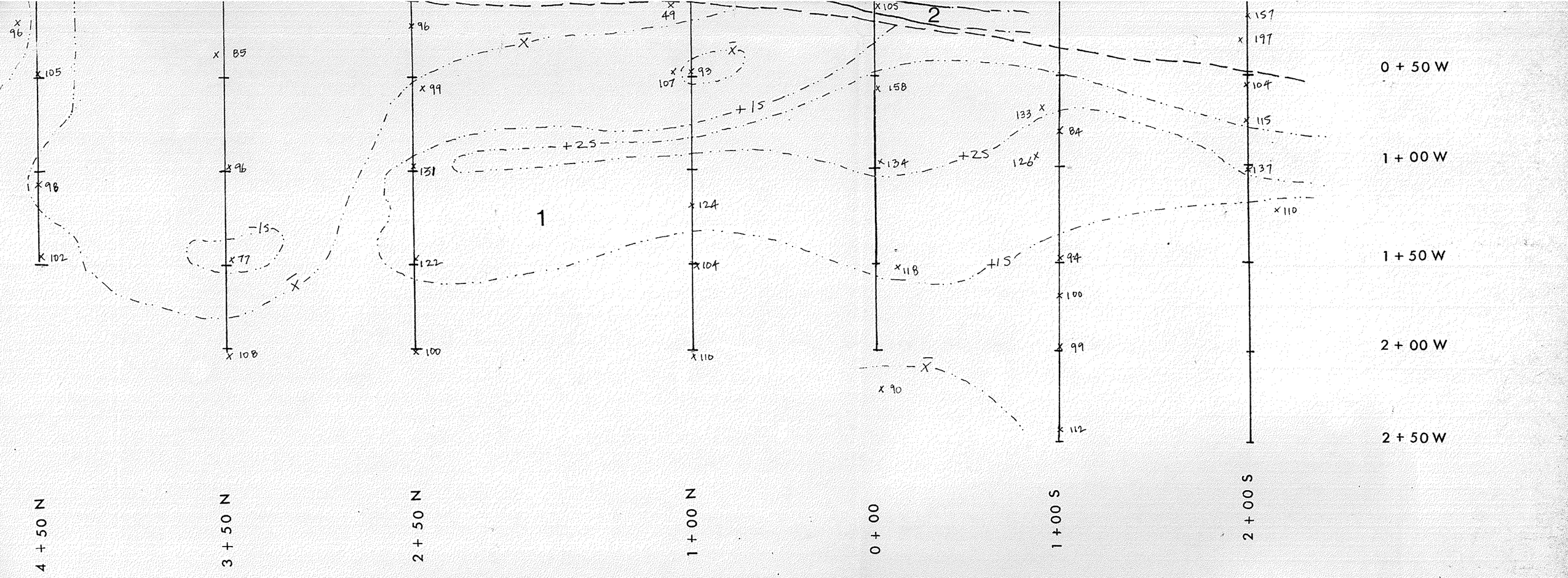

D

$\bar{X}$ = 98.25 counts/min.

s = 17 "

+1s = 115.25 "

+2s = 132.25 "

-1s = 81.25 "

-2s = 64.25 "

00' 250'